STUDY OF RADIATION HEAT FLUX FROM HIGH PRESSURE AIR ARCS

I Sub

C. H. Marston
General Electric Company

January 1965

ARNOLD ENGINEERING DEVELOPMENT CENTER
AIR FORCE SYSTEMS COMMAND
ARNOLD AIR FORCE STATION, TENNESSEE

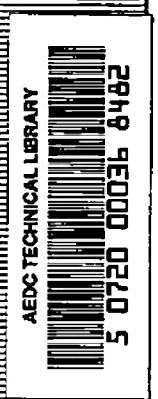

NOTICES

When U. S. Government drawings specifications, or other data are used for any purpose other than a definitely related Government procurement operation, the Government thereby incurs no responsibility nor any obligation whatsoever, and the fact that the Government may have formulated, furnished, or in any way supplied the said drawings, specifications, or other data, is not to be regarded by implication or otherwise, or in any manner licensing the holder or any other person or corporation, or conveying any rights or permission to manufacture, use, or sell any patented invention that may in any way be related thereto.

Qualified users may obtain copies of this report from the Defense Documentation Center.

References to named commercial products in this report are not to be considered in any sense as an endorsement of the product by the United States Air Force or the Government.

STUDY OF RADIATION HEAT FLUX FROM HIGH PRESSURE AIR ARCS

C. H. Marston
General Electric Company

FOREWORD

This report was prepared by the Space Sciences Laboratory of the General Electric Company Missile and Space Division for the Arnold Engineering Development Center (AEDC), Air Force Systems Command (AFSC). The work was performed from December 1963 to November 1964 under contract AF 40(600)-1080, Project 8952, Program Element 62405334, Task 895202, entitled "Study of Radiation Heat Flux from High Pressure Air Arcs."

Capt. J. Edwards and Capt. J. R. Cureton were the Technical Monitors.

C. H. Marston and T. K. Pugmire were the principal investigators. The spectrographic temperature profiles were obtained by H. Sadjian and B. A. Bellinger. Dr. H. E. Weber's continuing advice and comment and particularly his assistance with the applications section are gratefully acknowledged. The invaluable assistance of A. M. Schorn, who prepared the ARCRAD computer program, and V. L. Chesser, who ran the arc facility, is also gratefully acknowledged.

Some sections of this report were originally prepared by T. K. Pugmire, who is no longer with the company. These include the discussion of thermal equilibrium in section 2, some parts of section 5, and all of Appendix E. Appendix B was written by A. M. Schorn.

The reproducibles used for the reproduction of this report were supplied by the author December 28, 1964.

This technical report has been reviewed and is approved.

John R. Cureton
Captain, USAF
Gas Dynamics Division
DCS/Research

Donald R. Eastman, Jr.
DCS/Research

ABSTRACT

A computational model has been developed and applied for calculating radiant heat flux from an electric arc using real gas properties and taking into account both self absorption and space varying temperature. The model requires knowledge of the temperature profile as an input. Temperature profiles were measured spectrographically using an air arc at one and 2.4 atmospheres. These measured profiles plus some simple analytic ones which satisfied boundary conditions were used to calculate radiant heat flux at pressures from 1 to 300 atmospheres. The experimental program also included measurements of radiant flux density at 2.2 and 5.7 atmospheres for comparison with calculations based on the measured profiles. Estimates were made of radiation losses in the AEDC 20-megawatt arc air heater now under development.

CONTENTS

ILLUSTRATIONS

Figure

NOMENCLATURE

A	Transition probability (Appendix E only)
A	Area
dA	Radiating element of surface area
B	Total radiant flux density leaving a surface
B′	Total radiant flux density incident on a surface
c_2	Planck's second radiation constant 1.4380 (cm^oK)
D	Fraction of black body energy at wavelengths between 0 and λ
E	Voltage gradient
E	Excitation energy (Appendix E only)
e	2.718.....
F	View factor between radiating surfaces
g	Statistical weight of an energy state
h	enthalpy
h	Planck's constant (Appendix E only)
H	Dimensionless enthalpy (RT_o = 35.58 BTU/lbm)
I	Radiation intensity (watt/cm^2 - steradian) (Section 2 only)
I	Electric current
J	Total spectral radiance (watts/cm^3 - steradian)
k	Boltzmann constant (Appendix E only)
k	Linear absorption coefficient (cm^{-1})

$\overline{kR}$	Dimensionless absorption length
L	Length along absorbing path (Section 2 only)
L	Length
m	Number of constant temperature subdivisions of the arc column
N	Atom number density
n	Wavenumber (reciprocal of wavelength), (cm^{-1})
P	Power
p	Pressure
q	Radiant power (watts)
R	Sector radius (Section 2 only)
R	Radius
r	Annulus radius (Section 2 only)
s	Number of sector subdivisions in an absorbing quadrant
dV	Element of radiating volume
v	Dimensionless variable, c_2n/T
$W_{B,n}$	Monochromatic emissive power of a black body
W	Mass flow rate
x	Exponent on arbitrary profiles
x	Radial distance (Appendix E only)

GREEK SYMBOLS

α	Absorptivity
β	Angle whose sine is the annulus radius ratio r_{j+1}/r_j. Also, an angle defined in Fig. 2. 1a
γ	Angle defined in Fig. 2. 1a
δ	Arc column radius (cm)
ϵ	Emissivity
η	Fraction of black body energy radiated within a wavenumber interval
θ	Angle defined in Fig. 2. 1b
λ	Wavelength
ν	Frequency
π	3. 14 .....
ρ	Density
σ	Stefan-Boltzmann constant
σ_e	Electrical conductivity
τ	Transmissivity
ϕ	Angle at which absorption length is calculated (see Figs. 4 and 5)
χ	Angle used in cylinder absorptivity calculation
ψ	Angle defined in Fig. 2. 1
ω	Solid angle

INDEXING SUBSCRIPTS

The following subscripts are used to indicate that the subscripted quantity varies stepwise with the subscript (listed in reverse order of summation).

n	Wavenumber
j	Index on radiating annulus, counting from the outermost
	Angle at which absorption lengths are calculated (see Figs. 2.4 and 2.5)
q	Index on absorbing annulus, counting from the outermost (see sect. 2.4)

GENERAL SUBSCRIPTS

a	Arc column
b	Heated bulk gas
c	Constrictor or arc chamber
CL	Centerline
E	Exterior
g	Gas
HF	High frequency
I	Interior
i	Non-black surface at which net radiation is calculated
k	Non-black surface radiation to surface i

LF	Low frequency
LL	Lower limit
ref	Reference
UL	Upper limit
w	wall

SECTION I
INTRODUCTION

One of the primary limitations on entry simulation facilities, such as hotshot tunnels, arc driven shock tubes and electric arc heaters in general, is radiation heat loss. This report describes a project which consisted of a computer study of arc radiation using tabulated spectral absorption properties of high temperature air, combined with spectrographic measurements of temperature profiles and experimental determination of radiation heat transfer rates.

The geometric configuration studied was an idealization of a D.C. arc column in the form of an infinitely long right circular cylinder whose temperature is a known function of radius only. The basic approach, which makes use of detailed spectral absorption data (Refs. 1, 2) developed by Breene and Nardone for analysis of the radiating gas cap of a re-entry vehicle, has application to any reasonably simple geometry with space-varying temperature.

An upper bound on radiation heat flux can be calculated by assuming the arc to be a black body at arc centerline temperature. Another upper bound can be established by assuming the gas heated by the arc to be optically thin so that all the energy radiated by each infinitesimal volume element reaches the chamber walls. At a given pressure, and for a known or assumed temperature profile, radiant flux density can then be calculated by integrating total radiance over the volume of a unit length of arc column and multiplying by 4π steradians. The energy leaving this unit length of arc column is, of course, distributed over the entire column length but, assuming an infinitely long column, the energy radiated from a unit length must be equal to the energy (originating throughout the column) crossing a unit length of boundary surface.

These upper bounds are perfectly adequate as long as radiation is only a small part of the total heat flux. However, at the pressure and temperature levels which are now the goals of, for example, arc heater development, radiation is the predominant heat transfer mode and a more accurate prediction is needed.

Absorption and emission of radiant energy in air depend on temperature, density and frequency. Thus, radiation energy from a particular element of volume will have a spectral distribution of intensity which is characteristic of the temperature and density of that element. The amount of energy reabsorbed along a particular

path will depend on the path length and also on the absorption characteristics (hence temperature and density) of each volume element along the path. A complete solution of the radiation heat transfer problem with self-absorbing gas therefore requires detailed knowledge of the radiation characteristics of air plus calculation for all volume elements (or a representative sample if advantage can be taken of symmetry), all possible paths for each volume element and all frequencies for each path.

As a practical matter some approximations are necessary. By means of the method described in this report, sufficiently tight upper and lower bounds can be placed on the effect of self-absorption that the calculation of radiant flux density is limited in accuracy by the state of knowledge of radiation properties, and of arc column temperature profiles.

SECTION II
ANALYSIS

2.1 THE ARC COLUMN MODEL

Consider an infinite cylindrical column of radiating gas at constant pressure with a known or assumed radial temperature profile. Let the column boundaries be cold and non-reflecting because, for structural reasons, the wall must be kept sufficiently cool that re-radiation can be neglected and, while cold compared with the arc plasma, it is still too warm to retain a high reflectivity. A correction for the effect of non-black walls is discussed in Section 2.7.

Complete equilibrium cannot be attained in the arc column, which exists only because of continuous energy transfer processes. However, a considerable body of evidence, both experimental and theoretical (Refs. 3, 4, 5, 6 and 7), indicates that local thermal equilibrium among electrons, ions, atoms and molecules can be assumed, with certain restrictions, so that equilibrium properties may be used in the computation.

Finkelnburg (Ref. 3) has indicated that according to existing analytical and experimental evidence, local thermal equilibrium exists to a good approximation in the plasma of all arcs operating at one atmosphere or greater except near the electrodes where strong electric fields (hundreds of volts per centimeter) are present. Lochte-Holtgreven (Ref. 4) concluded from his theoretical studies of the arc column that, at atmospheric or higher pressures, both the temperature of excitation and the "temperature" of ionization are for practical purposes equal to the electron temperature, with the possible exception of constricted arcs having an electric field intensity of 300 volts/cm or more. Cobine (Ref. 5) has shown that bulk gas temperature and electron temperature are essentially identical for a constant current discharge whenever the pressure is above 17 mm hg. Maecker's (Ref. 6) experimental studies support these conclusions.

The arc heater used in this study was designed to isolate completely the constricted region from electrode contamination (a major source of column and flow perturbation). The only part of the arc column used for this study was the constricted region, well separated from the electrodes, with a voltage gradient less than one hundred volts/cm (Ref. 8).

A given temperature distribution implies the existence of a steady state; each element of volume, dV, has presumably struck a balance among heat generated, radiated, absorbed and conducted in and out. Each such element within the column radiates in all directions with an intensity which is a known function of temperature, density and frequency. The assumptions of cylindrical symmetry and constant pressure make temperature and density dependent on radius only, so that intensity and transmissivity reduce to functions of radius and frequency only.

The arc column was divided into a constant temperature core and a series of constant temperature annuli* with radiant heat flux originating in the core and in each annulus considered separately in terms of equivalent surface emissivities. Radiant flux densities for each surface are given by an equation of the form

$$q/A = \int_0^\infty \epsilon_n W_{B,n} \, dn \tag{2.1}$$

where $W_{B,n}$ is the monochromatic emissive power of a black body at the radiator temperature and n is the wavenumber.** Over a small but finite wavenumber interval the flux density is of the form

$$(q/A)_{\Delta n} = \sigma T^4 \epsilon_n \eta_n \tag{2.2}$$

where ϵ_n is the average emissivity within the wavenumber interval and η_n is the fraction of the total energy radiated by a black body at temperature T which is radiated within the interval Δn.

*Each annulus was denoted by the index number j assigned to its exterior surface, counting from the outside surface of the arc column inward to the core.

**Wavenumber is the reciprocal of wavelength and is therefore proportional to frequency. Tabulation of properties by wavenumber proves convenient so the term will be used interchangeably with frequency in the sense of frequency dependence.

Upper and lower limits were placed on the fraction of emitted radiant energy which actually leaves the arc column by considering two assumed sets of absorbing paths. One set of paths was so chosen that absorption is always less than or equal to the true absorption while along the other set of paths radiation absorption was always greater than or equal to the true value.

2.2 INFINITE HALF CYLINDER ABSORPTIVITY

The basic element from which the absorption model was built up is an infinite half-cylinder of gas, of radius R, absorbing radiation from an element of area on its axis. Associated with the cylinder is a linear absorption coefficient k which is a function of radial distance only. The angles shown in Fig. 2.1 (a) are related by

$$\cos \gamma = \sin \theta \cos \psi \tag{2.3}$$

From Fig. 2.1(b), the solid angle $d\omega$ can be written

$$d\omega = \frac{R}{L} \, d\theta d\psi \tag{2.4}$$

If the surface element dA is radiating with an intensity I (energy flux per unit solid angle) and absorption takes place along the path according to Beer's law, then

$$d^2q = (I \cos \gamma dA) \, d\omega \, \exp\left(- \int_o^L k \, d\ell \right) \tag{2.5}$$

Integration of Eq. (2.5) over the half cylinder would yield the total radiant flux originating from dA and escaping the half cylinder. With the further definition

$$(\overline{kR}) \equiv \int_o^R k dr = \frac{1}{\sin \theta} \int_o^L k d\ell \tag{2.6}$$

the radiant flux density from dA which escapes the half cylinder is

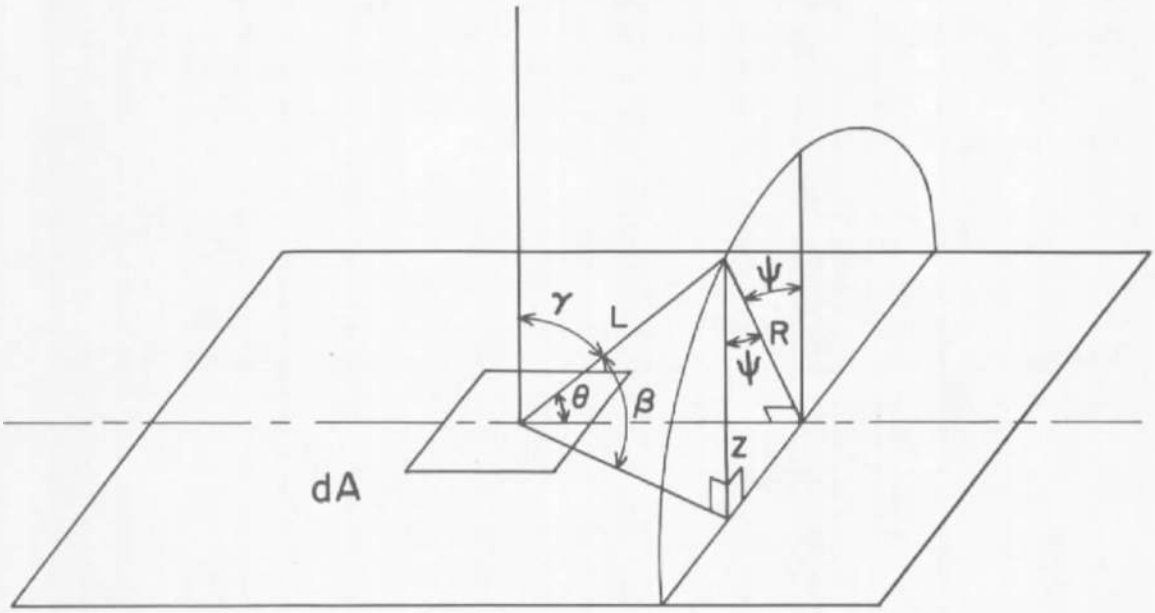

a) Geometry

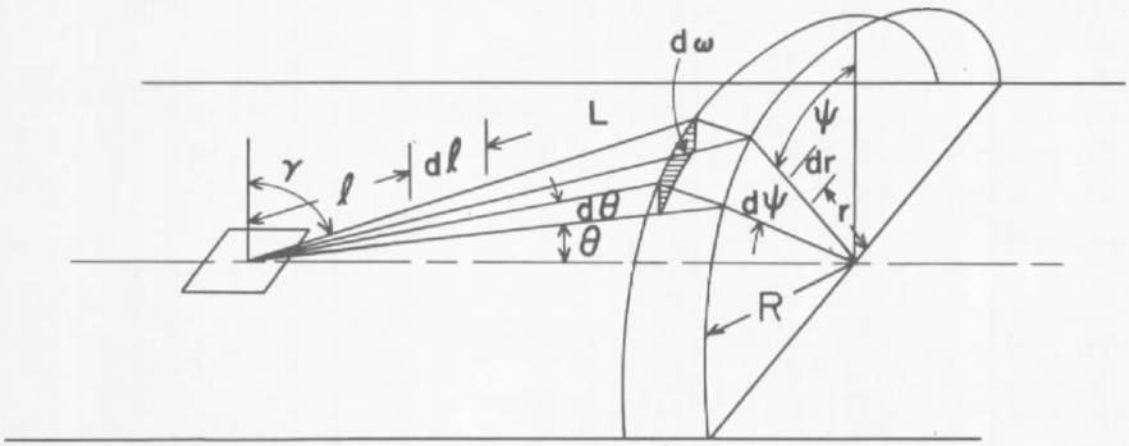

b) Typical Absorption Path.

Figure 2.1 Absorption by an Infinitely Long Half Cylinder.

$$\frac{dq}{dA} = 4I \int_0^{\pi/2} \cos\psi\, d\psi \int_0^{\pi/2} \exp\left(-\frac{\overline{KR}}{\sin\theta}\right) \sin^2\theta \tag{2.7}$$

For the case of no absorption

$$q/A = \pi I \tag{2.8}$$

Therefore if kR $\neq f(\psi)$ transmissivity and absorptivity are given by

$$\tau_n = 1 - \alpha_n = \frac{4}{\pi} \int_0^{\pi/2} \cos\psi d\psi \int_0^{\pi/2} \exp\left[-\frac{(\overline{kR})n}{\sin\theta}\right] \sin^2\theta d\theta \tag{2.9}$$

where subscript n denotes dependence on wavenumber. Equation (2.9) cannot be integrated inclosed form but numerical evaluation is straightforward and the result is shown in Fig. 2.2. Note that α_n and τ_n depend only on $(k\bar{R})_n$ hereafter called the absorption length. When k_n is assumed to undergo a series of step changes with radius, Eq. (2.6) is replaced by an appropriate summation but Eq. (2.9) is unchanged.

2.3 ABSORPTION OF EXTERIOR RADIATION

An element of the exterior surface of any annulus but the outermost "sees" the annuli exterior to it as a segment of a cylinder. The segment was approximated by two or more sectors of cylinders centered at the radiating surface element is shown in Fig. 2.3. In this way, calculation of absorption became simply a matter of determination of absorption lengths plus application of Eq. (2.9).

The boundaries of a typical sector are at angles ψ and $\psi + \Delta\psi$ from the normal to the radiating surface element. It is clear from Fig. 2.3 that an upper limit transmission approximation -- all absorption lengths less than or equal to the true absorption lengths -- corresponds to the case where sector coincides with segment at the ψ boundary. Likewise, a lower limit on transmissivity corresponds to sector-segment coincidence at the $\psi + \Delta\psi$ boundary.

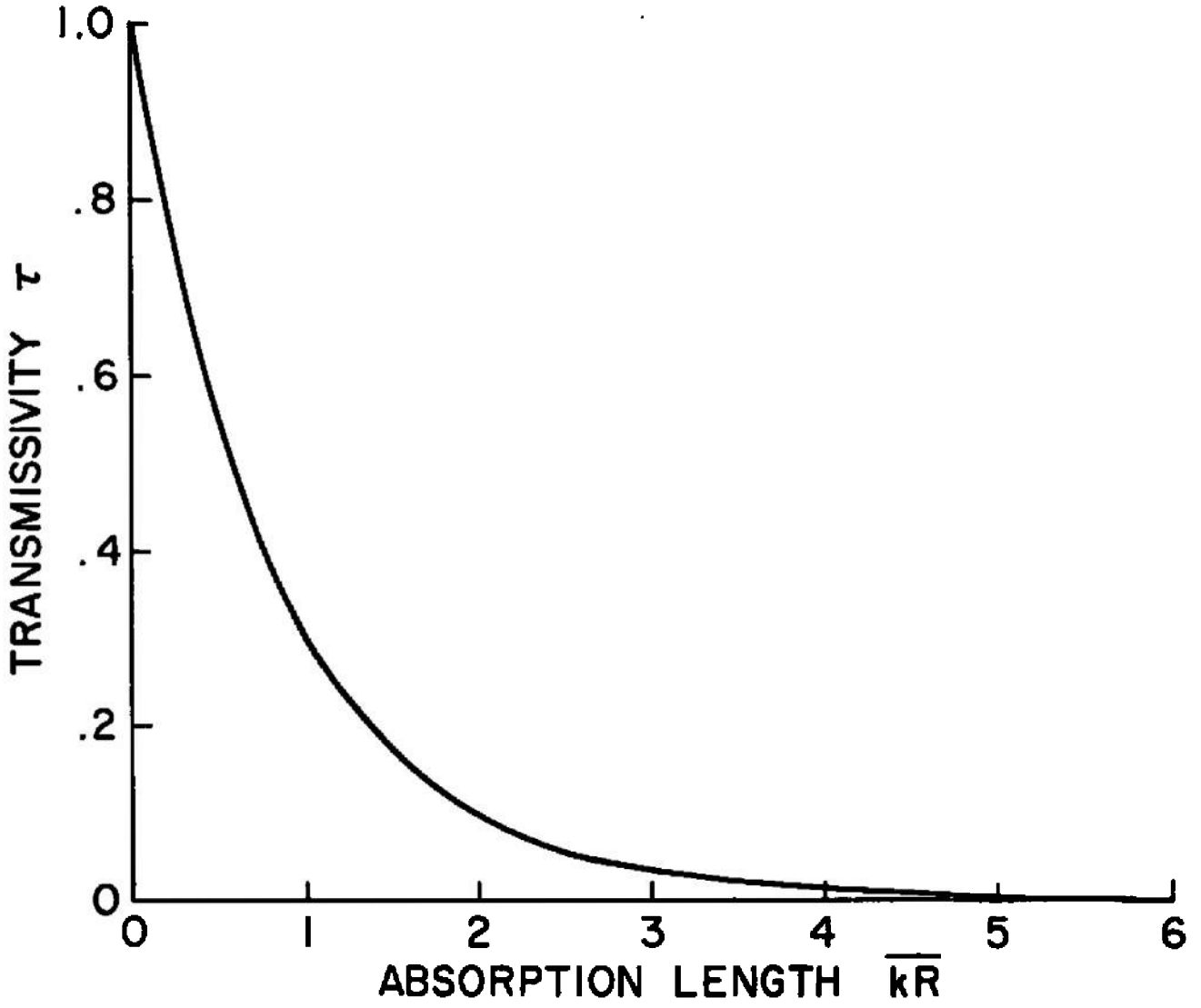

Figure 2.2 Transmissivity of an Infinitely Long Half Cylinder.

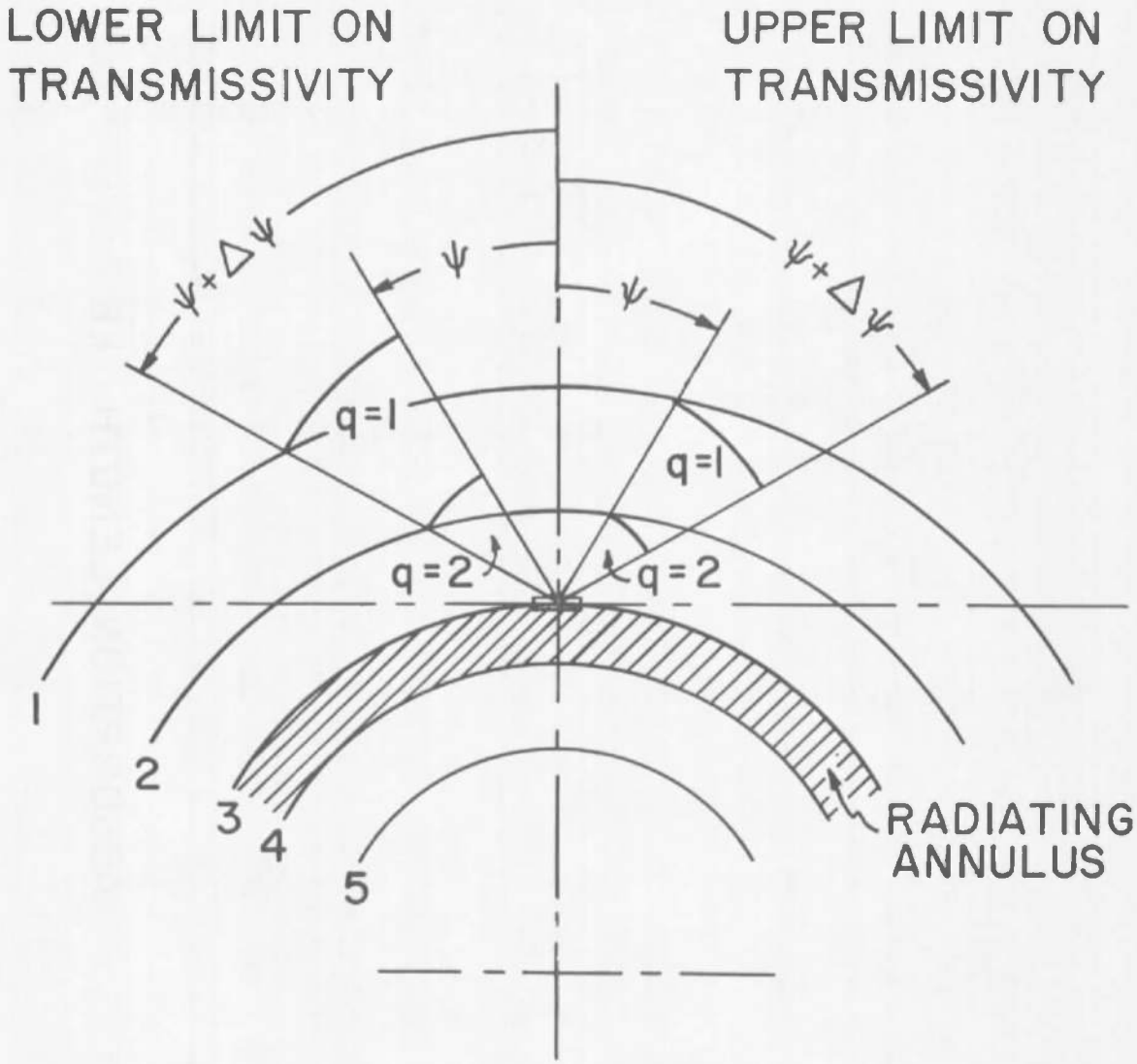

Figure 2.3 Absorption of Exterior Radiation. The j=3 Annulus is Shown as a Typical Example.

The absorption geometry calculation must be done separately for all but the outermost (j = 1) annulus. Referring to Fig. 2.4 there are q = j - 1 sector radii* $R_{j,\phi,q}$ exterior to the j^{th} annulus within each sector. Calculation of each $R_{j,\phi,q}$ is straightforward trigonometry since r_j and r_q are known and ϕ is equal to either ψ for the upper limit calculation or $\psi + \Delta\psi$ for the lower limit calculations. Absorption lengths are then

$$\overline{(kR)}_{n,\,j,\,\phi} = \sum_{q=1}^{j-1} k_{n,q} \left(R_{j\,\phi,q} - R_{j,\phi,\,q+1} \right) \tag{2.10}$$

The magnitude of $\Delta\psi$ depends on the number of sectors into which the quadrant $0 \le \psi \le \frac{\pi}{2}$ was divided. Let s be the number of sectors, so that

$$\Delta\psi = \frac{\pi}{2s} \tag{2.11}$$

Transmissivity is then given by

$$\tau_{n,j} = \frac{4}{\pi} \sum_{i=1}^{s} \left[\sin(i\,\Delta\psi) - \sin\left[(i-1)\,\Delta\psi\right] \right] \int_0^{\pi/2} \exp\left[\frac{-(kR)_{n,j,\phi}}{\sin\theta} \right] \sin^2\theta\, d\theta \tag{2.12}$$

*Subscript j on sector radius, absorption length and transmissivity refers to the respective quantities as "seen" from the j^{th} annulus. Subscript q is used to denote annuli absorbing radiation from the j^{th} annulus, again counting inward from the outermost radius. Capital R is used to distinquish sector radii from annulus radii and the angle $\psi \le \phi \le \psi + \Delta\psi$ designates the angle at which absorption lengths for a particular sector were calculated.

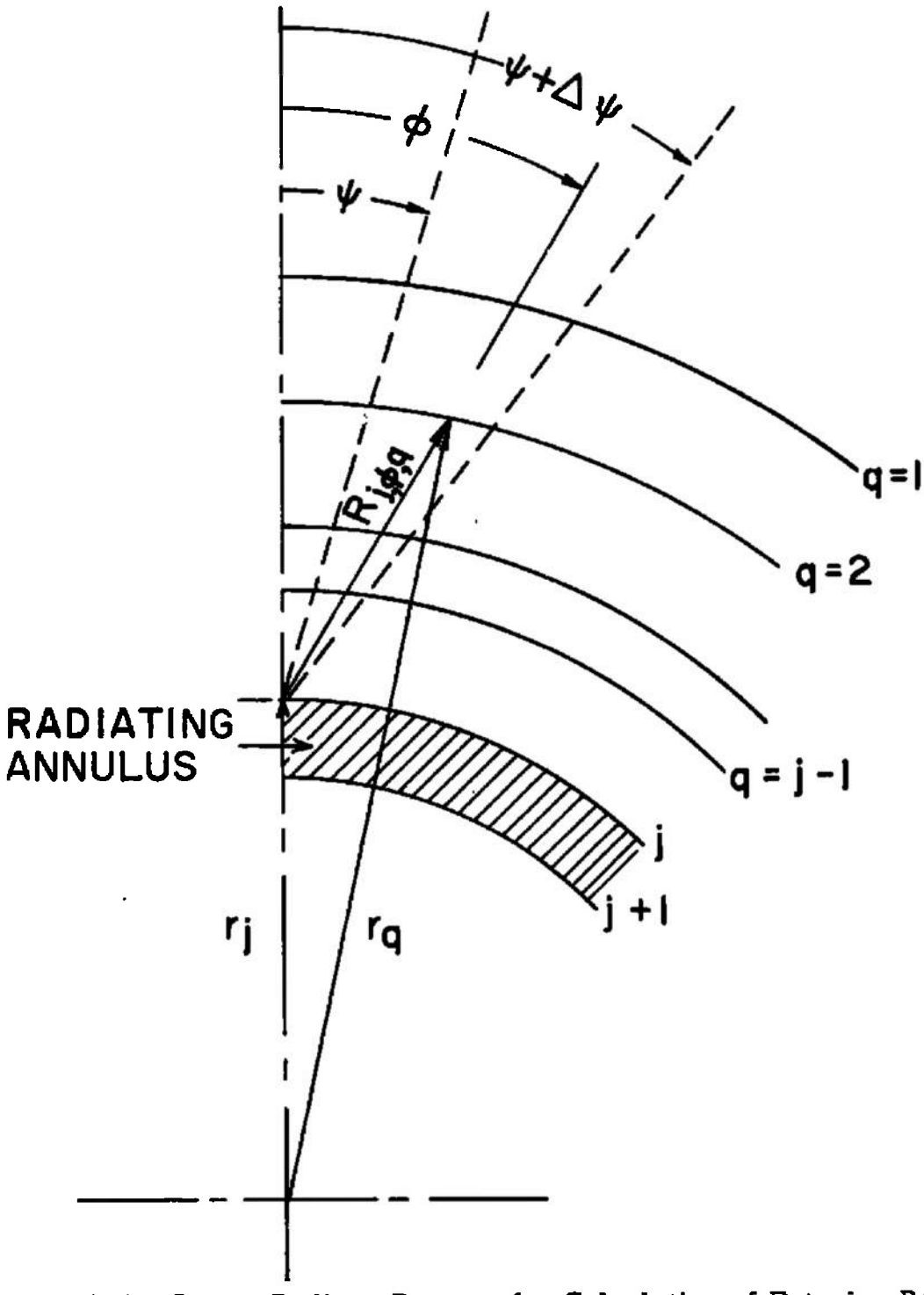

Figure 2.4 Sector Radius, $R_{j,\phi,q}$ for Calculation of Exterior Radiation Absorption Length.

Upper and lower limits on transmissivity depend on choice of ϕ

$$\phi = i\,\Delta\psi;\quad \tau = (\tau_{n,j})_{E,LL} \qquad (2.13a)$$

$$\phi = (i-1)\Delta\psi;\quad \tau = (\tau_{n,j})_{E,UL}$$

where subscripts E, LL and UL refer to exterior, lower limit and upper limit respectively.

2.4 ABSORPTION OF INTERIOR RADIATION

The parts of annuli "visible" to a radiating element of interior surface are no longer segments, but similar sector approximations can be applied. Calculation of absorption lengths is somewhat complicated by the fact that, depending on ϕ, a radiation path can cross an annulus boundary twice, once, or not at all, corresponding to the existence of two, one, or no solutions to the triangle specified by r_{j+1}, r_q and ϕ, Fig. 2.5. Sector radii* are given by

$$R^{+}_{j,\phi,q} = \frac{r_q}{\sin\phi}\left\{\sin\left[\phi + \sin^{-1}\left(\frac{r_{j+1}}{r_q}\sin\phi\right)\right]\right\} \qquad (2.14a)$$

when

$$r_{j+1}\sin\phi \le r_q$$

and by

$$R^{-}_{j,\phi,q} = \frac{r_q}{\sin\phi}\left\{\sin\left[\phi + \pi - \sin^{-1}\left(\frac{r_{j+1}}{r_q}\sin\phi\right)\right]\right\} \qquad (2.14b)$$

when

$$r_{j+1}\sin\phi < r_q \le r_{j+1}$$

*Sector radii equal to or larger than r_{j+1} are designated R^{+} while those smaller than r_{j+1} are designated R^{-}.

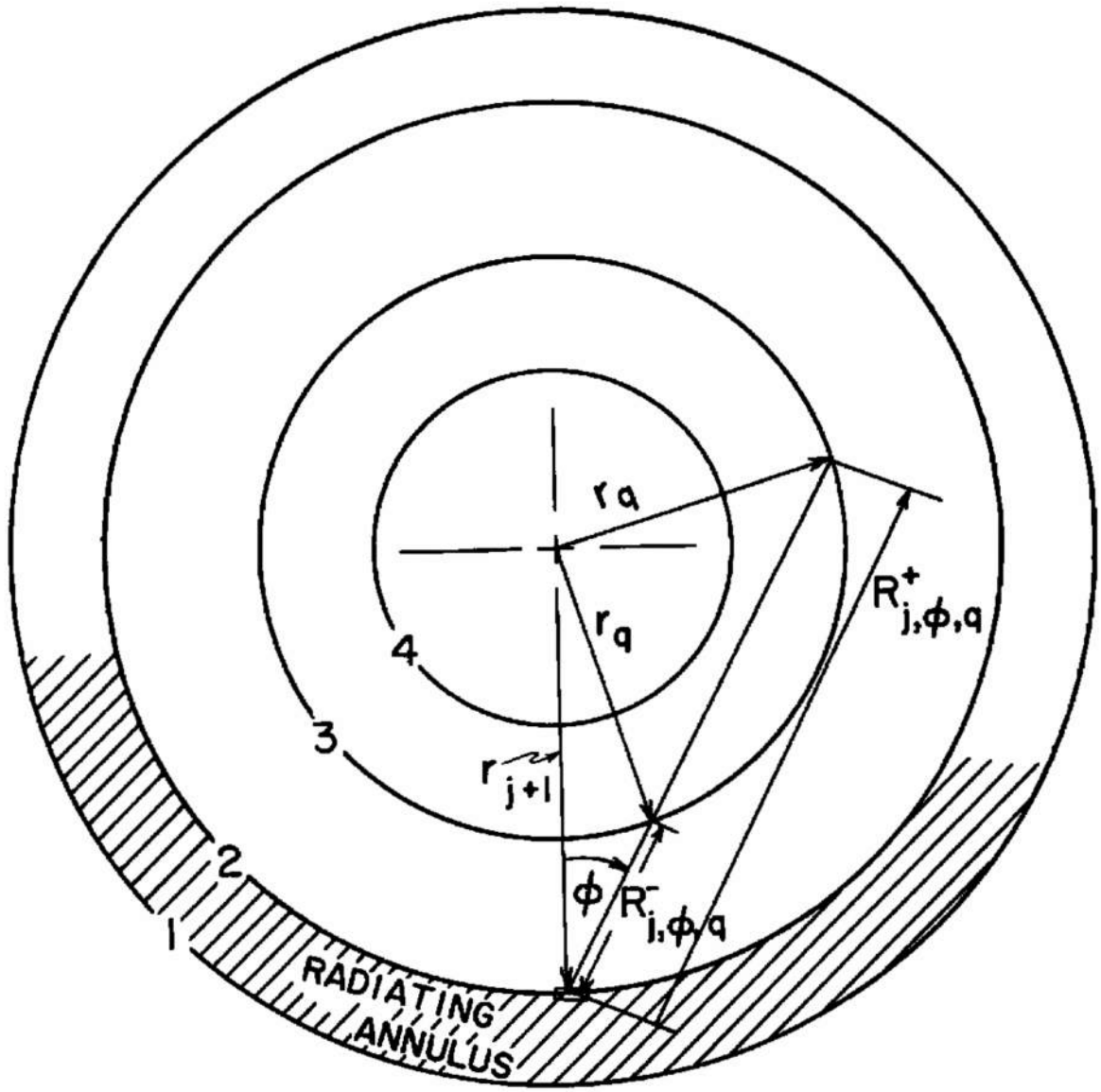

Figure 2.5 Geometry of Absorption of Interior Radiation Illustrated for Radiation from the Outermost Annulus (j=1) with q=j+2.

Defining q' as the maximum value of the index q (corresponding to the smallest r_q) for which two solutions exist, the absorption lengths are given by

$$\overline{(kR)}_{n,j,\phi} = \sum_{q=2}^{q'} k_{n,q-1}\left[\left(R^{+}_{j,\phi,q-1}\right) - \left(R^{+}_{j,\phi,q}\right)\right] \qquad (2.15)$$

$$+ k_{n,q'}\left[\left(R^{+}_{j,\phi,q'}\right) - \left(R^{-}_{j,\phi,q'}\right)\right]$$

$$+ \sum_{q=j+2}^{q'} k_{n,q-1}\left[\left(R^{-}_{j,\phi,q-1}\right) - \left(R^{-}_{j,\phi,q}\right)\right]$$

Because absorption coefficient is not necesarily a monotonically increasing function of temperature, the extremals of of absorption length within any sector do not always correspond to the values at sector boundaries ψ and $\psi + \Delta\psi$. Therefore, a third computation of $(\overline{KR})_{n,j,\phi}$ was made within each sector at $\phi = \psi + \Delta\psi/2$. The smallest and largest of these were used for computing interior transmissivities $(\tau_{n,j})_{I,LL}$ and $(\tau_{n,j})_{I,UL}$ respectively from Eq. (2.12).

2.5 EMISSIVITY CALCULATIONS

Radiation from the exterior and interior surfaces of each constant temperature annulus was also considered separately. Emissivity of the exterior surface was obtained by modifying the limits on the absorptivity integral for a complete cylinder. At the interior surface emissivity was obtained using a modification of the transmissivity calculation already discussed.

The basis for calculating emissivity of the exterior surface is the integral expressing absorptivity of an infinitely long gaseous cylinder relative to an element of its surface. The integral is given by Jakob (Ref. 9)as

$$\alpha = \frac{k}{\pi} \int_{-\pi/2}^{+\pi/2} \int_{-\pi/2}^{+\pi/2} \cos^2 \chi \cos \psi \left[\int_0^L e^{-kr} dr \right] d\chi d\psi \tag{2.16}$$

where ψ is defined in Fig. 2.6 and χ is the angle between the vertical and L measured in a plane passing through the surface element normal to the plane of Fig. 2.6.

Instead of evaluating the complete double integral, a closed form solution was obtained for the case where kL is sufficiently small that the inner integral reduces to

$$\int_0^L e^{-kr} dr \cong L \qquad kL << 1 \tag{2.17}$$

This solution was extended to optically denser conditions using the mean beam length concept (Ref. 10).

Replacing the cylinder by a cylindrical annulus, Fig. 2.6, only the unshaded part of the annulus is considered because radiation which passes through the hollow is included in the emissivity of the interior surface. The integration of Eq. (2.16) over ψ must therefore be performed in two steps:

$$0 \le \psi \le \beta : L = \frac{r_j}{\cos \chi} \left[\cos \psi - \sqrt{\sin^2 \beta - \sin^2 \psi} \right] \tag{2.18a}$$

$$\beta \le \psi \le \frac{\pi}{2} : L = \frac{2 r_j \cos \psi}{\cos \chi} \tag{2.18b}$$

where β is the angle at which L is tangent to the inner surface and is related to the ratio of annulus radii by

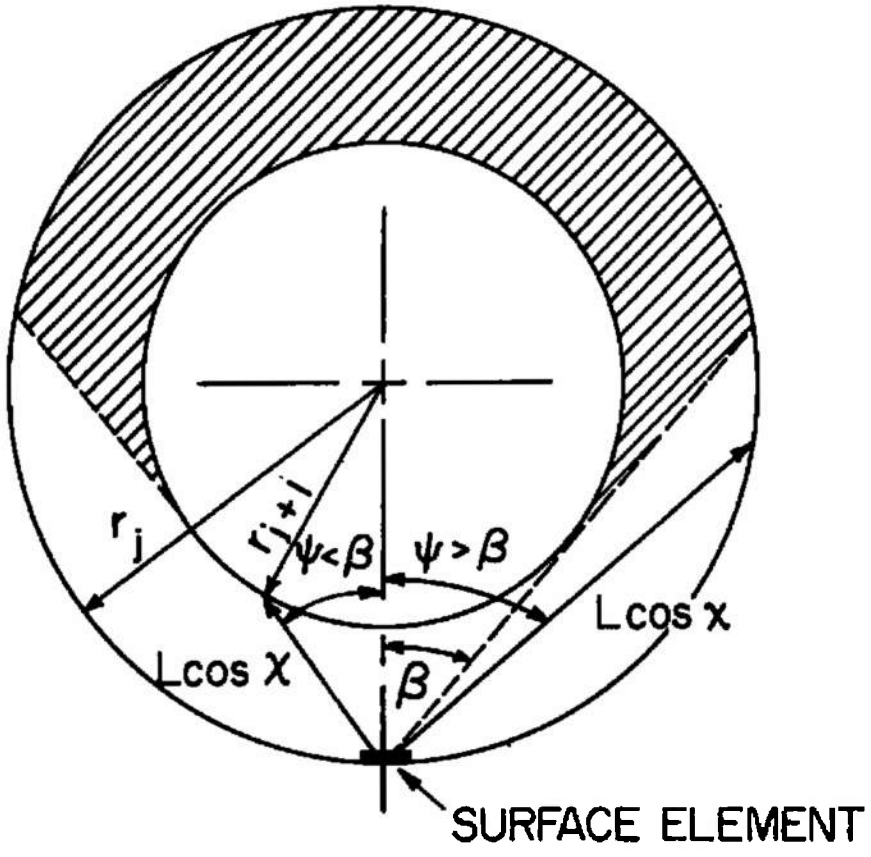

Figure 2.6 Absorption Paths for Calculation of Exterior Emissivity from an Infinitely Long Cylindrical Annulus. Only the Unshaded Part of the Annulus is Directly Visible to the Surface Element.

$$\sin \beta = \frac{r_{j+1}}{r_j} \tag{2.19}$$

Combining Eqs. 2.16, 2.17 and 2.18 the absorptivity of an annulus can be expressed by

$$\alpha_j = \frac{2kr_j}{\pi} \left[\int_{-\frac{\pi}{2}}^{+\frac{\pi}{2}} \cos \chi \, d\chi \right] x \tag{2.20}$$

$$\left[\int_0^{\beta} \left(\cos \psi - \sqrt{\sin^2 \beta - \sin^2 \psi} \right) \cos \psi \, d\psi + 2 \int_{\beta}^{\pi/2} \cos^2 \psi \, d\psi \right]$$

Integrating and dividing by $2kr_j$, which is the limiting absorptivity of a cylinder of radius r_j

$$\frac{\alpha_j}{2kr_j} = \left[1 - \frac{\sin^2 \beta}{2} - \frac{\beta}{\pi} - \frac{\sin 2\beta}{2\pi} \right] \tag{2.21}$$

Equation (2.21) is plotted in Fig. 2.7. If the factor 2 is changed to 1.9, the mean beam length of a cylinder is obtained and the absorptivity over the range from optically thin to black body is given within $\pm 5\%$ (Ref. 10) by

$$\alpha = \left[1 - \exp \left(-1.9 \, kr_j \right) \right] \tag{2.22}$$

Combining Eqs. (2.21) and (2.22) and noting that the assumption of local equilibrium implies $\alpha = \epsilon$, the following expression for "exterior" emissivity $(\epsilon_{j,n})_E$ results

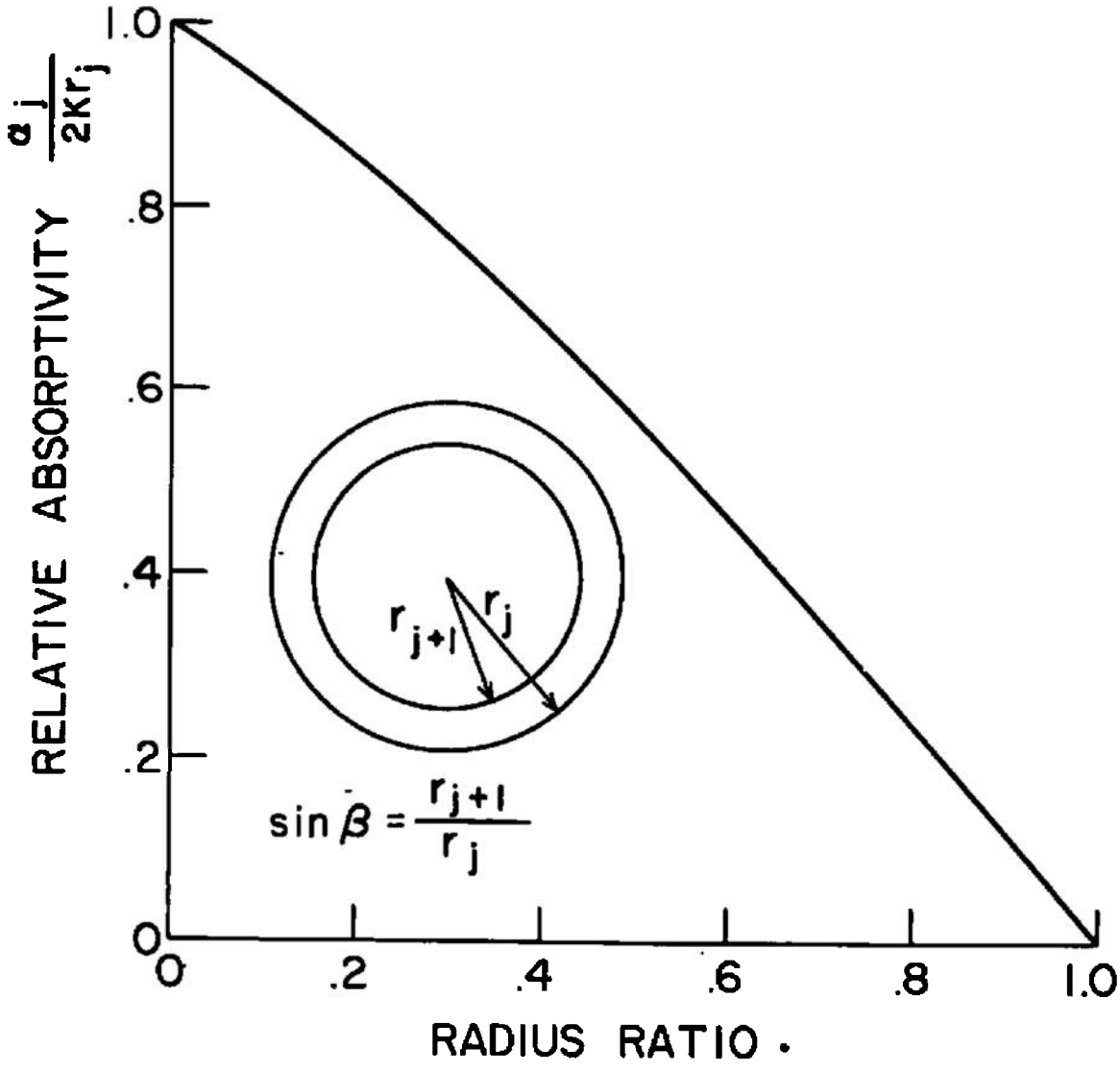

Figure 2.7 Absorptivity of a Cylindrical Annulus Relative to Absorptivity of a Cylinder (both infinitely long).

$$\left(\epsilon_{j,n}\right)_E = 1 - \exp\left[-1.9\, k_n r_j \left(1 - \frac{\sin^2\beta}{2} - \frac{\beta}{\pi} - \frac{\sin 2\beta}{2\pi}\right)\right] \tag{2.23}$$

Equation (2.23) includes the emissivity of the cylindrical core as the special case $\sin\beta = 0$.

The interior emissivity of an annulus is identical with the absorptivity of a single annulus relative to a radiating element at its inner surface. The sum of absorptivity and transmissivity is unity so transmissivity of a single annulus can be calculated from Eq. (2.12) using absorption lengths given by

$$(\overline{kR}) = (k_{n,j})\,(R_{j+1,\phi,j}) \tag{2.24}$$

The arithmetic mean of the upper and lower limits on τ was used to calculate interior emissivity

$$\left(\epsilon_{n,j}\right)_E = 1 - \frac{\tau_{UL} + \tau_{LL}}{2} \tag{2.25}$$

2.6 COMPLETE EXPRESSION FOR RADIANT HEAT FLUX

Radiant heat flux, expressed as power per unit surface area of arc column boundary, may now be written as a double summation of terms like Eq. (2.2), each multiplied by the appropriate transmissivity

$$q/A = \sigma \sum_n \left\{ \left[\sum_{j=1}^{m} T_j^4 \left(\frac{r_j}{\delta}\right)\left(\eta_{n,j}\right)\left(\tau_{n,j}\right)_E \left(\epsilon_{n,j}\right)_E \right] + \left[\sum_{j=1}^{m-1} T_j^4 \left(\frac{r_{j+1}}{\delta}\right)\left(\eta_{n,j}\right)\left(\tau_{n,j}\right)_I \left(\epsilon_{n,j}\right)_I \right] \right\} \tag{2.26}$$

The radius of the arc column is δ, m is the number of constant temperature subdivisions (core plus annuli) and τ and ϵ are given by Eqs. (2.13), (2.23) and (2.25). Black body energy fraction, η, is proporational to the integral of the Planck radiation function over each wavelength interval Δn. Methods used for calculation of η are discussed in Appendix A.

2.7 CONSTRICTED ARC WITH NON BLACK WALLS

As pointed out in Section 2.1 the arc chamber wall will have a low reflectivity (high emissivity). However, wall emissivity will not be unity* as has been assumed thus far, and a means of evaluating its effect on the magnitude of the radiant heat flux actually absorbed by the wall is desirable.

A complete calculation of the radiant interchange between the arc and the constrictor walls adds a very substantial complication to the analysis already presented and, in addition requires data on the frequency and angular dependence of wall surface emissivity. Fortunately the effect of a non-black wall can be accounted for quite closely in the following way.

Radiant interchange between a non-black wall and a radiating gas can be expressed, following Eckert (Ref. 10)

$$(q/A)_i = - B_i + \sum_k F_{i-k}(1 - \alpha_{i-k,g})\, B_k + (q/A)_g \qquad (2.27)$$

where $(q/A)_i$ is the net radiant flux density absorbed at surface i, B_i and B_k are the total radiant flux densities leaving surface i and surface k respectively, F_{i-k} is a view factor between surface i and each surface k, $\alpha_{i-k,g}$ is the absorptivity of the gas between surface i and each surface k as determined by integration over the solid angle corresponding to the particular F_{i-k}, and $(q/A)_g$ is the radiant flux density from the gas incident on surface i. Equation 2.27 expresses the net radiant flux density to surface i as the algebraic sum of radiant flux density leaving surface i, radiant flux density arriving from surfaces k and radiant flux density from the gas.

*McAdams (Ref. 17) gives a total normal emissivity of 0.57 for a copper "plate heated at 1110°F".

Let surface i be an infinitesimal element of the chamber wall and consider as a single surface k the remainder of the infinitely long cylindrical arc chamber wall. Then

$$(q/A)_g = (q/A)_a \frac{\delta}{R_c} \tag{2.28}$$

where $(q/A)_a$ is the radiant flux density from the arc as given by Eq. 2.26 and R_c is the constrictor radius. Also

$$B_i = B_k = B_w \tag{2.29}$$

$$F_{i-k} = 1 \tag{2.30}$$

$$\sum_k F_{i-k}(1 - \alpha_{i-k,g}) B_k = (1 - \alpha_{w,g}) B_w \tag{2.31}$$

where B_w is the radiant flux density leaving the wall at any point and $\alpha_{w,g}$ is the "average" absorptivity of the gas between surface element i and all other parts of the wall surface. Further, defining B'_w as the total radiant flux density incident on the wall at any point we can write, where ϵ_w is the emissivity of the wall

$$B_w = \epsilon_w \sigma T_w^4 + (1 - \epsilon_w) B'_w \tag{2.32}$$

By definition

$$(q/A)_w = B'_w - B_w \tag{2.33}$$

so that, neglecting radiation at wall temperature,

$$B_w = \frac{1 - \epsilon_w}{\epsilon_w} (q/A)_w \tag{2.34}$$

Combining eqs. 2.27, 2.28, 2.31 and 2.34 we obtain

$$\frac{(q/A)_w}{(q/A)_a \left(\frac{\delta}{R_c}\right)} = \frac{1}{1 + \alpha_{w,g} \left(\frac{1 - \epsilon_w}{\epsilon_w}\right)} \tag{2.35}$$

which has been plotted as Fig. 2.8.

The quantity $\alpha_{w,g}$ is an "average", over all frequencies and angles, of the absorptivity of the gas relative to radiation which has been reflected one or more times from the constrictor wall. Reflection may itself vary with frequency and angle, and multiple relfection will be more likely at those frequencies at which gas absorption is relatively low. However, if the arc fills the constrictor, $\alpha_{w,g}$ cannot differ greatly from the average emissivity of the arc column and, as arc radius becomes small compared to wall radius, $\alpha_{w,g}$ approaches zero. A reasonable estimate of $\alpha_{w,g}$ and Fig. 2.8 shows that the correction is relatively insensitive to the precise value of $\alpha_{w,g}$, particularly for the relatively high values of emissivity expected in practice.

All results in Sections 3, 4, and 5 are presented in terms of heat flux from the arc and a wall emissivity correction may be applied as required.

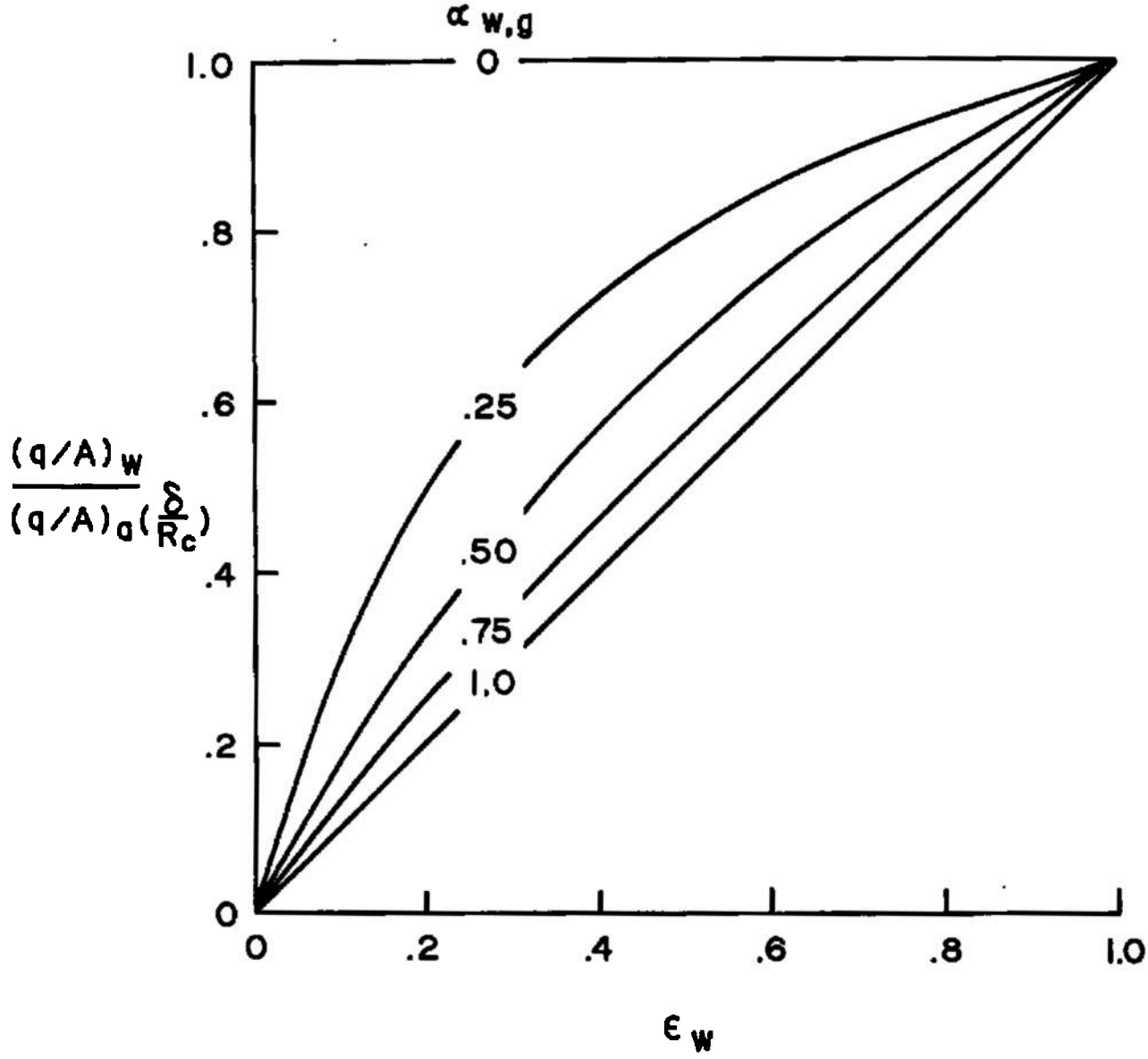

Figure 2.8 Influence of Arc Chamber Emissivity on Radiant Heat Transfer.

SECTION III

DIGITAL COMPUTATION

3.1 PROGRAM ARCRAD

The FORTRAN computer program which enabled an IBM 7090 digital computer to produce solutions to Eq. 2.23 is called ARCRAD and is included as Appendix B. It requires as input information the temperature, density and inner and outer radii of each annulus, absorption coefficient data and some programming data discussed in Appendix B. Its standard output includes

1. A repeat of the temperature-density-radius input.

2. Radiant flux density based on upper and lower limit transmissivities tabulated by wavenumber interval and also summed over all wavenumbers.

3. Radiant flux density with all transmissivities set equal to unity, again both tabulated by wavenumber interval and summed.

4. Optionally, an output tape which can be converted automatically to a graph of tabulations 2) and 3) above.

3.2 LIMITS ON FREQUENCY RANGE OF CALCULATIONS

Although radiant energy is distributed throughout the electromagnetic spectrum, all but a negligible fraction is contained within rather narrow limits which are a function of temperature. These limits are conveniently expressed in terms of a parameter v defined as

$$v = \frac{c_2 n}{T} \tag{3.1}$$

where c_2 is Planck's second radiation constant and is equal to 1.4380 cm-°K. For a black body radiating at a given temperature, only 0.25% of the total energy is radiated at frequencies corresponding to $v < 0.3$ or to $v > 13$.. Therefore the only energy considered was that at frequencies (wavenumbers) bracketed by the above values of v. Figure 3.1 shows these limits, along with the curve $v = 1$, which was the dividing line for application of two different methods for calculating η (see Appendix A).

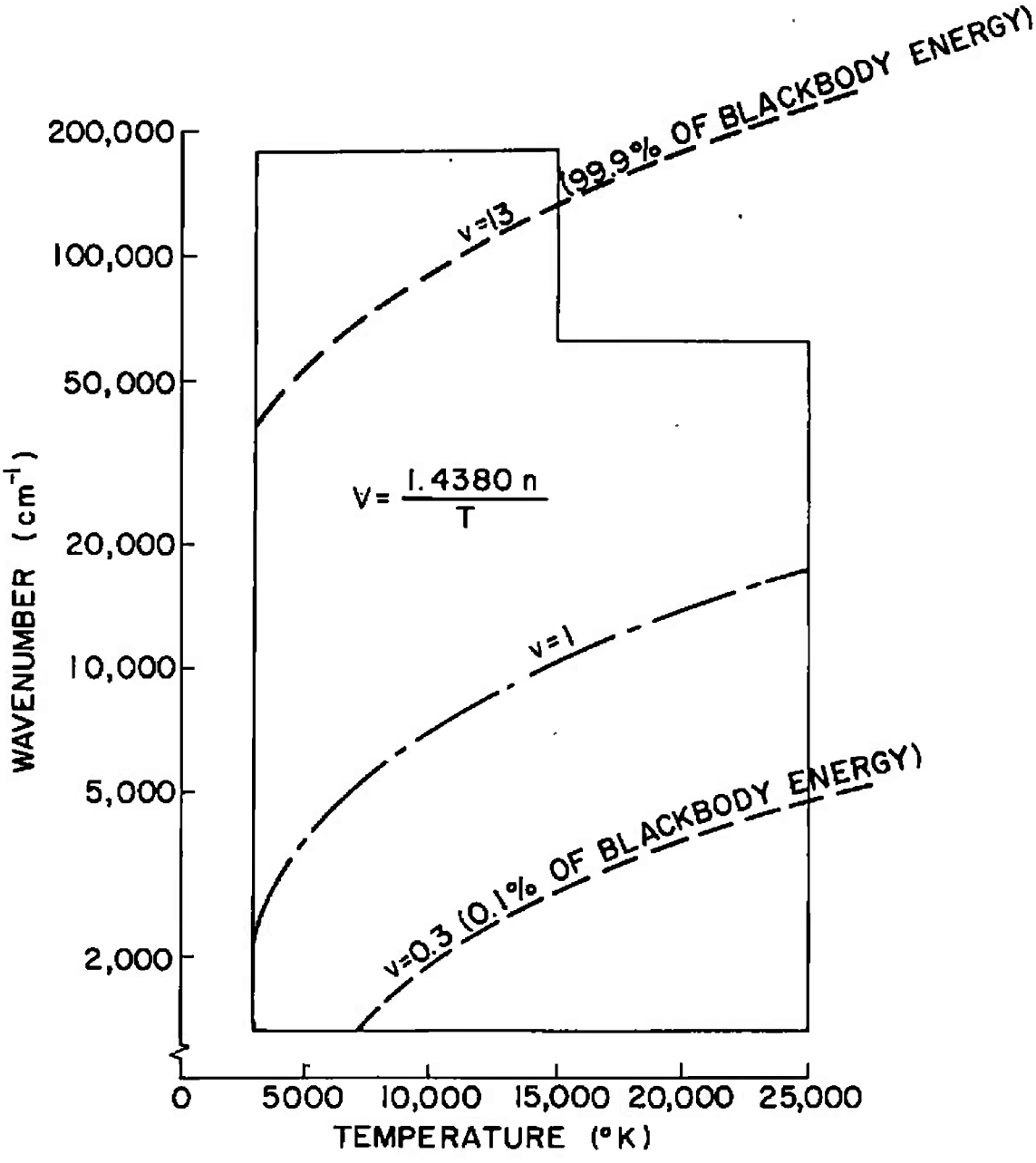

Figure 3.1 Frequency and Temperature Ranges of Spectral Absorption Coefficient Data. The Solid Outline Represents Available Data.

The solid outline of Fig. 3.1 represents the range of temperature and frequency of the Breene and Nardone results (Refs. 1, 2) plus additional as yet unreported work. Data above 61,500 cm^{-1} are not precise but are known to provide an upper bound within a factor of 2. Temperatures near the centerline on the measured profiles exceeded the 15000°K upper limit on available high frequency data. An upper bound on the possible contribution in the high frequency range was therefore established by considering annuli at temperatures above 15000°K to be black bodies in the wavenumber range for which data was not available.

$$(q/A)_{HF} = \sigma \sum_{j=j_{16,000}}^{m} T_j^4 \left(\frac{r_j}{\delta}\right) (D_{61,5000})_j \qquad (3.2)$$

where D is defined by Eq. A.2 and is here the fraction of black body energy above 61,5000 cm^{-1}. The dependence of $D_{61,500}$ on temperature is shown in Fig. 3.2. Both D and (r/δ) are generally small in this case so use of the upper bound does not greatly increase the uncertainty of the results.

3.3 PRELIMINARY PROCESSING OF ABSORPTION COEFFICIENT DATA

The Breene and Nardone data from 1300 cm^{-1} to 62,000 cm^{-1} is recorded on magnetic tape but the tape contains much information extraneous to this study and the absorption coefficients are tabulated at unnecessarily fine frequency intervals. A preliminary processing of these tapes was therefore necessary to obtain a data tape containing linear absorption coefficients tabulated at 500 cm^{-1} intervals.

Data above 62,000 cm^{-1} was available only in printed form so punched cards were prepared which were then converted to magnetic tape. The wavenumber interval was increased to 1000 cm^{-1} because at higher frequencies a given increment represents a smaller fraction of the total energy.

3.4 TEMPERATURE AND DENSITY PROFILES USED IN COMPUTATION

As has been stated, temperature distribution in the arc column is presumed known. With the assumption of local thermal equilibrium

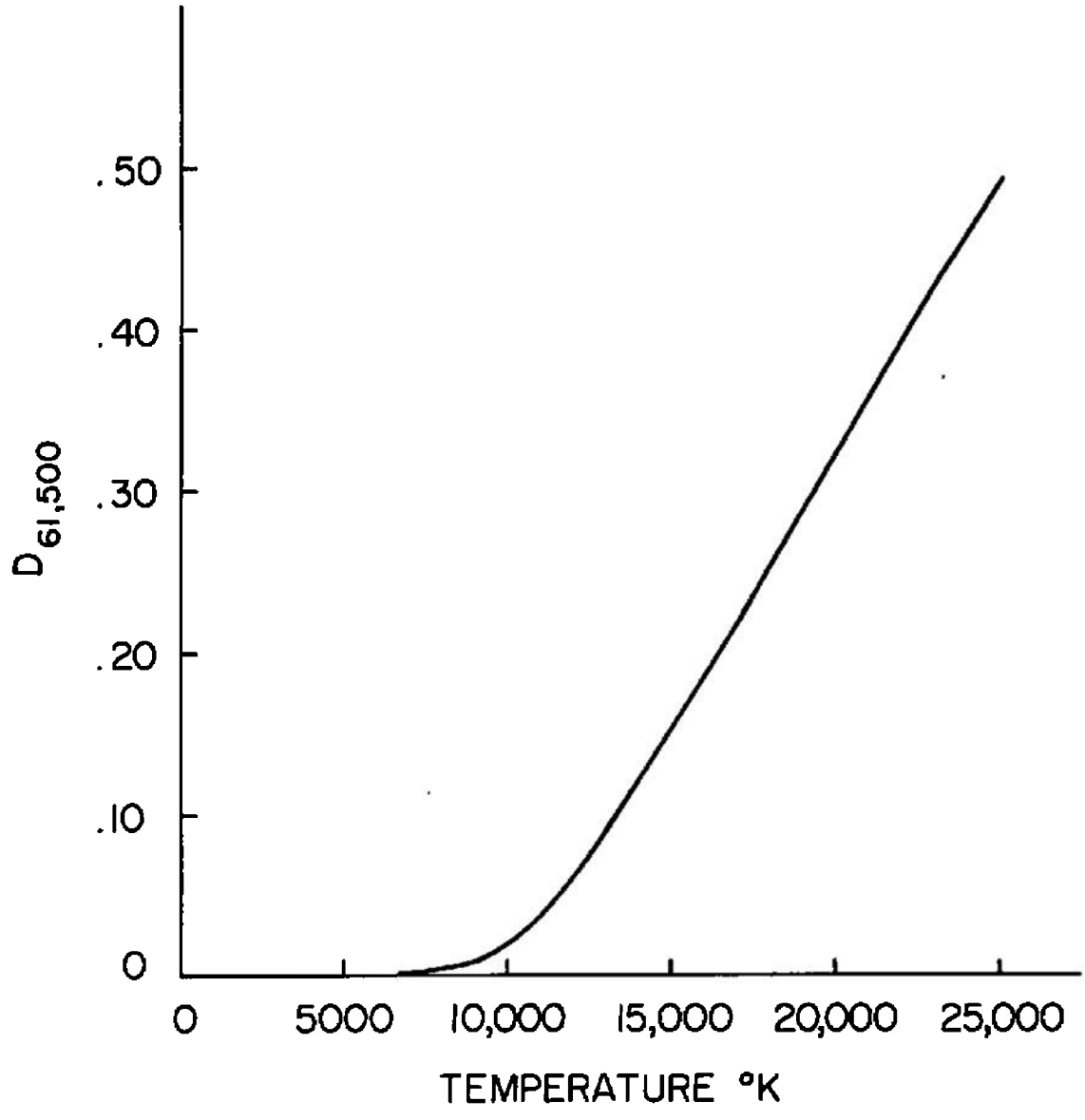

Figure 3.2 Fraction of Black Body Energy Emitted at Wave Numbers Greater Than 61,500 cm^{-1}.

and a given pressure level, the density distribution can then be determined from a table or chart of thermodynamic properties. A limited amount of temperature profile data was available from direct spectroscoptic measurement (see Section 5.2 for further discussion) which provided a basis for comparison of results with direct measurements of radiant heat flux.

Based on the results of direct measurements plus application of reasonable boundary conditions, a series of simple analytic (polynomial) profiles were also used for computation. These profiles were chosen to provide a systematic comparison of the effect on radiant heat flux of temperature level and fullness of the temperature profile. These analytic profiles, shown in Fig. 3.3 along with a profile, measured by Maecker, (Ref. 6) were of the form

$$\frac{T - T_{ref}}{T_{CL} - T_{ref}} = 1 - \left(\frac{r}{\delta}\right)^{x} \tag{3.3}$$

The spectral absorption coefficient data were tabulated at temperature intervals of 1000°K and decade density intervals. In order to avoid double interpolation for temperature and density, the thickness of each annulus was selected in such a way that the weighted avarage temperature of each annulus was a tabulated temperature, see Appendix C. Absorption coefficients were then interpolated logarthmically with density. Calculation of weighted average annulus temperatures requires a polynomial representation of the temperature profiles so measured profiles were reduced to this form using a modification of a standard least squares polynomial curve fit program, Appendix D.

3.5 TRANSMISSIVITY APPROXIMATION

Numerical evaluation of the integral appearing in Eq. 2.12 leads to the curve of Fig. 2.2 with $(\overline{kR})_{n,j,\phi}$ as a parameter. Rather than perform the numerical integration for each different $(\overline{kR})_{n,j,\phi}$ empirical approximations were used in Program ARCRAD which took advantage of the similarity of Fig. 2.2 to a simple exponential decay. The approximations were made over three regions as follows:

1) $0 \leq \overline{kR} \leq 1.1 \qquad \tau = \exp -1.206\,(\overline{kR})$

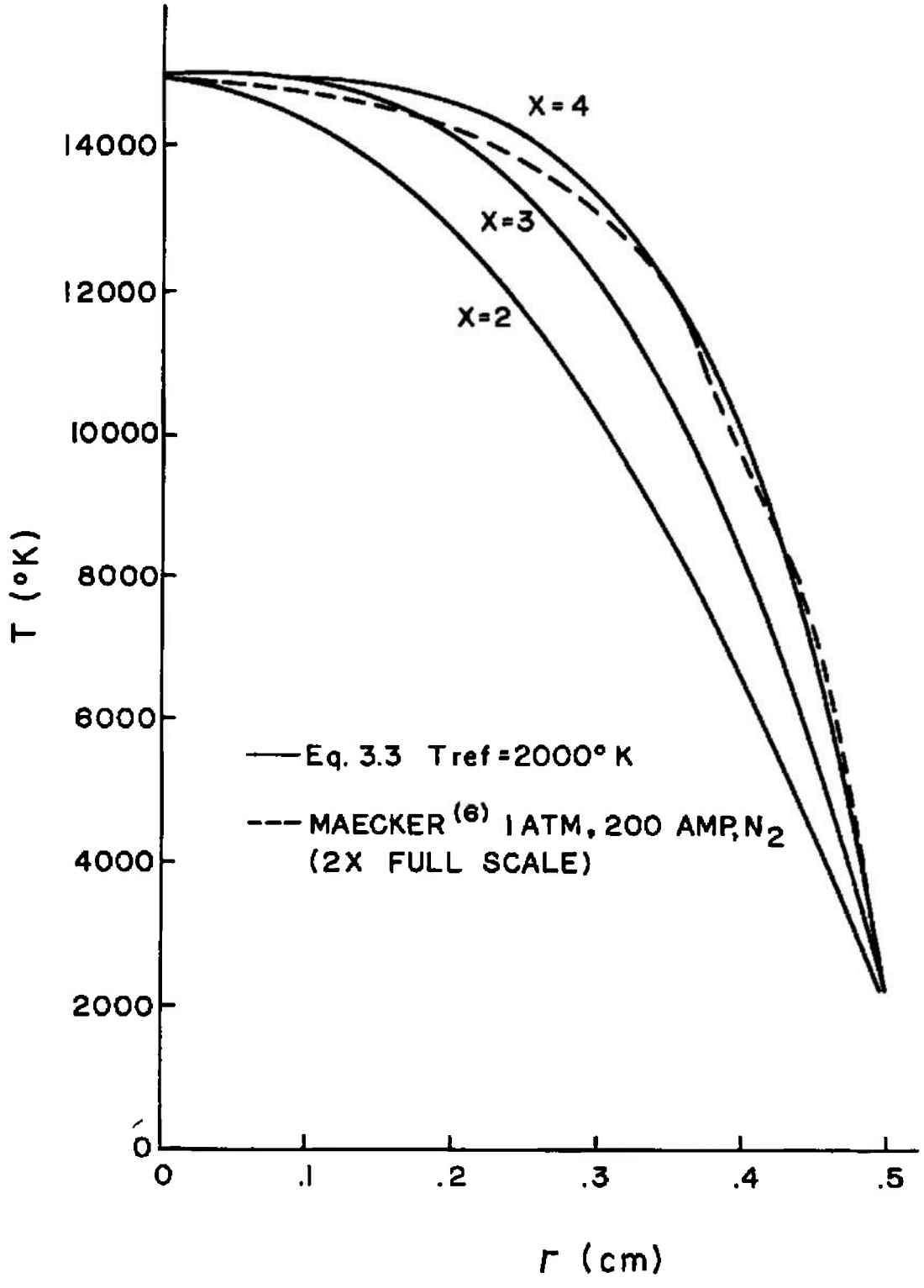

Figure 3.3 Arbitrary Polynomial Profiles and a Nitrogen Profile Measured by Maecker.

2) $1.1 < \overline{kR} \leq 16$ $\quad \tau = \{\exp[-1.206\,(\overline{kR})]\}\{1.0774 - .09539\,(\overline{kR})$

$$+ .055577\,(\overline{kR})^2 - .004291\,(\overline{kR})^3$$

$$+ .00020826\,(\overline{kR})^4\}$$

3) $\overline{kR} > 16$ $\quad \tau = 0$

Introduction of this approximation resulted in roughly halving the computer time per case.

SECTION IV
COMPUTER RESULTS

4.1 WAVENUMBER RANGE OF RESULTS

Because of the limitations on available data discussed in Section 3.2, curves presenting results of calculation are labeled as follows to indicate the wavenumber range they cover

Label	Meaning	Wavenumber Range (cm^{-1})	Temperature Range (^{o}K)
LF	Low Frequency	up to 61,5000	3,000 - 25,000
HF	High Frequency	61,500 and up	9,000 - 15,000
BBL	Black Body Limit given by Eq. 3.2	61,500 and up	16,000 - 25,000

Table 4.1 - Frequency Range of Results

As will be discussed in Section 5.4 the break at 61,500 cm^{-1} is also convenient from the standpoint of comparisons with experimental measurements since this frequency is just about the cutoff frequency of the fused quartz window used to protect the radiant heat flux gage.

4.2 CONVERGENCE OF UPPER AND LOWER BOUNDS

The computational model described in Section 2 of this report was designed to bracket the effect of self absorption on radiant heat flux from an arc column. The effectiveness of this approach depended on just how close to each other were the upper and lower bounds and this could not be established without actually performing some numerical calculations.

As originally conceived and proposed, the absorption model postulated a lower limit on absorption (maximum radiant heat flux) in which all radiation was considered to be "exterior" in the sense of section 2.3. For this case the absorption paths were represented by half-cylinders whose radii were equal to the difference between annulus outside radii and the arc column boundary radius. The upper limit on absorption (minimum radiant heat flux) was established by assuming

all radiation to be "interior" and absorbed by half-cylinders whose radii were equal to the sums of the annulus radii and the arc column boundary radius. Results with this model gave an upper bound practically indistinguishable from the optically thin case and a lower bound which was lower by an order of magnitude.

A second computational model was then developed, as described in detail in Section 2. Division of the half cylinders into sectors and separate calculation of "exterior" and "interior" radiation for both upper and lower bounds greatly reduced the spread between them. By retaining the number of sectors as variable, more sectors could be used at higher pressures, where the spread is large, than are needed at lower pressures.

The additional flexibility achieved by retaining the number of sectors as a variable can be used in two ways. Figure 4.1 illustrates the effect of varying the number of sectors while keeping all else constant. Within the limits of roundoff error, increasing the number of sectors improves the approximation. A price is paid of course, in additional computer time. The form of convergence indicates that an average of upper and lower bound calculations will give an excellent approximation to the "exact" result.

In addition to justifying an average of the two limit calculations as representative of the "exact" result, Fig. 4.1 is a useful guide to economic choice of the number of sectors. At pressures equal to or greater than 100 atm, s was set equal to 3. Below 100 atm a value of s=2 sufficed.

4.3 RESULTS WITH ASSUMED TEMPERATURE PROFILES

If one starts with the postulate that the arc column is axially symmetric and that the temperature decreases monotonically from a peak at the centerline to some relatively low temperature at the outermost radius, than the general shape of the profile is reasonably well determined. This is true even though local bumps may exist due to changes in ionization level or other phenomena.

Let us define a full profile as one in which arc temperature remains near arc centerline temperature until very near the outer boundary. Fullness is dependent on details of the local energy balance and is therefore certain to change with, for example, changes in the relative importance of the conduction and radiation modes of heat loss to the boundary.

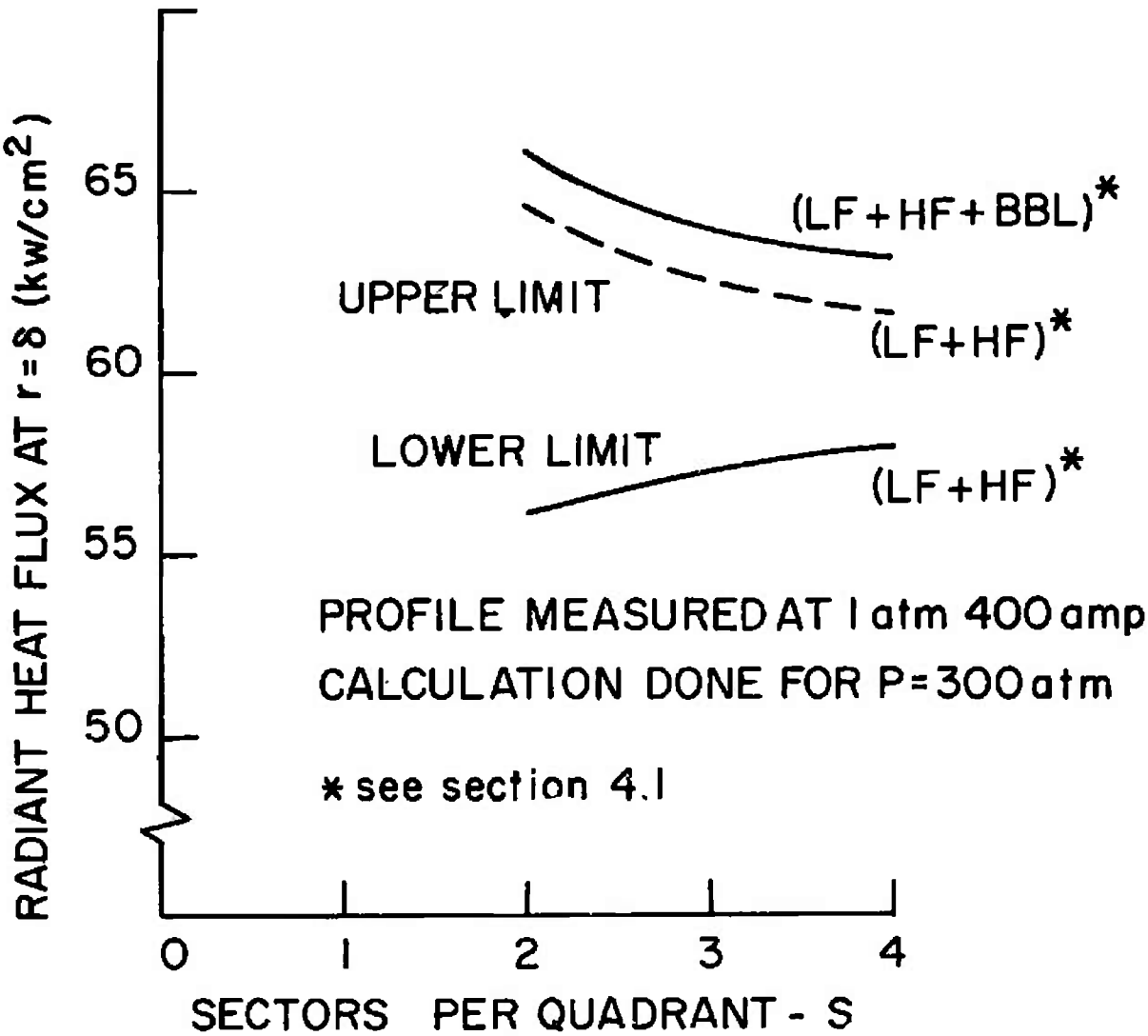

Figure 4.1 Convergence of Upper and Lower Limit Calculations as Number of Sectors Increases.

The family of curves given by Eq. 3.3 satisfies the aforementioned postulates and contains a single parameter, the exponent x, to characterize the fullness. The effect of fullness may then be judged by a plot such as Fig. 4.2 which shows radiant flux density vs. x at 3 pressure levels. Fig. 4.2 also shows, for comparison, the asymptotic value which each curve approaches as x becomes very large. The asymptotes were computed assuming a cylinder of gas uniformly at centerline temperature. The limiting case of a blck body at centerline temperature is also included. Lacking knowledge of temperature profiles at the higher pressures, these curves help narrow the possible range of radiant flux densities and will be more useful if and when more becomes known about temperature profiles at high pressure.

The sensitivity of radiant heat flux to temperature was investigated for a sequence of profiles of the form of Eq. 3.3 (with x=3) in which centerline temperature was varied from 12,000 to 15,000°K, Fig. 4.3. Over the range calculated the radiant heat flux increases approximately as the 8.4 power of arc column centerline temperature at 100 atm and below.

4.4 SENSITIVITY TO CHANGES IN OUTER RADIUS

Weber's estimates of constricted arc column growth (Ref. 12) indicate that the arc may not entirely fill the constrictor of the arc heater used in the experimental work. Temperature could not be measured over the entire column, so for one of the measured profiles, Fig. 5.4, two different outer edge parabolas were matched to the polynomial which was fitted to the data (in this case also a parabola). The part of the profile for which data existed was unchanged and the sensitivity of the calculation to changes in the outer part of the profile was checked in this way. Comparison made on the basis of heat flux at the constrictor wall (0.5 cm radius) indicated that exact arc column diameter made little difference, Table 4.2.

Because only the outer few annuli were changed this result does not contradict Fig. 4.2 where the entire profile was systematically varied.

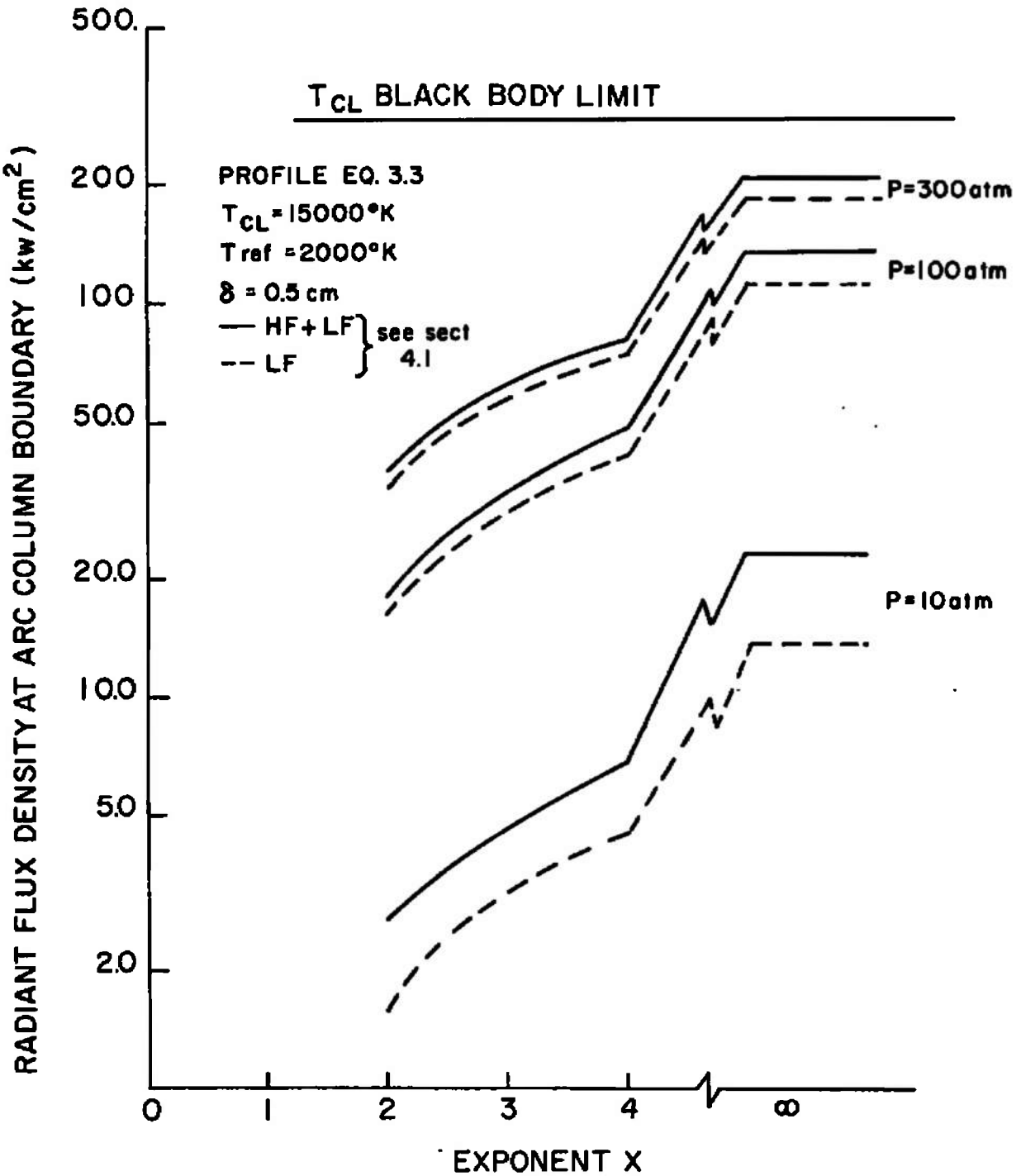

Figure 4.2 Effect of Profile Fullness on Radiant Flux Density.

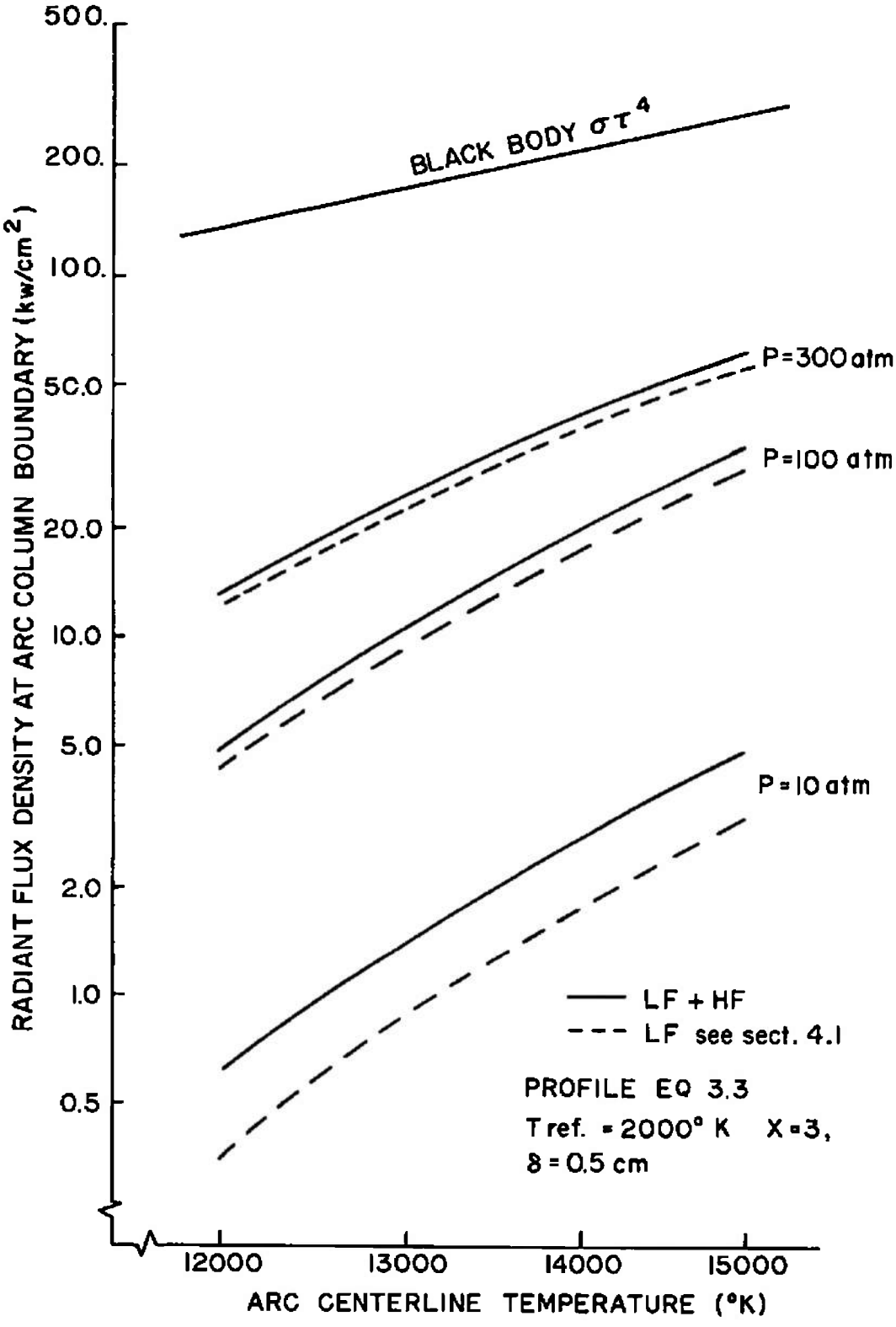

Figure 4.3 Temperature Level Dependence of Arc Radiant Heat Flux.

Pressure (atm)		Radiant Flux Density at 0.5 cm radius (kw/cm^2)	
		δ = .35 cm	δ = .5 cm
1	HF	.44	.62
	LF	.18	.20
	SUM	.62	.82
2	HF	.88	.93
	LF	.55	.59
	SUM	1.43	1.52
10	HF	1.87	1.65
	LF	4.62	4.88
	SUM	6.49	6.53
100	HF	2.5	3.2
	LF	45.1	45.6
	SUM	47.6	48.8

Table 4.2 - Radiant Flux Density at Constrictor Boundary
2.4 atm 455 amp measured profile

4.5 QUASI-THIN MODEL AND FREQUENCY DISTRIBUTION

The quasi-thin model was obtained by setting all transmissivities equal to unity in Eq. 2.26. Because the computation of emissivities takes into account self absorption within each annulus, the quasi-thin model will yield a radiant heat flux known to be closer to the true value than the optically thin model. The extent of the difference between quasi-thin and optically thin depends on the magnitude of the dimensionless absorption lengths associated with each annulus, so choice of number of annuli will have an effect on the quasi-thin result. The quasi-thin result, however, is a very simple extra step for the computer and provides a useful indication of the importance of self-absorption.

As mentioned in section 3.1, an option in the program permits automatic plotting of radiant flux density in each wavenumber interval, both quasi-thin and self-absorbing, Fig. 4.4. In general the higher the intensity of radiation the greater the difference between self-absorbing and quasi-thin.

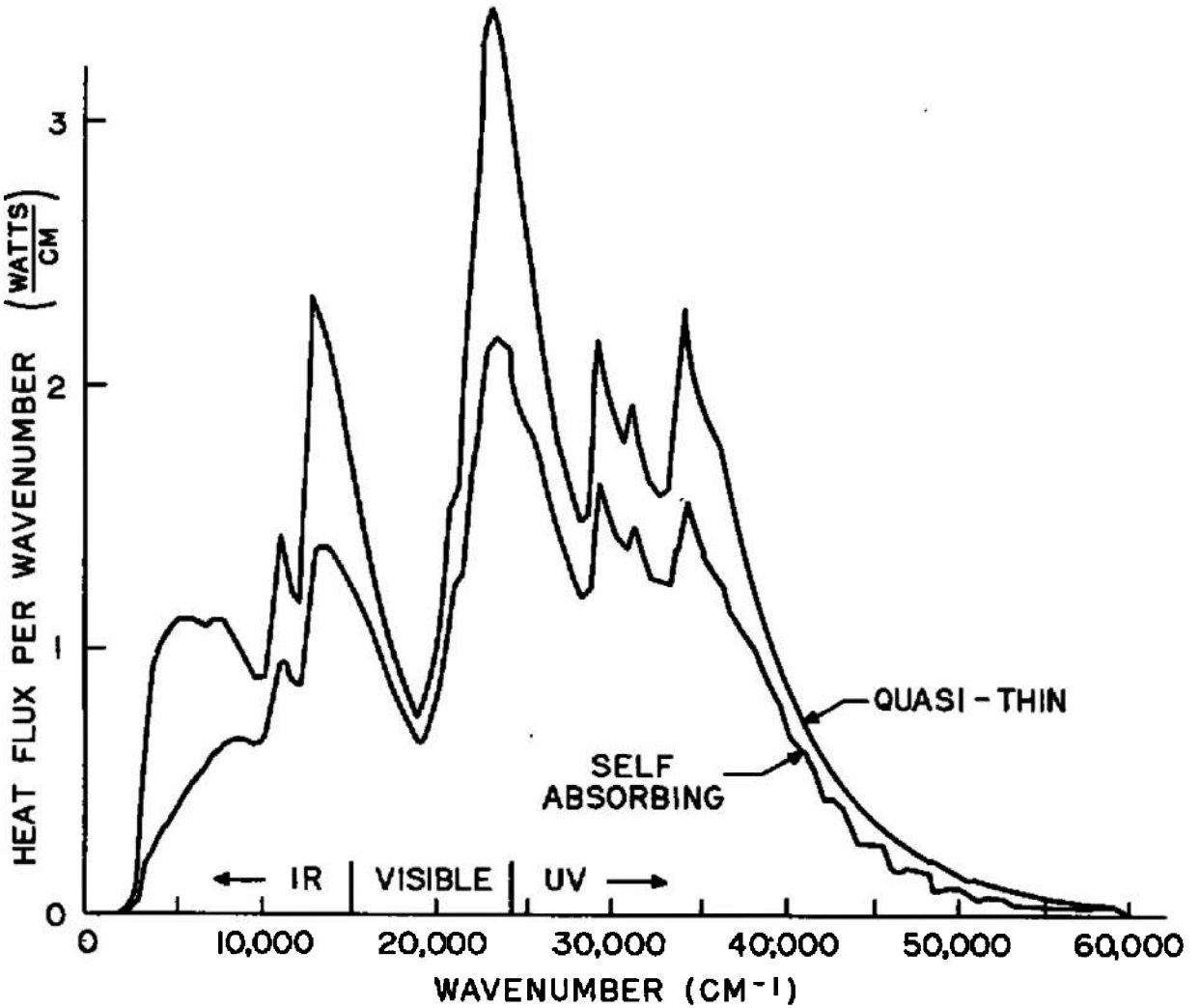

Figure 4.4 Frequency Distribution of Radiant Heat Flux. Arc Profile Measured at 2.4 atm, 455 amp. Computed at 100 atm.

4.6 TWO TEMPERATURE MODEL

In order to gain some idea of the effect of a body of heated plasma in reducing the intense radiation from the arc column proper, a two temperature cylindrical model, which is compatible with that discussed in section 2, was investigated. Figure 4.5 presents results with the arc at 16,000°K and the surronding plasma at 6,000°K with the dimensions investigated shown in the inset sketch. As pressure is increased, the shielding effect of the lower temperature surrounding plasma may be sufficient to cause the total radiant flux to pass through a maximum and then decrease somewhat. As pressure is increased the energy radiated by the cooler surrounding gas to the walls will continue to increase and the large equivalent radiating surface tends to magnify the increase. However, the fraction of energy reabsorbed from the arc column will also increase and the possibility that the latter effect could result in a net decrease in radiant flux to the walls in confirmed by Fig. 4.5. The calculation was repeated with the arc at 15,000°K in order to include the high frequency radiation, Fig. 4.6.

It must be emphasized that the existence of such an effect is controlled by geometry, operating conditions and arc behavior at high pressures -- all of which affect the temperature distribution and its (here neglected) pressure dependence.

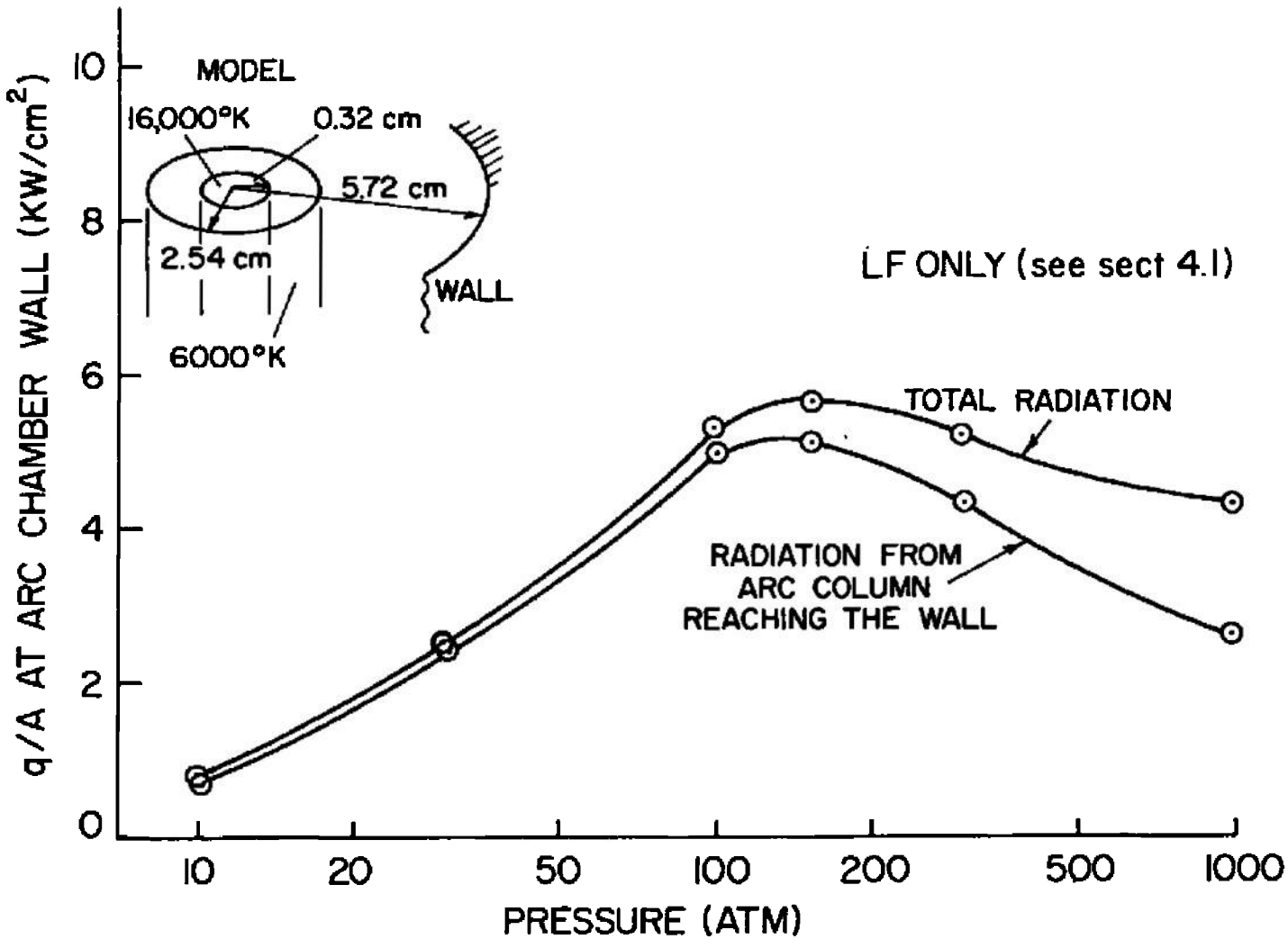

Figure 4.5 Reduction in Intensity of Radiation from a High Pressure by Surrounding Plasma - Two Temperature Model with Arc at 16,000°K.

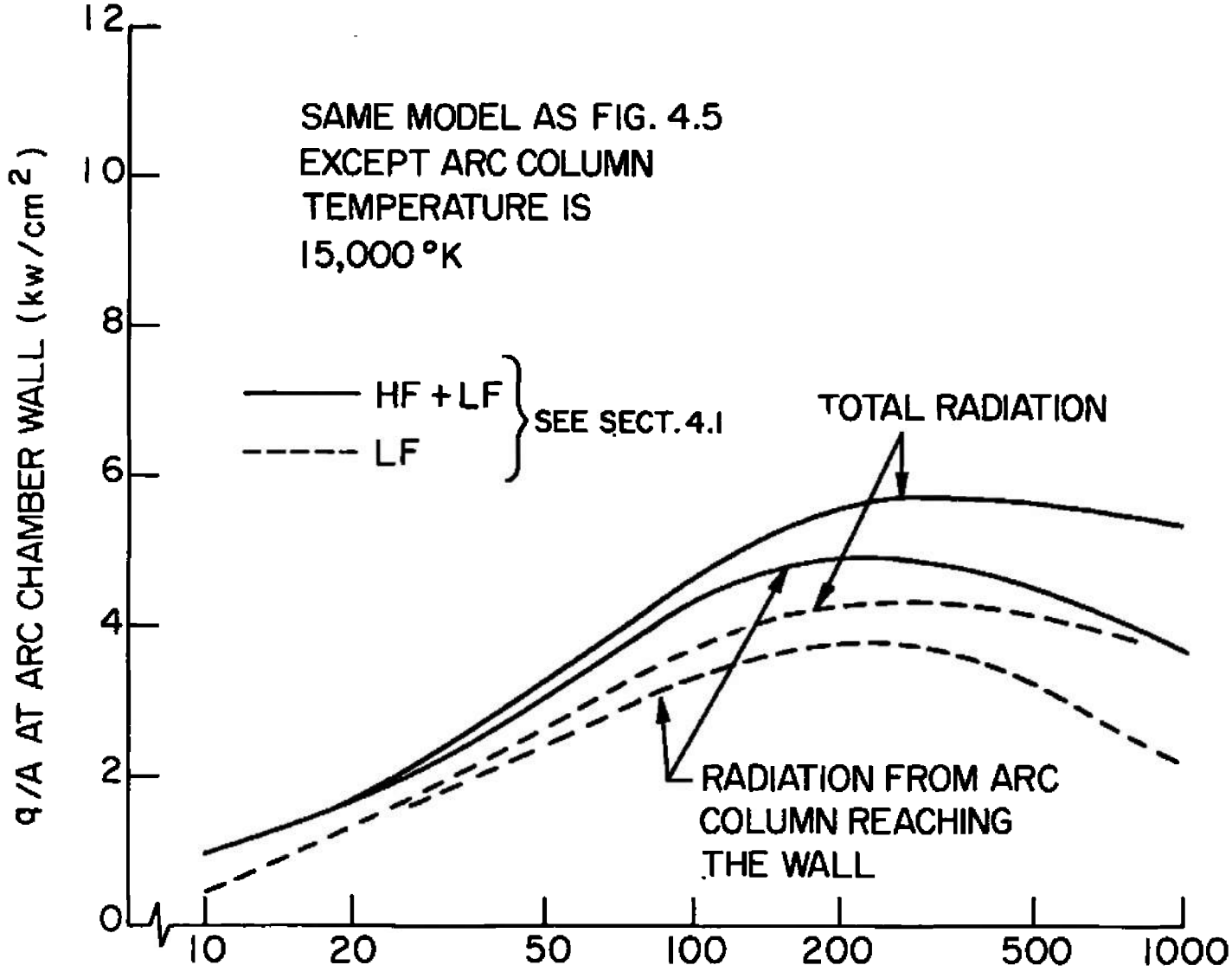

Figure 4.6 Two Temperature Model Including High Frequency Radiation with Arc at 15,000°K.

SECTION V
EXPERIMENTAL STUDY

5.1 OBJECTIVES

The objectives of the experimental work were:

1) measurement of temperature profiles for use as an input to the analysis.

2) measurement of total radiant heat flux to compare with results of the analysis.

5.2 ARC HEATER

The Gerdien type arc heater used for this study is shown in Fig. 5.1. This heater produces a uniform uncantaminated air plasma in a test section (constricted region) instrumented with voltage probes, a spectrographic observation window and a shuttered channel for radiation measurements. The heater has been more completely described in Ref. 8. The constrictor section can be replaced by a somewhat shorter non-constricting section which has a window for photographic observation.

Available power supply voltage limits maximum operating pressure in the unconstricted mode to 15 atmospheres although the heater is capable of withstanding higher pressures. The greater length of the constrictor section reduced the voltage limitation on pressure to about 5 atmospheres.

5.3 TEMPERATURE PROFILES AND CENTERLINE TEMPERATURES

Two temperature profiles were obtained at one atmosphere and one at 2.4 atmospheres. These are shown in Figs. 5.2, 5.3, and 5.4. The reason for two fitted curves in Fig. 5.4 was discussed in Section 4.4.

Relative intensities of several emission lines were used with Abel's integral equation to establish arc column temperature gradients. A description of the technique is included as Appendix E. Additional measurements of arc centerline temperature were made at 2.2 atmospheres and several current levels as shown in Fig. 5.5. These are based on average intensities in a narrow slice through the center of the arc. Therefore evaluation cannot make use of Abel's integral

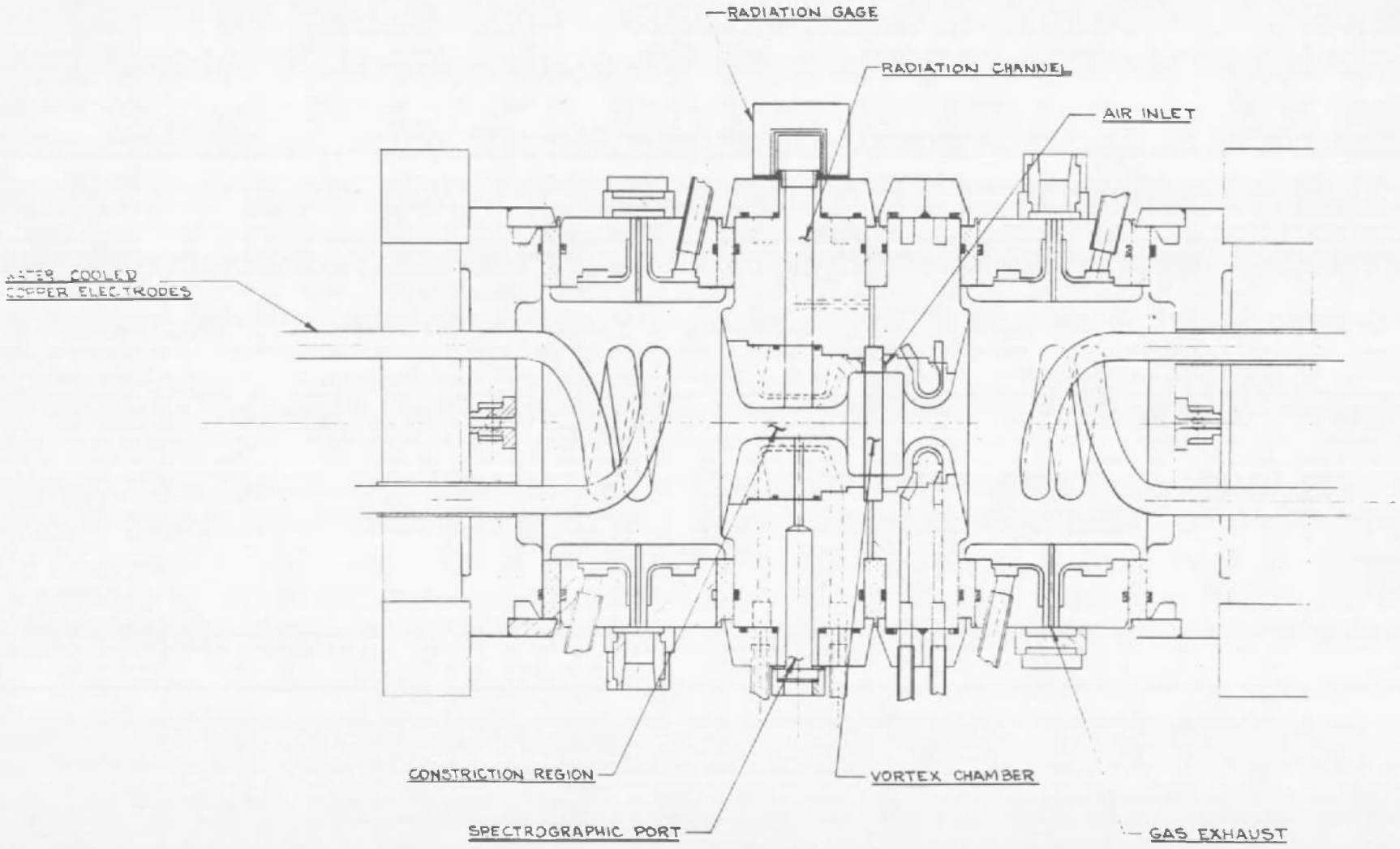

Figure 5.1 High Pressure Air Arc-Constructed Column.

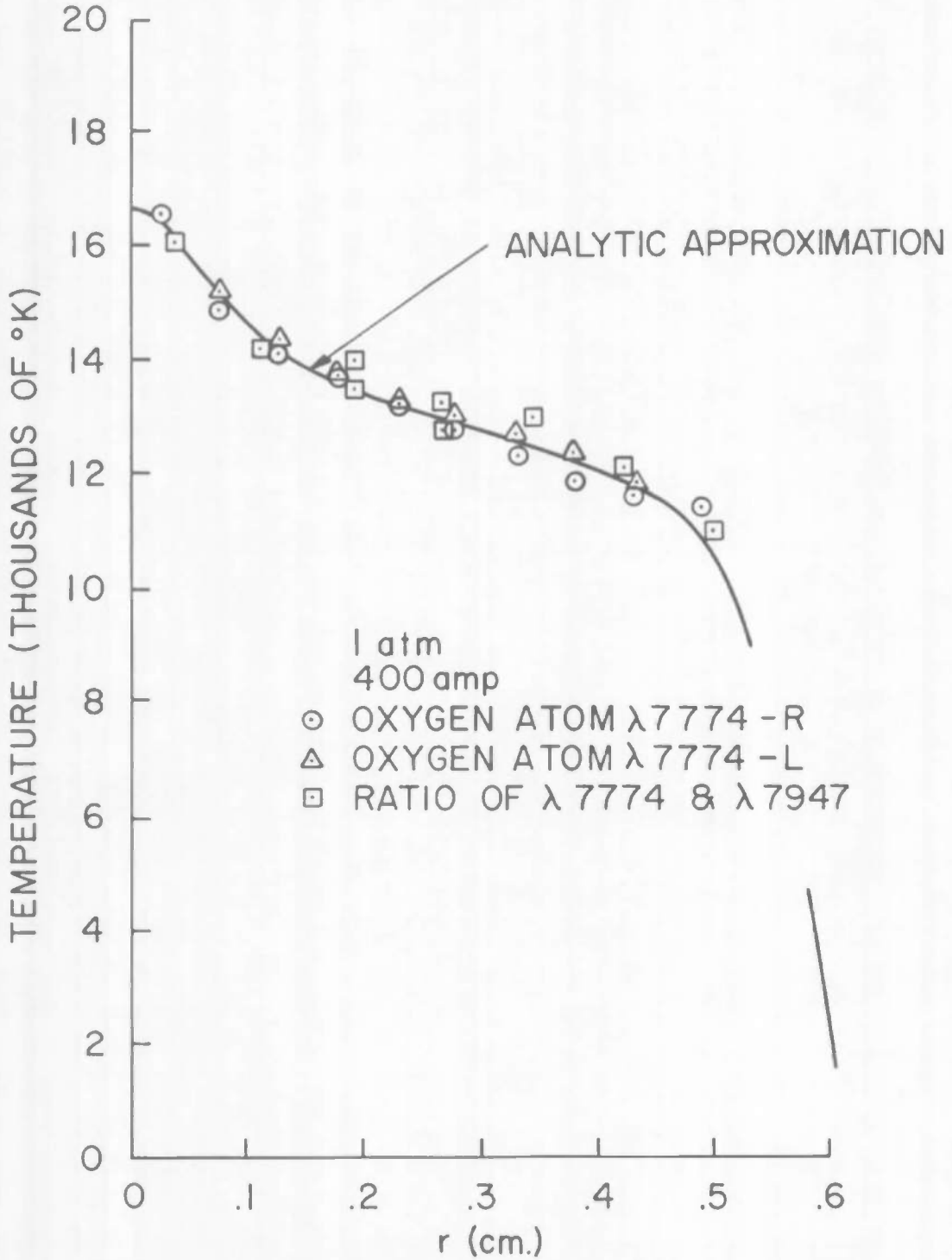

Figure 5.2 Spectrographically Measured Profile, 1 atm, 400 amp.

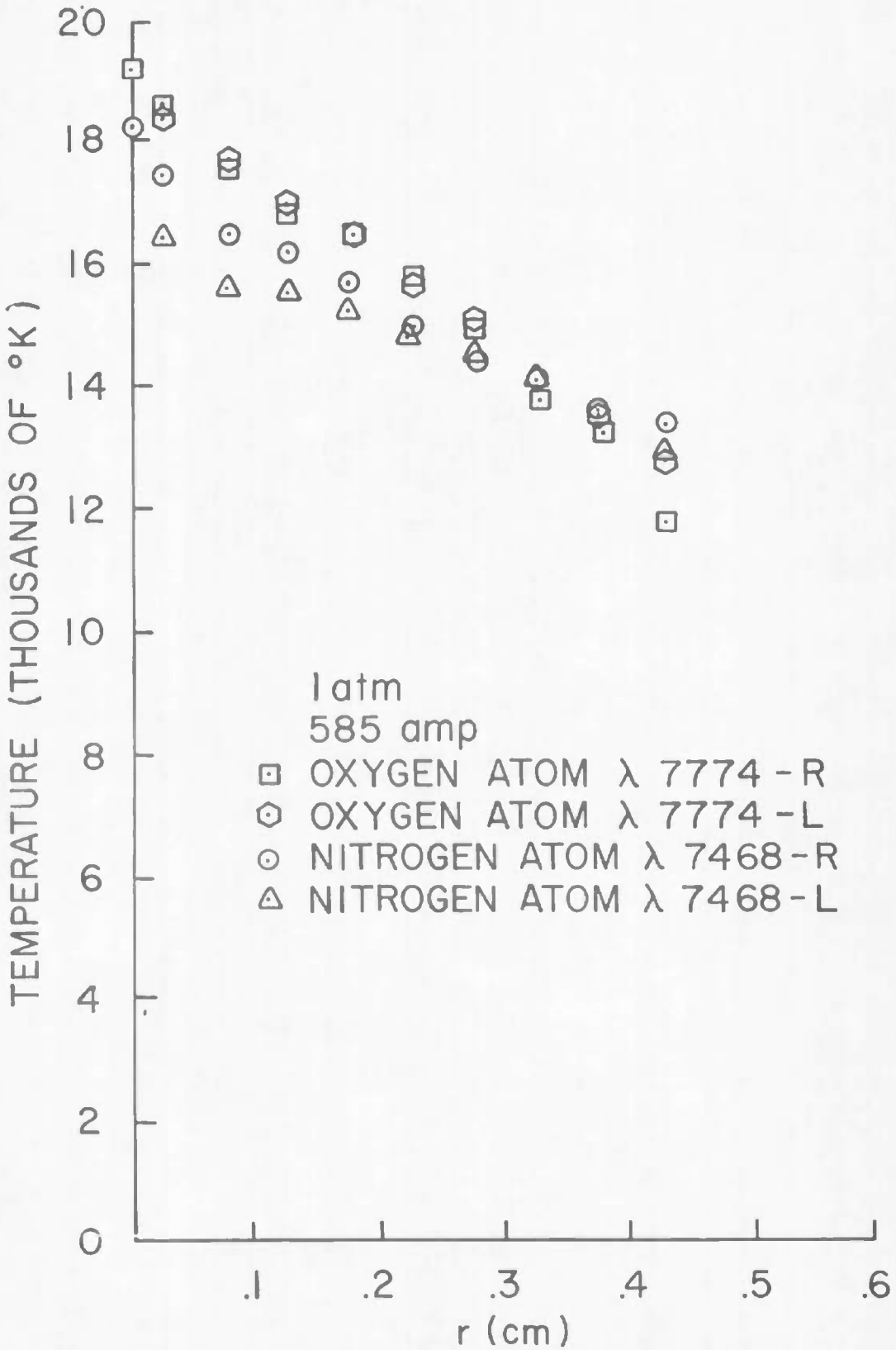

Figure 5.3 Spectrographically Measured Profile, 1 atm, 585 amp.

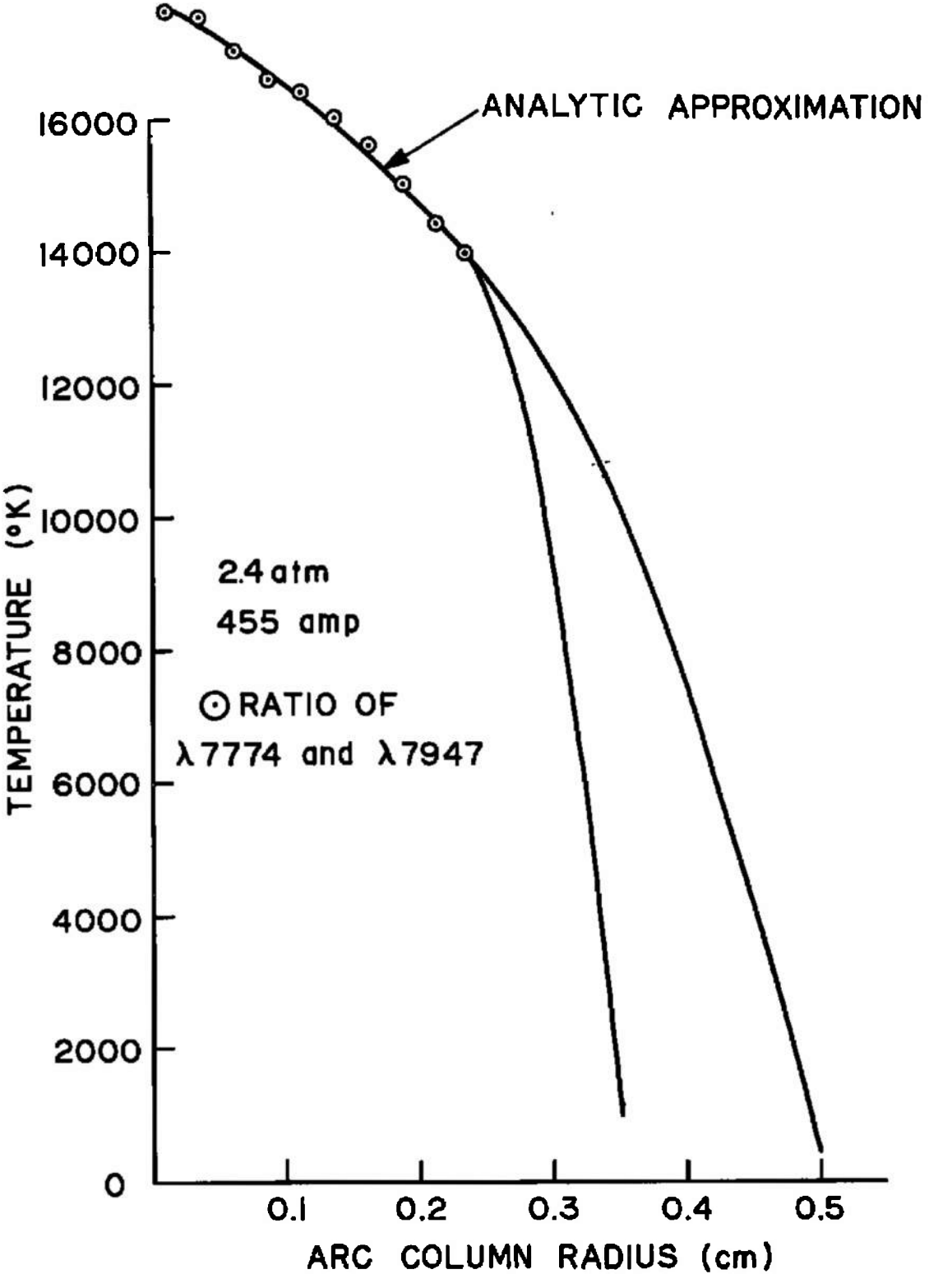

Figure 5.4 Spectrographically Measured Profile, 2.4 atm, 455 amp with Curve Fit to Two Different Boundary Conditions.

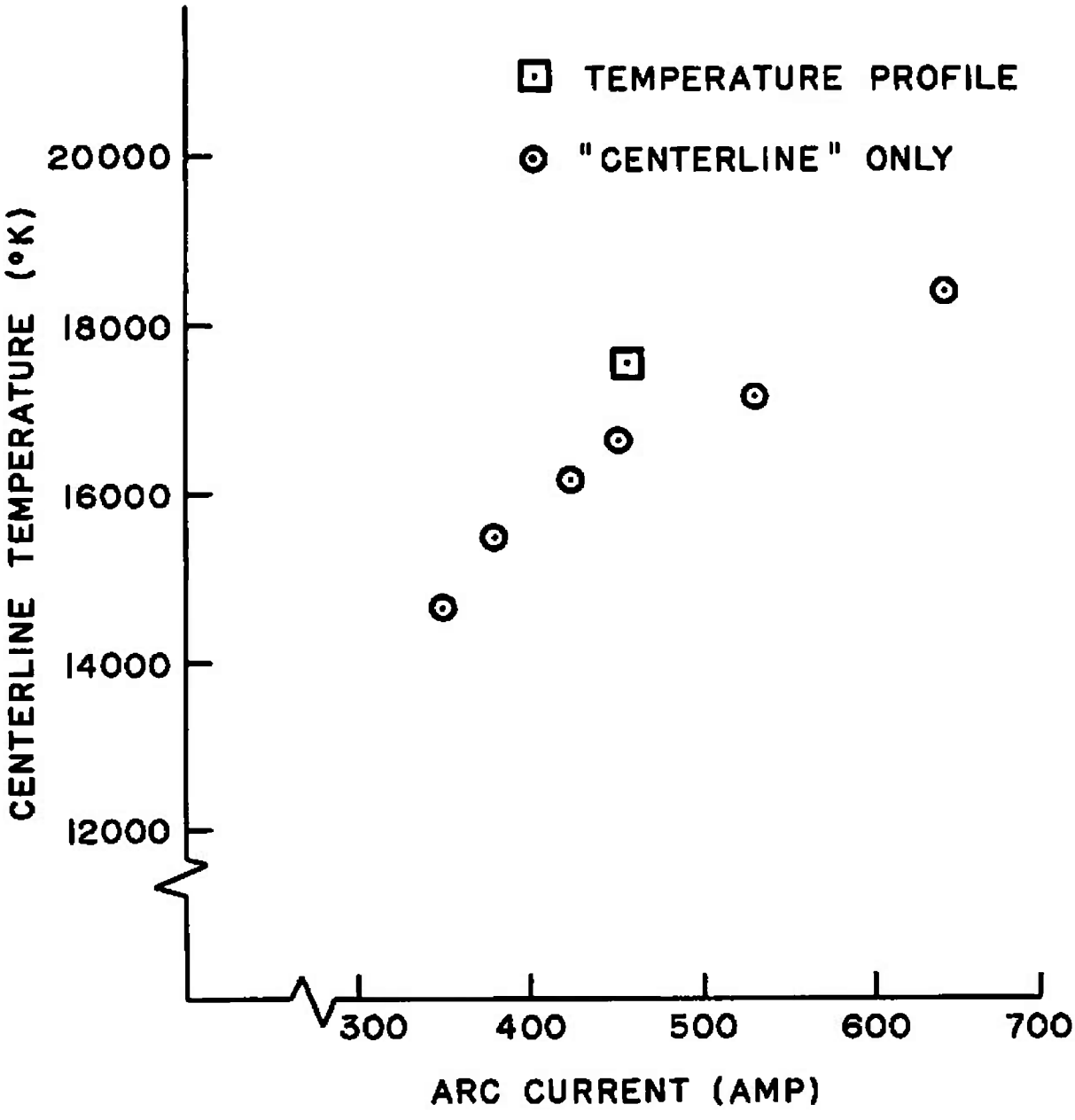

Figure 5.5 Arc Column Centerline Temperature Variation with Arc Current P=2.2 to 2.4 atm.

to allow for the cooler gas ahead of and behind the centerline region and the resultant temperatures are slightly lower that the "true" centerline temperature as obtained by measurements over a significant fraction of the profile.

Spectrographic data were not obtained at higher pressures because the measurements depend on observed spectral lines being nearly optically thin. The line reversal technique which is applicable at high pressures requires of the order of 70% absorption and is therefore most applicable at pressures substantially above 5 atm.

5.4 RADIANT HEAT FLUX MEASUREMENTS

Three types of gages were considered for measuring radiant heat flux while avoiding convective heating. The first gage was a cavity type, recessed in a channel 5 cm from the arc column. The channel eliminated convection and conduction without the necessity of a transparent window, but temperature rise of the cavity was barely detectable. At the other extreme a thermopile proved too sensitive.

The gage actually used, Fig. 5.6, was a cylindrical copper slug mounted with one base coated with lampblack and covered by a 1/16"thick quartz window. Remaining surfaces were thermally insulated by a teflon sleeve which also held the window in place. Temperature rise in the slug was measured by a chromel-alumel thermocouple directly connected to a recording oscillograph.

A shutter shielded the gage until the arc had stabilized at the desired conditions. Then the shutter was opened and the gage moved rapidly forward to one of several preselected positions in the channel. In the first position the gage surface was recessed 1/2" from the constrictor wall. Fully extended the gage surface was recessed 1/16" so that the exposed surface of the quartz was tangent to the constrictor wall.

Radiant heat flux to the gage was calculated from the rate of temperature rise of the copper slug, assuming constant specific heat and no heat losses. A typical data trace is shown in Fig. 5.7. Radiation ot the constrictor wall can be inferred by plotting heat flux data at several points along the channel and extrapolating to zero distance.

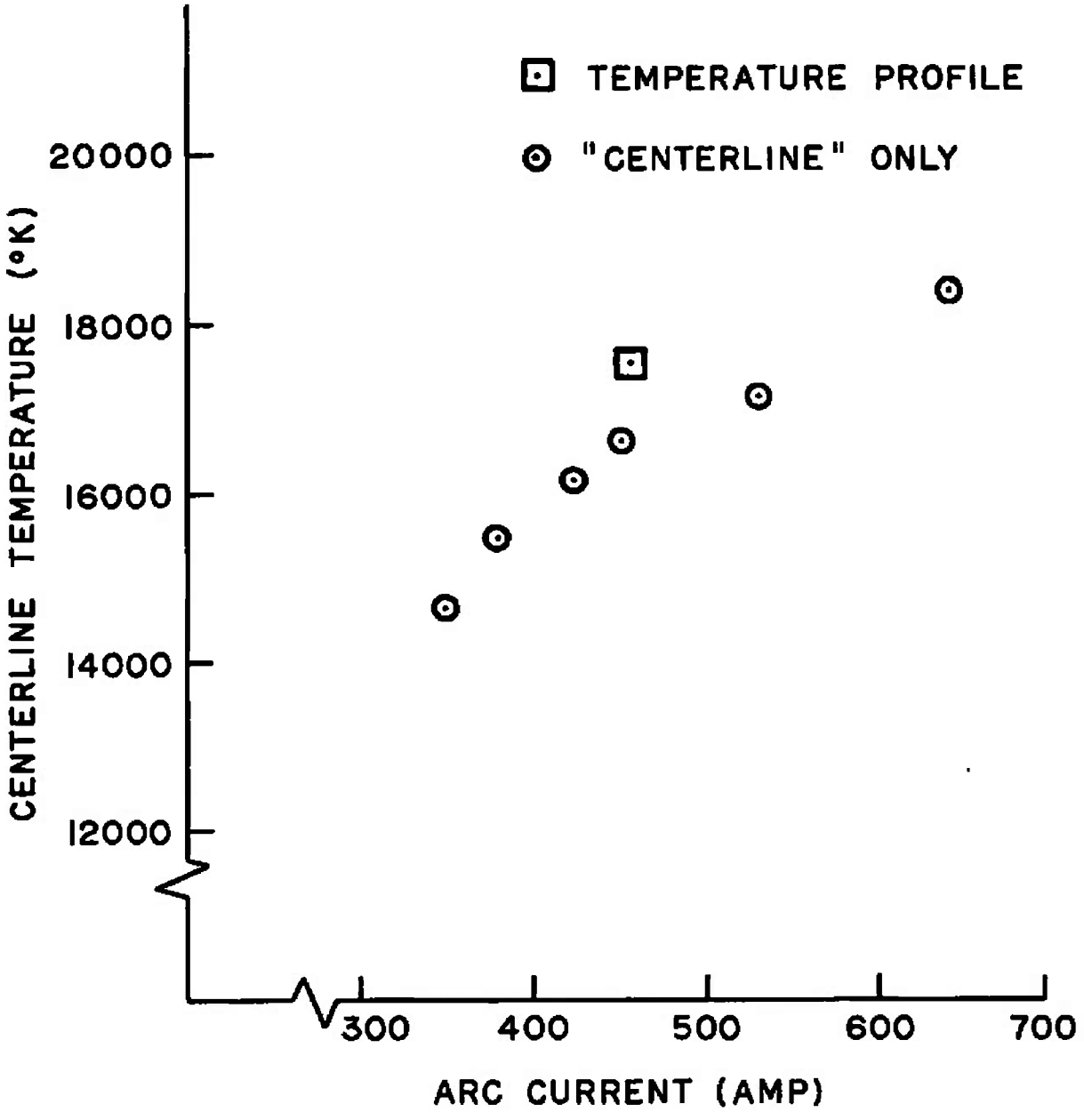

Figure 5.5 Arc Column Centerline Temperature Variation with Arc Current P=2.2 to 2.4 atm.

to allow for the cooler gas ahead of and behind the centerline region and the resultant temperatures are slightly lower that the "true" centerline temperature as obtained by measurements over a significant fraction of the profile.

Spectrographic data were not obtained at higher pressures because the measurements depend on observed spectral lines being nearly optically thin. The line reversal technique which is applicable at high pressures requires of the order of 70% absorption and is therefore most applicable at pressures substantially above 5 atm.

5.4 RADIANT HEAT FLUX MEASUREMENTS

Three types of gages were considered for measuring radiant heat flux while avoiding convective heating. The first gage was a cavity type, recessed in a channel 5 cm from the arc column. The channel eliminated convection and conduction without the necessity of a transparent window, but temperature rise of the cavity was barely detectable. At the other extreme a thermopile proved too sensitive.

The gage actually used, Fig. 5.6, was a cylindrical copper slug mounted with one base coated with lampblack and covered by a 1/16"thick quartz window. Remaining surfaces were thermally insulated by a teflon sleeve which also held the window in place. Temperature rise in the slug was measured by a chromel-alumel thermocouple directly connected to a recording oscillograph.

A shutter shielded the gage until the arc had stabilized at the desired conditions. Then the shutter was opened and the gage moved rapidly forward to one of several preselected positions in the channel. In the first position the gage surface was recessed 1/2" from the constrictor wall. Fully extended the gage surface was recessed 1/16" so that the exposed surface of the quartz was tangent to the constrictor wall.

Radiant heat flux to the gage was calculated from the rate of temperature rise of the copper slug, assuming constant specific heat and no heat losses. A typical data trace is shown in Fig. 5.7. Radiation ot the constrictor wall can be inferred by plotting heat flux/data at several points along the channel and extrapolating to zero distance.

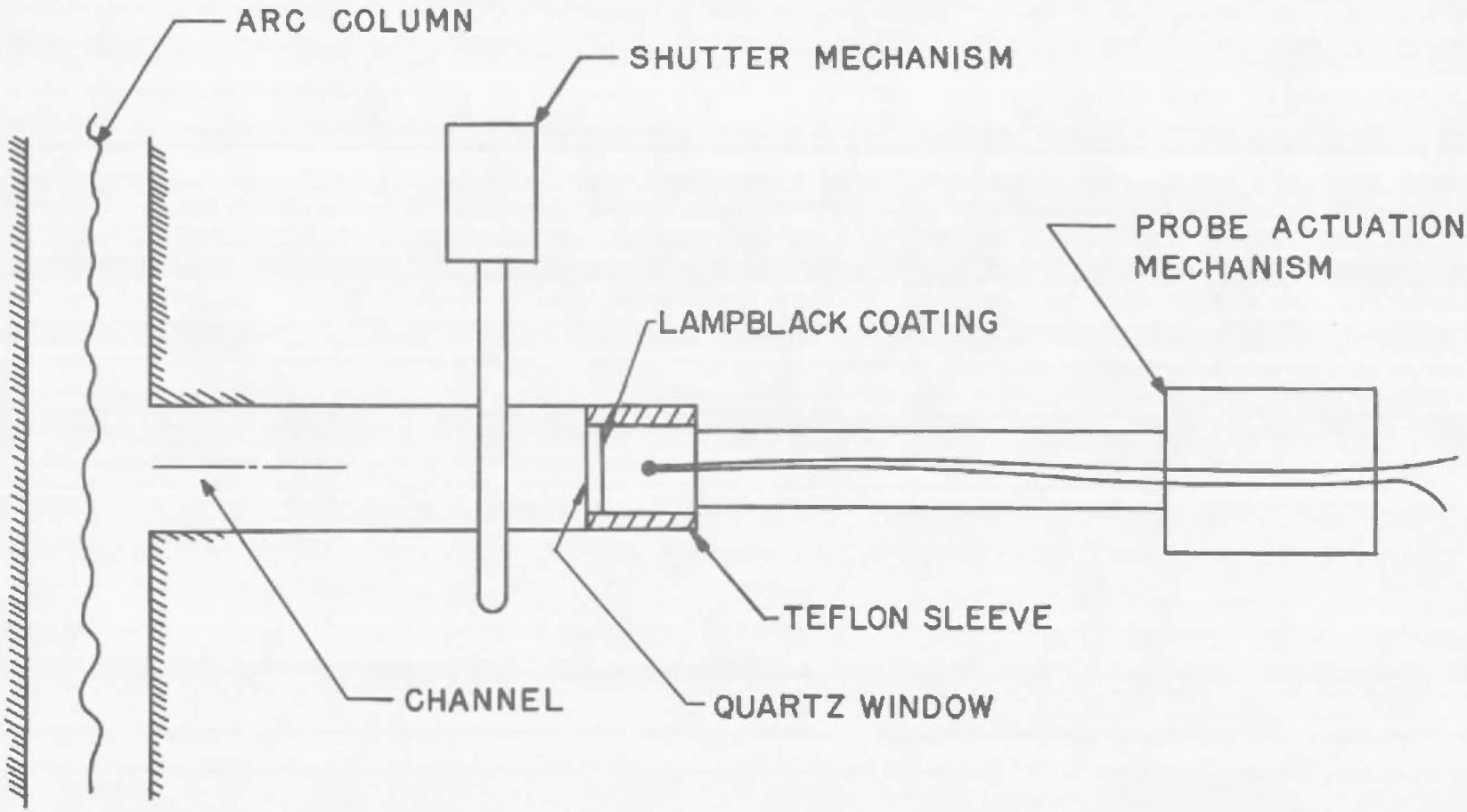

Figure 5.6 Copper Slug Gage for Total Radiant Heat Flux Measurement Shown in Retracted Position.

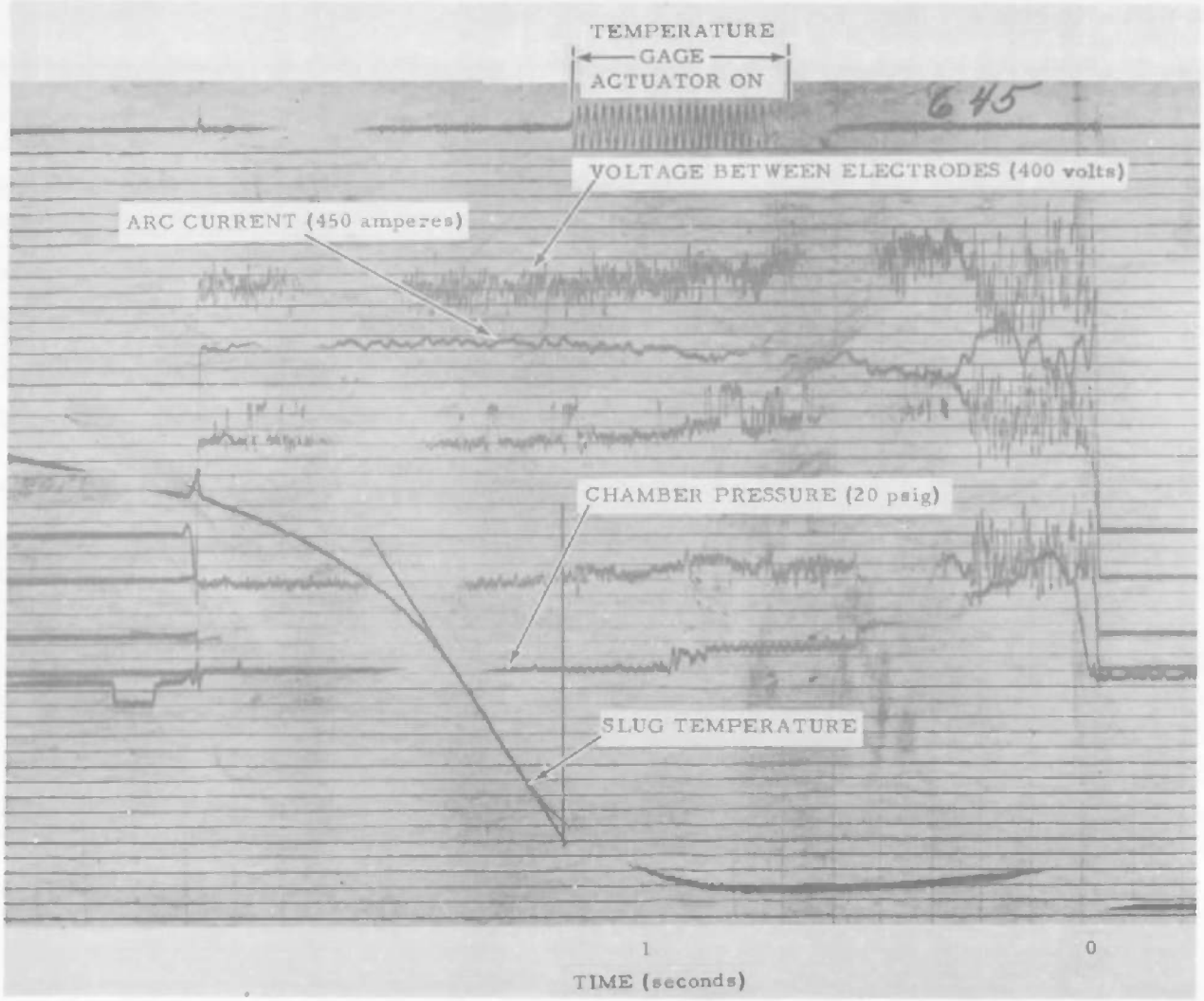

Figure 5.7 Typical Recording Trace for Determination of Radiant Heat Flux.

Allowances must be made for losses through the window and at the gage surface. The percentage of light reflected by a glass surface of refractive index 1.55 (about that of quartz) is tabulated as a function of angle of incidence in Ref. 13 and a graphical integration based on this tabulation indicates that approximately 92% of the incident energy is transmitted when the gage is fully in. Taking the absorptivity of lampblack as .95, the radiant energy measured by the gage at the arc chamber wall must be increased by a factor of 1.14. This correction is approximate but extrapolation to the arc column wall leads to considerable uncertainty in any event. The transmission characteristic of type 101 fused quartz, Fig. 5.8, coincides very nearly with the Low Frequency Range computer output so comparison will be made with LF curves.

An additional uncertainty introduced by the quartz window is the possible change in transmission characteristic when the glass is exposed to the high temperature arc. The transmission characteristic in the visible range was checked for a few windows using a standard lamp and photomultipliers. The ratio of photomultiplier outputs with and without the window inserted gave the fraction of energy transmitted (i.e., energy neither reflected nor absorbed). A clean window gave values from .89 to .90. Transmission of windows which has been exposed to the arc ranged from .40 to .79. The time at which the changes took place is unknown so no correction has been made for this effect.

Results are shown in Table 5.1 and Fig. 5.9. For the first series the insulator used to jacket the copper slug was melamine, and the quartz window was fastened to the melamine with an adhesive. This was not entirely satisfactory since the glass did not always remain in place. In the second series tabulated the teflon sleeve arrangement shown in Fig. 5.6 proved to be much more reliable.

The effect of the quartz window in shielding the gage from conduction is evident in the comparison of table 5.2.

Figure 5.10 is a comparison of calculations based on two measured profiles and the results of direct measurement. Complete confirmation of the calculation model and absorption coefficient data requires measurements at substantially higher pressures but at least the magnitude and trend are consistent.

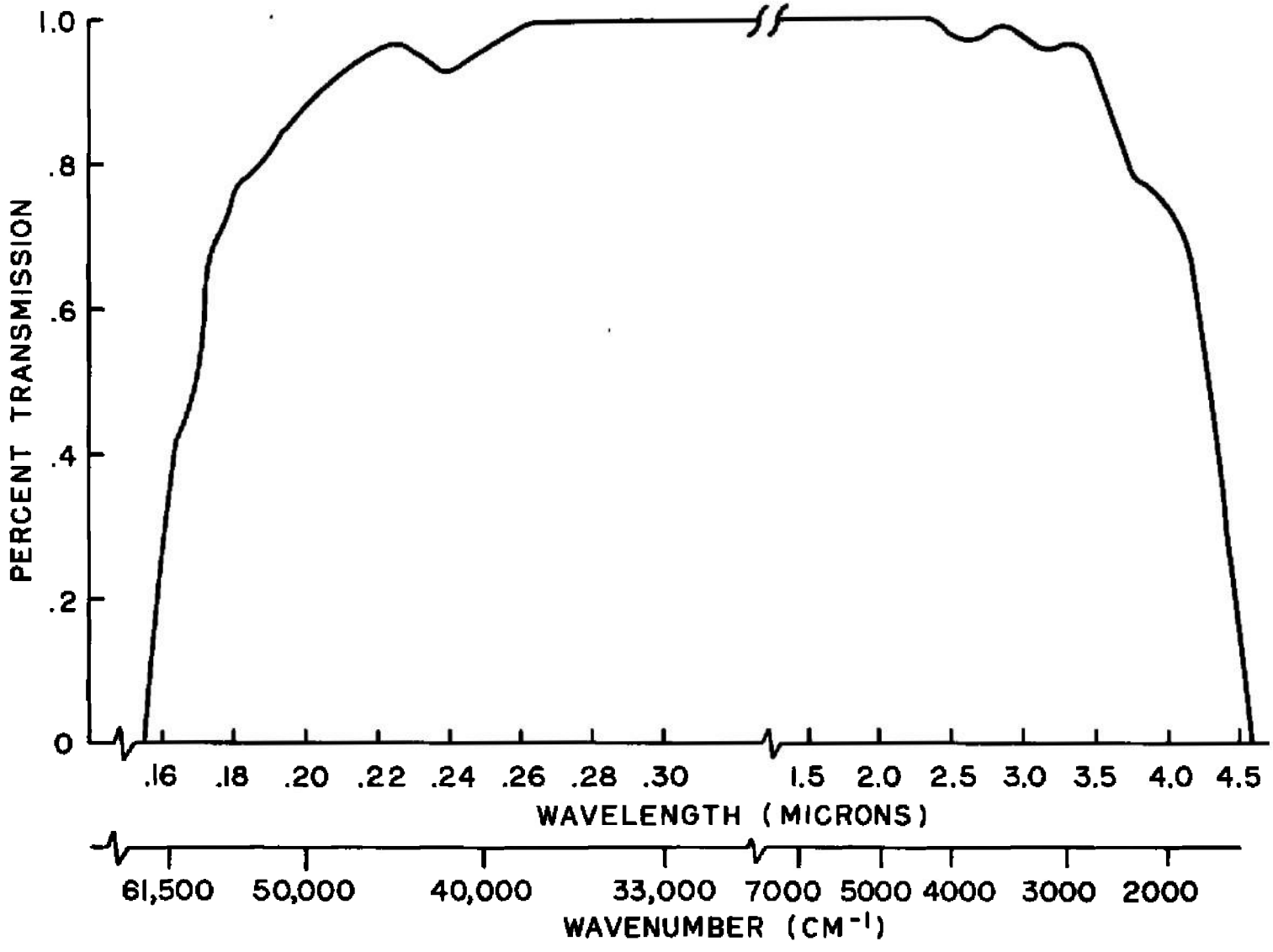

Figure 5.8 Average Transmission of General Electric Type 101 Quartz Excluding Surface Reflection Losses (Thickness=1/16").

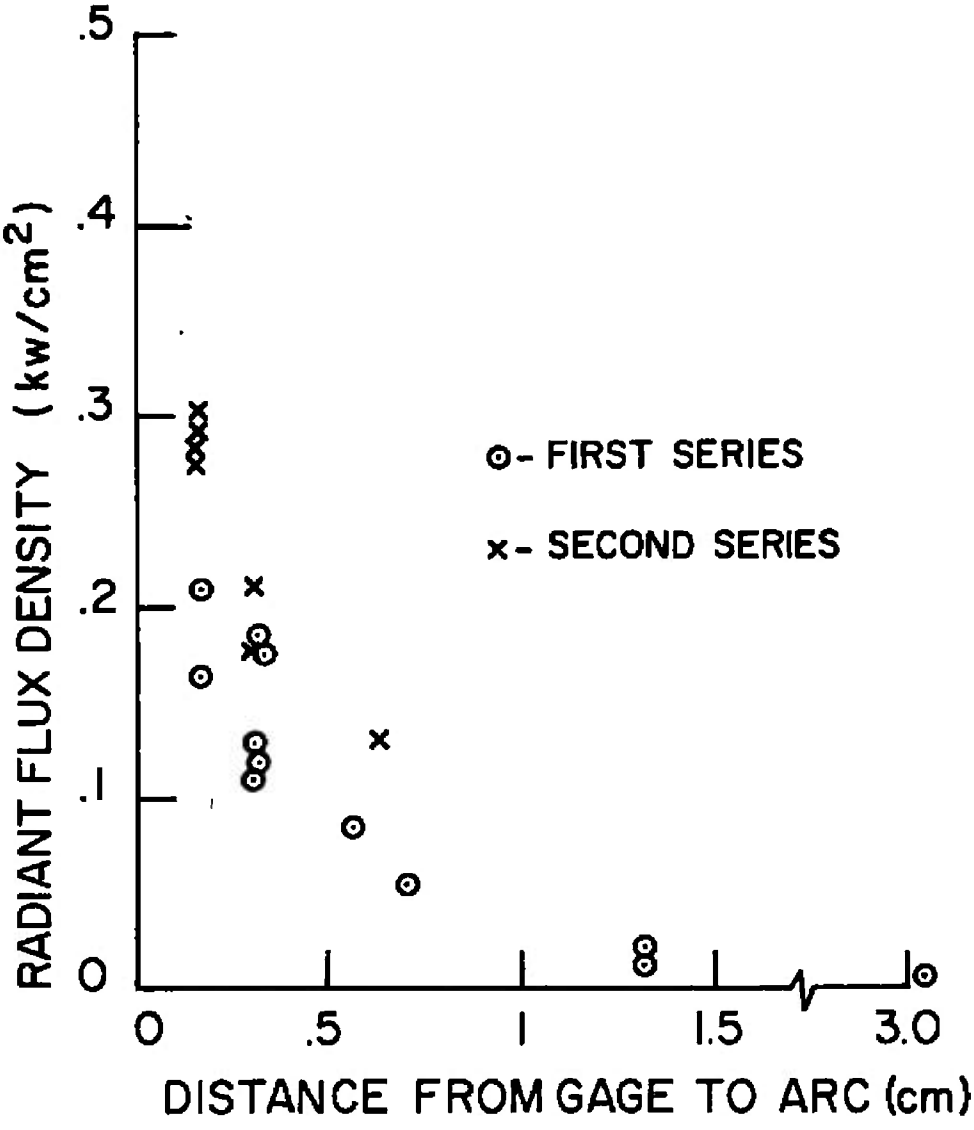

Figure 5.9 Radiant Heat Flux at 2.2 atm.

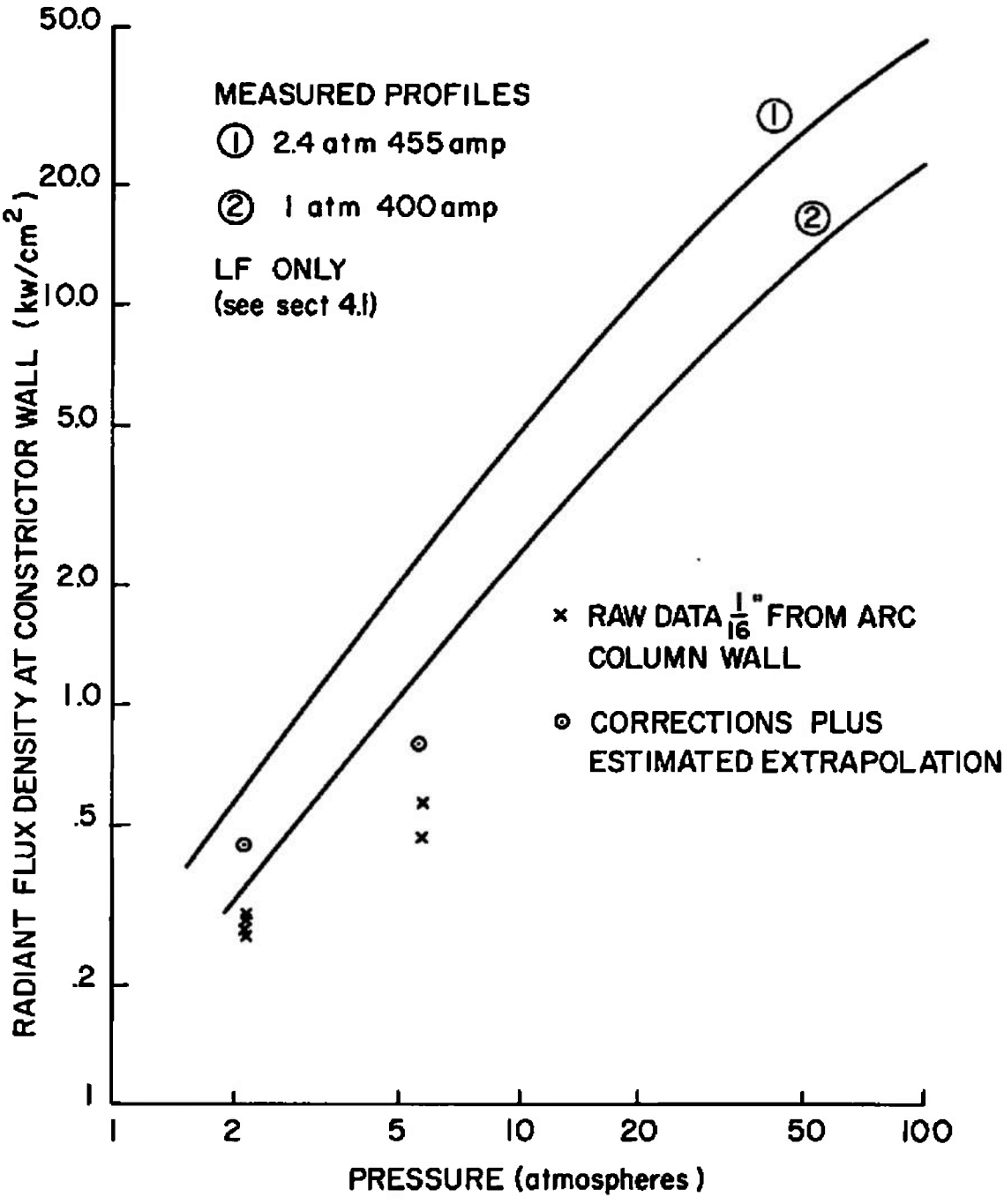

Figure 5.10 Comparison of Computations Using 2 Measured Profiles with Direct Radiant Flux Density Measurements

Distance of Gage Face from Arc Column (in)	Arc Current (amp)	Arc Voltage (volts)	Rate of Temperature Rise (°F/sec)	Mass of Slug (gm)	Radiant Flux Density (w/cm^2)
		First series, P=2.2 atm			
1.25	460	350	6.86	1.64	7.7
1.25	400	410	5.8	1.64	6.5
1.25	430	410	6.7	1.64	7.5
1.25	405	390	5.8	1.64	6.5
1.25	430	415	8.1	1.64	9.1
1.25	525	355	6.9	1.75	8.2
.50	450	390	11.86	1.64	13.3
.50	440	350	21.0	1.64	23.6
.50	425	405	11.60	1.64	13.0
.28	440	360	50.2	1.64	56.4
.22	500	365	76.4	1.64	85.7
.13	500	356	172.0	1.53	179.5
.13	550	340	175.0	1.53	183.0
.13	545	345	94.5	1.75	112.
.13	555	340	109.0	1.75	129.
.13	555	330	99.0	1.75	117.0
.06	485	372	179.0	1.72	210.5
.06	550	350	136.0	1.75	161.0
		Second series, P=2.2 atm			
.06	400	430	249	1.67	284
.06	480	410	244	1.67	278
.06	440	408	252	1.67	292
.06	450	410	266	1.67	302
.13	450	405	156	1.67	178
.13	455	415	185	1.67	211
.25	425	415	123	1.67	141
		Second series, P=5.7 atm			
.06	600	505	479	1.76	575
.06	610	480	385	1.76	454

Table 5.1 - Radiant Heat Flux to Slug Gage

Distance of Gage Face from Arc Column (cm)	Radiant Flux Density (watts/cm^2)	Total Flux Density (No Window on Gage) (watts/cm^2)
.559	85.7	214.0
.159	210.5	636.0
.159	161.0	648.0

Table 5.2 - Comparison of Total and Radiant Heat Flux at a Pressure of Two Atmospheres

SECTION VI
APPLICATION TO ARC HEATER CONFIGURATIONS

6.1 GENERAL

A variety of configurations for heating plasma by means of an electric arc are in use today. Two of the more common basic arc heater geometries are the constricted arc and the ring electrode rotating arc. Application of the model developed in Section 2 applied fairly well to the constricted arc since axial symmetry is maintained in most of the heater and some measurements of arc column temperature profiles are available.

Analysis of the ring electrode rotating arc is considerably more difficult because arc temperature measurements are not available and arc behavior is influenced by such new factors as the ratio of ring diameter to separation distance, the magnitude and direction of self-induced or externally applied magnetic driving fields, and the magnitude and direction of cold air flow transverse to the arc column.

Under some circumstances for instance, the rotating arc may bow inward to the extent that, except near the electrodes, it is stationary on the axis of symmetry, Fig. 6.1. Fastax films taken of a rotating arc between ring electrodes separated by a distance of about 4 ring radii tend to bear out this possibility. The column was photographed through a 3/8" wide x 1/8" high port midway between electrodes. At pressures above approximately 10 atmospheres the the column was visible and stationary, centered in the port. At lower pressures, down to about 2 atmospheres, changes in brightness indicated that the column was moving past the port. At 2 atmospheres pressure light from the port was uniform. These observations fit the hypothesis that at the highest pressure only the parts of the arc near the electrodes are moving, while the body of the column is aligned with the axis, while at low pressure the entire column may be moving too fast for the Fastax camera to "stop" the motion.

If the magnetic field which causes the arc to rotate is sufficiently strong, of the order of 20 kilogauss, the arc can be magnetically diffused (Ref. 14) thus radically altering its geometry and radiation characteristics. A transverse flow created by a rapidly moving arc column may destroy the axial symmetry of the column, probably tending to create a turbulent If this tail merges with the leading "edge" of the column a diffuse operating mode also results.

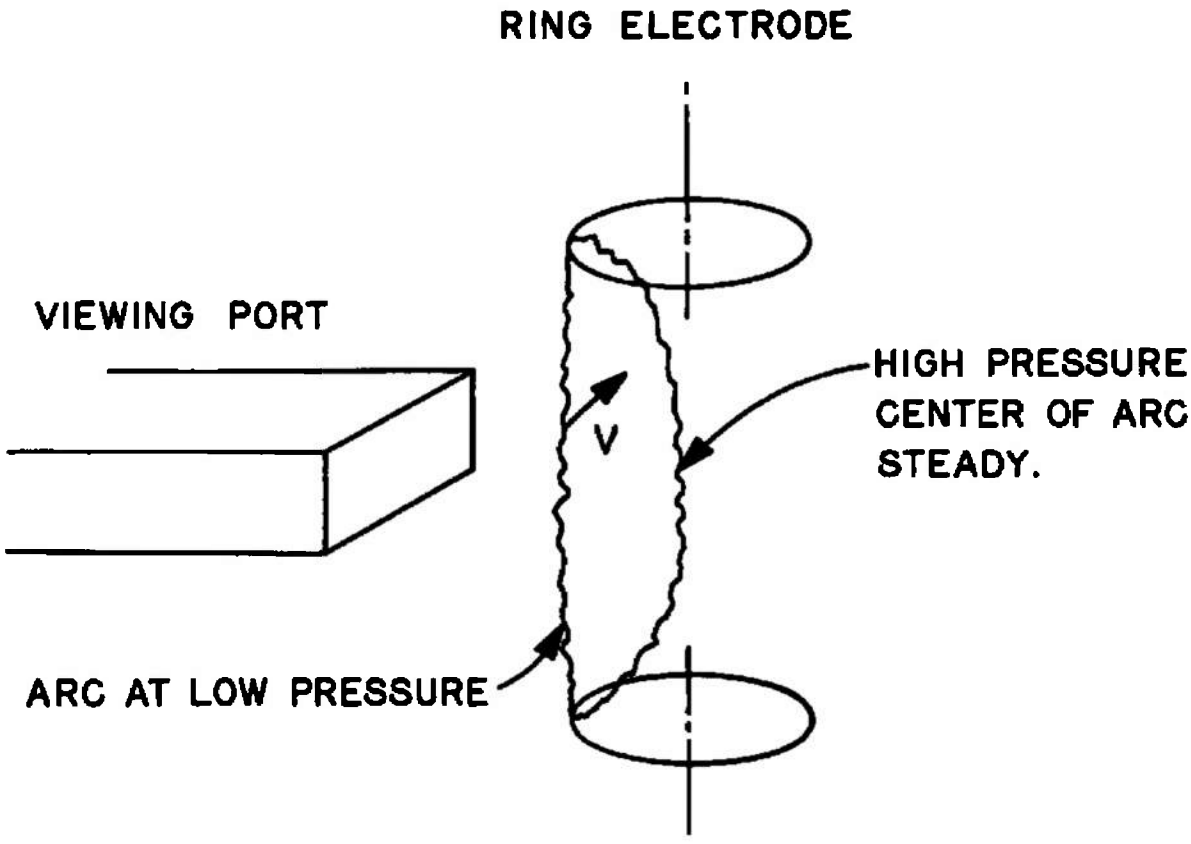

Figure 6.1 Ring Electrode Rotating Arc With Separation Distance of 4 Ring Radii.

6.2 SPECIFIC CONFIGURATION

An outline sketch of the arc heater of immediate interest is shown in Fig. 6.2. It is designed to operate at high pressure on 3 phase, 60 cps, alternating current with the arcs kept in rapid motion by a steady, externally applied, magnetic field. Cold air flows radially inward through the arcs, then axially to the nozzle.

Magnetic field strength is 5 kilogauss, which is probably not sufficient to cause magnetic diffusion, so the arc will be treated as a cylindrical column. Arc length cannot easily be established because, while electrode separation is only about one fourth that in the observations described in Section 6.1, pressure can be higher and there is a radially inward velocity component which will probably cause the arc to bow inward. Some estimated operating conditions at two pressures are shown in Table 6.1.

TABLE 6.1. AEDC 20 MEGAWATT ARC HEATER SPECIFICATIONS

	Dimensions*
Chamber Diameter (in.)	4
Insulator Diameter (in.)	6
Electrode Spacing (in.)	
center to center	4.5
Minimum Gap	1.5
Total Chamber Length (in.)	17.5

Estimated Operating Conditions	Low Pressure	High Pressure
Pressure (psia)**	75	3750
(atm)	5.1	255
Arc Voltage (volts zero to mean)**	1000	2000
Arc Current (amperes rms/phase)**	4000	3500
Power Input (MW)**	11	19
Exit Enthalpy (Btu/lbm)**	6100	7200
(h/RTo)	180	212
Exit Temperature (^{o}K)	6300	8000
Mass Flow (lbm/sec)**	1.20	1.0
Estimated Rotational Speed (rev/sec)**	1400	1300

*Scaled from Westinghouse Drawing AC09084
** Westinghouse letter of 11 September 1964

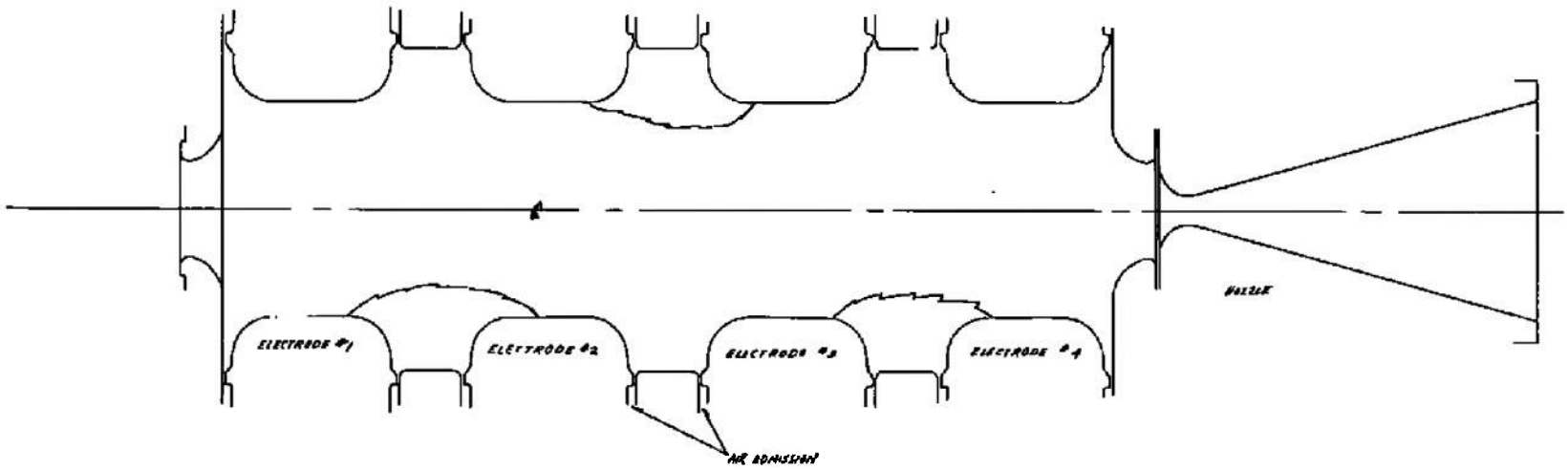

Figure 6.2 Outline of AEDC 20 MW Arc Heater Interior (based on drawing furnished by Westinghouse Electric Co.)

6.3 ARC COLUMN MODEL

Arc size and temperature distribution are not known, so some admittedly crude assumptions were made in order to arrive at an estimate. The arc was assumed to be cylindrical at a uniform temperature with air flow through it limited by aerodynamic choking or by the total flow, whichever was least. The choked flow function for flow through an arc has been computed by Weber (Ref. 15) and is shown in Fig. 6.3. For a known or assumed voltage gradient and current there is then a unique combination of arc radius and temperature which satisfies both an energy balance and Ohm's Law. In view of the approximate nature of the data and model, electrode drops (of the order of tens of volts) and back EMF due to interaction with the externally applied magnetic field (a few volts) were neglected in the estimates of voltage gradient. A further implicit assumption is that an AC arc may be treated by DC methods and that the RMS value of current gives acceptable mean values. In brief, both space and time variation of arc temperature (and bulk gas temperature too) were ignored.

6.4 LOW PRESSURE OPERATION

The gas is nearly optically thin at 5 atmospheres so that total radiance, J, as computed by Breene and Nardone (Ref. 2) was used to computed radiant heat fluxes. The energy balance for a unit length of arc column was written

$$\frac{I^2}{\sigma_e \pi \delta^2} - \left(\frac{W}{Ap}\right)^* p(2\delta)(h_a - h_o) - (4\pi J_a)(\pi \delta^2) = 0 \qquad (6.1)$$

where p is pressure, h_o is the enthalpy of the incoming air, h_a is enthalpy at arc temperature, δ is arc radius and $(\frac{W^*}{Ap})$ is the choked flow function, Fig. 6.3. Peng and Pendroh (Ref. 16) were the source for electrical conductivity σ_e. Equation 6.1 can be considered a function of radius and arc temperature, Fig. 6.4, since, at a given pressure, σ_e, J, $(\frac{W}{Ap})^*$ and h_a are all functions of temperature. Ohm's law in the form

$$E = \frac{I}{\sigma_e \pi \delta^2} \qquad (6.2)$$

is also shown on Fig. 6.4 for several values of E. The values selected are reasonable at the low pressure. Experience with rotating arcs indicates that the column radius should be less than about 0.5 cm and

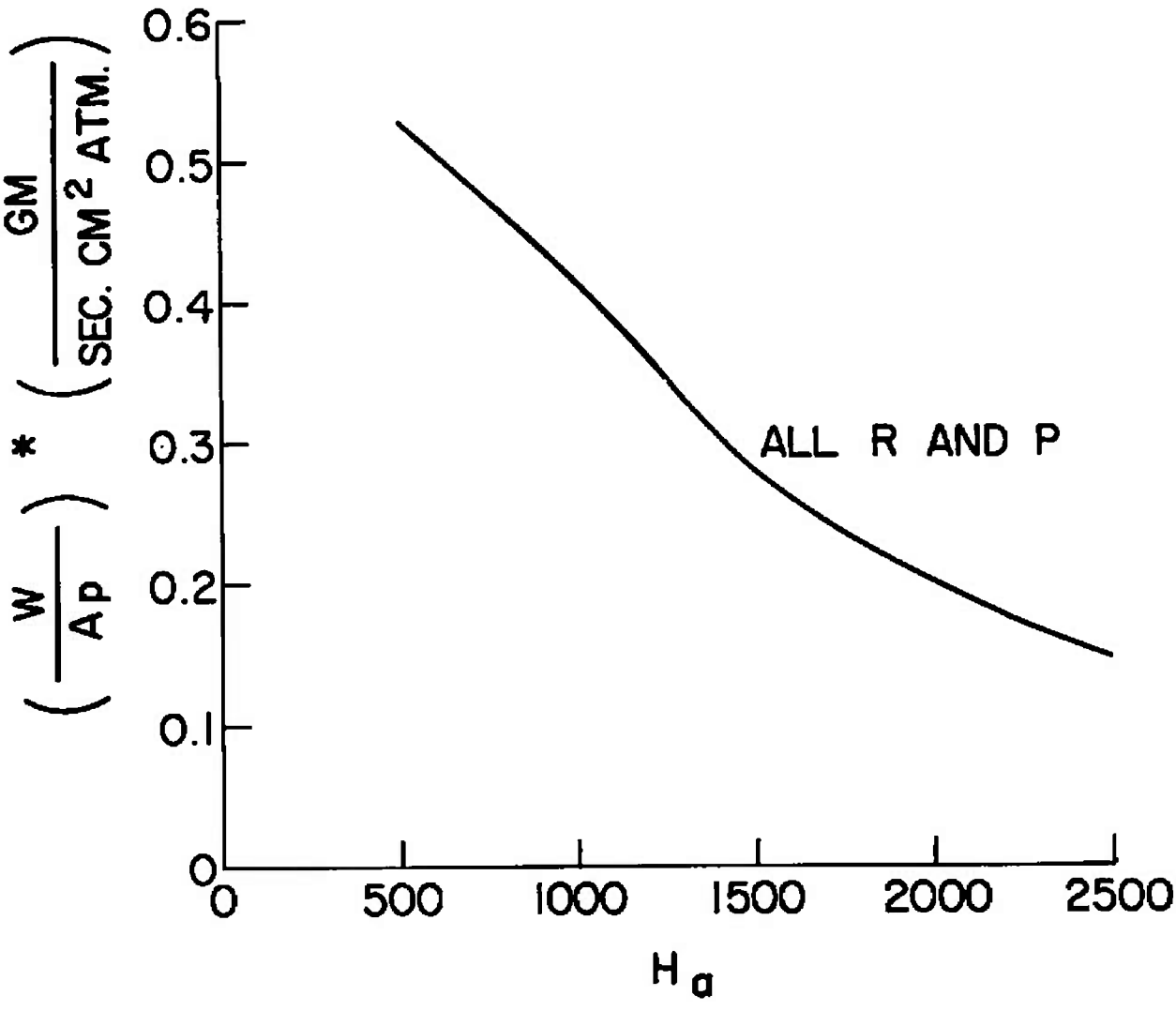

Figure 6.3 Choked Fully Developed Flow (Ref. 15)

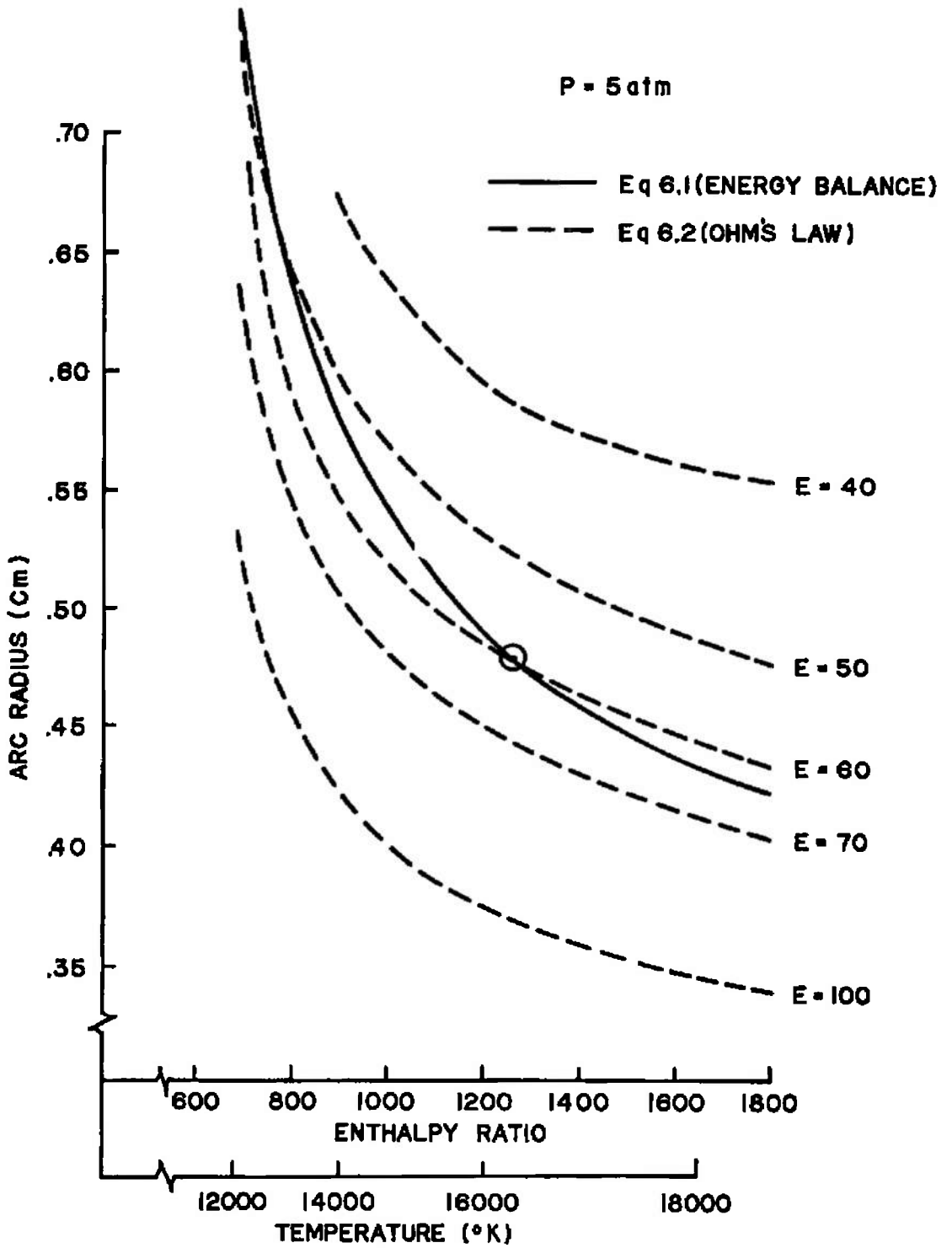

Figure 6.4 Energy Balance and Ohm's Law at 5 Atmospheres Chamber Pressure.

that 60 v/cm is a reasonable maximum voltage gradient. This is a local column gradient which cannot be obtained by simply dividing the voltage between electrodes by electrode spacing. Turbulence locally twists and turns the column extending its actual length to several times the distance between electrodes. The arc length used for calculations at 5 atm is then obtained by dividing the applied voltage by the voltage gradient.

Bulk enthalpy, h_b, of plasma leaving the arc chamber, was estimated from another energy balance. Consider 3 arcs, each of length L_a, in a cylindrical chamber of length L_c and radius R_c and assume that the only loss is the bulk gas radiation at bulk (exit) enthalpy. Then

$$\left(\frac{W}{Ap}\right)^{*} p\,(2\delta)\,(3L_a)\,h_a - W h_b = 4\pi J_b\,(\pi R_c^{\,2} L_c) \qquad (6.3)$$

where subscript b refers to bulk gas and L_a is the length of a single arc. The choked flow function and the total radiance are known functions of bulk enthalpy (or, equivalently, bulk temperature) so Eq. 6.3 uniquely determines h_b. Results are presented in Section 6.6 along with those for the high pressure case.

6.5 HIGH PRESSURE OPERATION

Essentially the same analysis was applied to the 255 atmosphere case except that the gas can no longer be considered optically thin and program ARCRAD was used to calculate radiation. For the conditions given, the entire flow can pass through the arc column without choking, so the arc column energy balance analogous to Eq. 6.1 was written

$$\frac{I^2}{\sigma_e \pi \delta^2} - \frac{W(h_a - h_o)}{3L_a} - (q/A)_a\, 2\pi\delta = 0 \qquad (6.4)$$

where $(q/A)_a$ is the radiant flux density at the arc column boundary, Fig. 6.5.

Again a unique combination of a radius and arc temperature exist which simultaneously satisfy Eq. 6.4 and Ohm's law (Eq. 6.2) for an established value of E.

Raezer, et. al., Ref. (17) indicate that voltage gradient varies as the 0.28 power of the pressure. Applying this to the 60 v/cm gradient at 5 atmospheres gives 174 v/cm and an arc length of 4.5

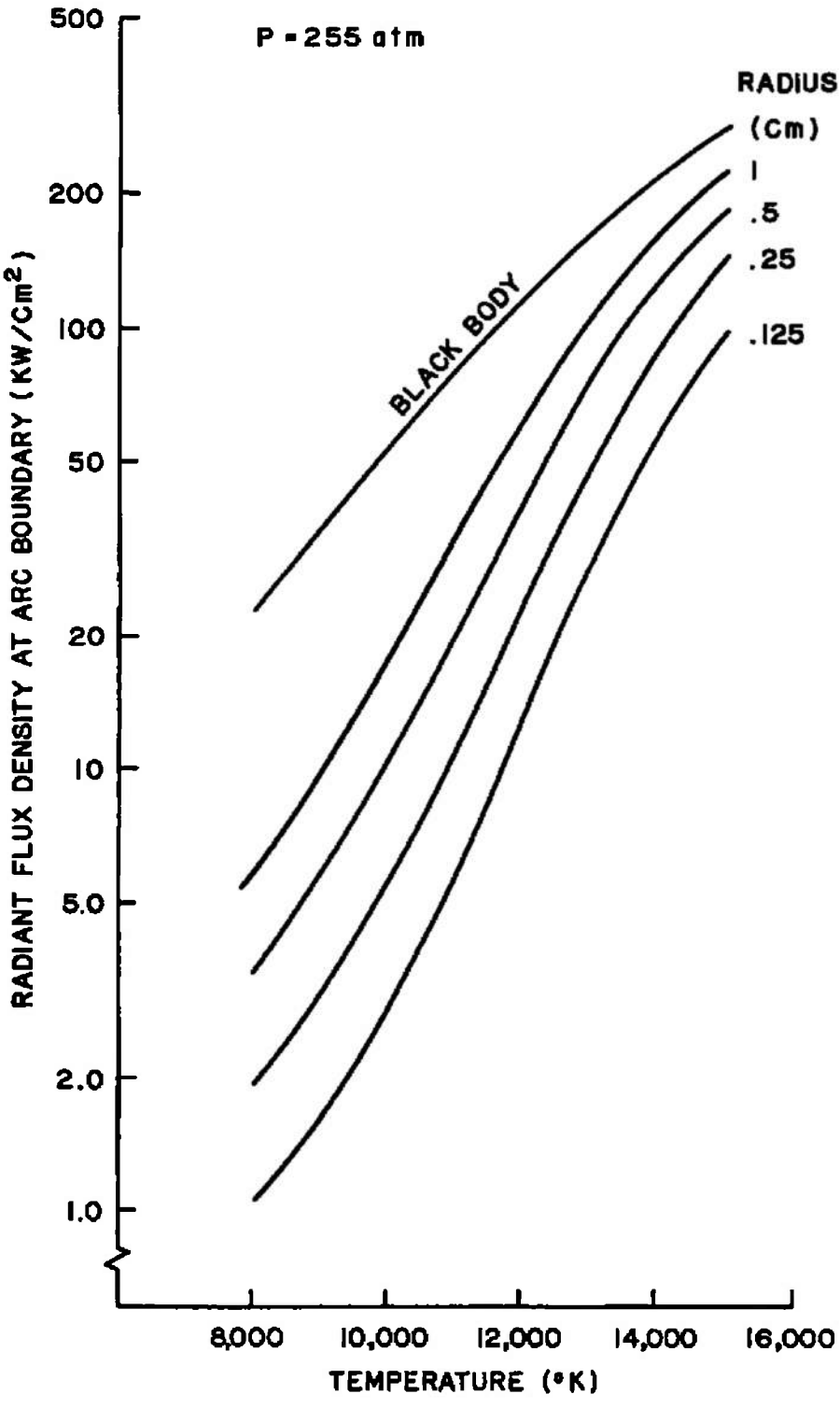

Figure 6.5 Radiant Flux Density at the Boundary of a Uniform Temperature Air Arc at 255 Atmospheres.

inches. The resulting arc radius is quite large, probably much too large, and the arc temperature and enthalpy are therefore low since the general trend of the curve is similar to Fig. 6.4. For this reason results are also included for an arbitrarily assumed arc length of 2 inches.

Exit enthalpy was again estimated from a simplified arc chamber energy balance. The bulk gas was taken to be a cylinder of arc chamber dimensions at a uniform temperature corresponding to exit enthalpy, with a smaller cylinder, the arc column, moving rapidly around its circumference. Both the bulk gas and the arc column radiate to the arc chamber wall but a part of the arc radiation is now reabsorbed by the bulk gas.

In cross section this geometry corresponds very closely to radiation of a surface element into a cylinder, so the Nusselt solution for absorptivity of a cylinder can be applied. By Lambert's cosine law the equivalent arc surface area per unit length radiating inward is equal to the arc column diameter so that q_{ab}, the power reabsorbed by the bulk gas, is given by

$$q_{ab} = 2\delta\,(3L_a)\,\sigma T_a^4 \sum_n \epsilon_{a,n}\,\eta_{a,n}\,\alpha_{b,n} \qquad (6.5)$$

Program ARCRAD was adapted to the computation of q_{ab}.

Neglecting all losses but radiation and assuming, optimistically, that radiation from the bulk gas takes place at bulk exit enthalpy, the equivalent of Eq. 6.3 is

$$W(h_a - h_b) + q_{ab} = q_b \qquad (6.6)$$

where power radiated by the bulk gas, q_b is given by

$$q_b = (q/A)_b\,(2\pi R_c)\,(R_c + L_c) \qquad (6.7)$$

and $(q/A)_b$ was computed using program ARCRAD. Strictly speaking, absorption lengths for radiation from the ends of the cylinder are slightly different than for the cylindrical surface, but the difference is of the order of 5% and the ends are only a small fraction of the total surface anyway so no distinction is made. It was convenient to solve for T_b graphically, Fig. 6.6, plotting Eqs. 6.6 and 6.7 as functions of temperature because both q_b and h_b are non-analytic.

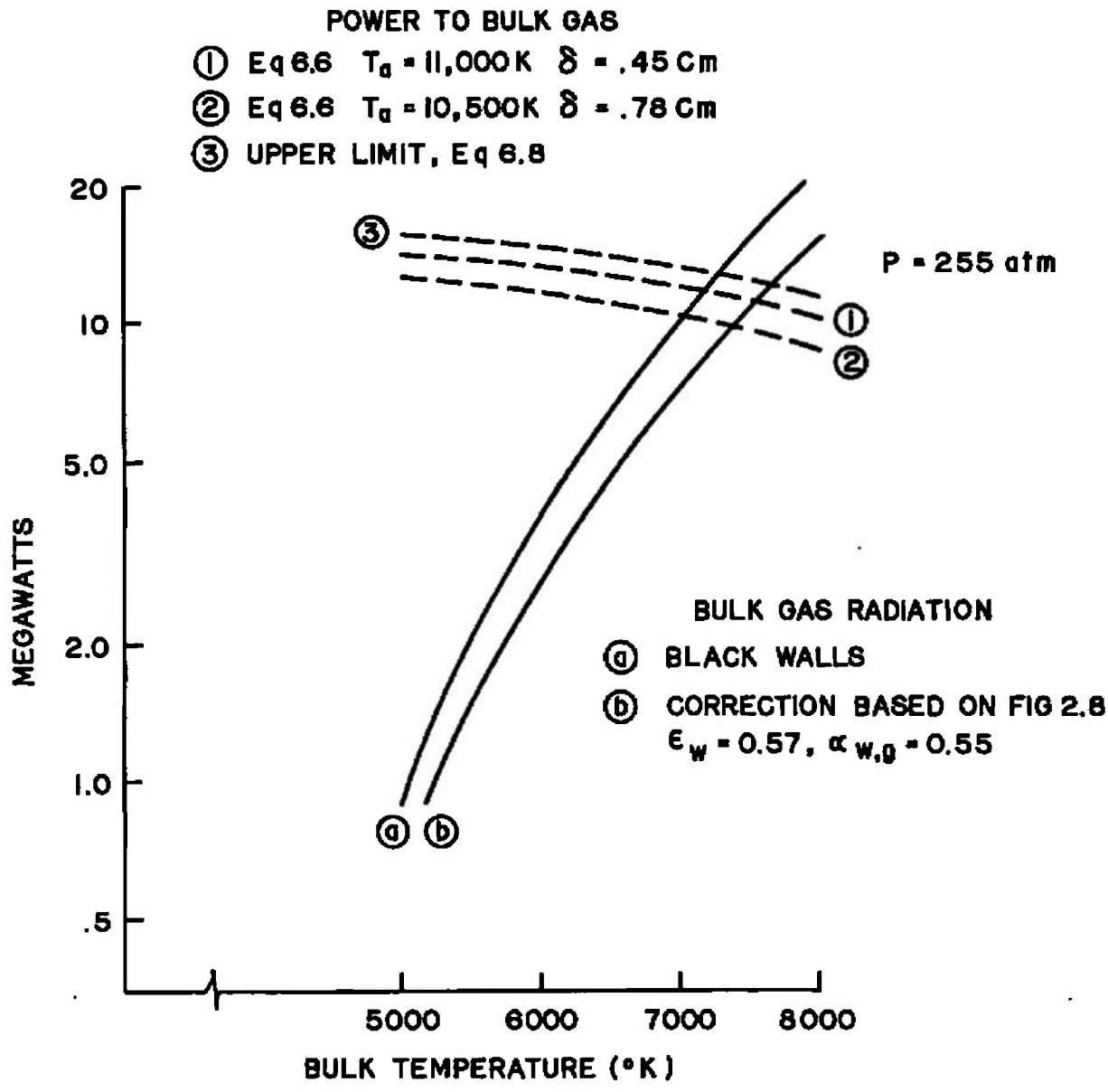

Figure 6.6 Arc Chamber Energy Balance at 255 atmospheres with an Input power of 19 megawatts.

Two curves are shown for q_b, one assuming that the chamber walls are black and the other applying the correction factor discussed in Section 2.7. The arc itself is small compared to the chamber so no correction is needed, but reabsorbtion by the bulk gas can be significant. In evaluating the correction factor for the bulk gas $\alpha_{w,g}$ was taken as the ratio of $(q/A)_b$ to black body radiation, both at 7500 ^{o}K.

If P_{loss} is defined as that part of the input power which is absorbed by processes other than net heating of the incoming air and P_{in} is the total input power then

$$P_{loss} \leq P_{in} - W(h_b - h_o) \tag{6.8}$$

A curve representing the equality is also plotted in Fig. 6.6 and its intersection with the radiation loss curve places an upper bound on bulk temperature.

6.6 RESULTS AND DISCUSSION

Results of calculations are summarized below.

TABLE 6.2. AEDC 20 MEGAWATT ARC HEATER, ESTIMATED ARC CONDITIONS AND RADIANT FLUXES

Pressure (atm)	5	255		255	
Voltage gradient (V/cm)	60	390		174	
Arc Length (cm)	15.7	5.1		11.5	
(in)	6.2	2.0		4.5	
Arc Radius (cm)	.48	.45		.78	
Arc Temperature (K)	16,000	11,000		10,500	
Wall Emissivity	--	.57	1.0	.57	1.0
Exit Temperature (K)	6,300	7500	7200	7400	7000
Exit Enthalpy (Btu/lbm)	6,100	6300	5900	6200	5600
Arc Radiation (mw)					
Total from arc	3.6	.9	.9	3.6	3.6
To Bulk gas*	0	.2	.2	.6	.6
To Wall*	3.6	.7	.7	3.0	3.0
Bulk gas radiation (mw)	.05	11.0	11.7	9.7	10.3
Total Radiation to Wall	3.65	11.7	12.4	12.7	13.3
Average Radiant Flux Density** (kw/cm^2)	2.3	7.4	7.8	8.0	8.4

* at 7500°K

** Based on a cylinder 17.5 inches long by 4 inches diameter.

At 5 atmospheres the bulk gas radiation loss is relatively small and the decrease in enthalpy from arc to bulk gas is primarily the result of mixing with cold gas which did not pass through the arc.

At 255 atmospheres bulk gas radiation alonge can consume practically all of the power input. Results presented in Fig. 6.6 and Table 6.2 tend to be optimistic in that conduction losses have been neglected and bulk gas radiation has been assumed to take place at exit temperature rather than somewhere between arc temperature and bulk temperature.

Total radiation to the wall includes radiation directly from the arcs. The arcs would tend to create local hot spots except that they are in rapid motion -- making about 10 revolutions for each half cycle of input voltage -- so the heat flux per unit length from the arc was considered as uniformly distributed around the arc chamber periphery.

SECTION VII

CONCLUSIONS

At high pressures there is no simple way to predict the radiant heat transfer from an arc column. The computational model described herein provides very tight upper and lower limits if the basic geometry assumptions of the model are satisfied and if the temperature distribution is known. Reasonable limiting assumptions about temperature profiles can be useful in bracketing the desired answer but one must know the temperature level either by measurement or calculation.

Incorporation of radiation including self-absorption into a solution of the energy equation such as Weber has done (Ref. 11) for the optically thin case, is the next logical step in the study of this problem. The temperature profile would then be a part of the result rather than a required input. A coordinated experimental program to measure radiant heat flux and/or temperature profiles at high pressure would also be very desirable.

REFERENCES

1. Breene, R. G. and Nardone, M., "Radiant Emission from High Temperature Equilibrium Air", General Electric Company, Philadelphia, Pennsylvania, MSD TIS R61SD2311, May 1961.

2. Nardone, M. C., Breene, R. G., Zeldin, S. S., and Riethof, T. R., "Radiance of Species in High Temperature Air", General Electric Company, Philadelphia, Pennsylvania, MSD TIS R63SD3, June 1963.

3. Finkelnburg, W. and Maecker, H., Handbuck der Physik, Vol. XXII, Berlin, Julius Springer, 1956, pp 305-315.

4. Lochte-Holtgreven, W., Reports on Progress in Physics, London, The Physical Society, 1958, pp 312-383.

5. Cobine, J. D., Gaseous Conductors, New York, Dover Publications, Inc., 1958, p 290.

6. Maecker, H., "Thermal and Electrical Conductivity of Nitrogen up to 15,000°K by Arc Measurements", AGARD Conference, Aachen, Germany, September 1959.

7. Cann, Gordon L., "Energy Transfer Process in a Partially Ionized Gas", Guggenheim Aeronautical Laboratory Memo No. 61, 1961, California Institute of Technology, Pasadena, California.

8. Pugmire, T. K., Weber, H. E., and Marston, C. H., "Arc Heater Development for Re-Entry Simulation", Third Hypervelocity Techniques Symposium, Denver, Colorado, March 1964.

9. Jakob, M., Heat Transfer, Vol II, New York, John Wiley and Sons, Inc., 1949, p 104.

10. Eckert, E. R. G. and Drake, R. M., Heat and Mass Transfer, 2nd ed., New York McGraw-Hill Book Co., 1959.

11. McAdams, Heat Transmission, 3rd ed., New York, McGraw-Hill Book Co., 1954, p 473.

12. Weber, H. E., "Constricted Arc Column Growth", Proceedings of the 1964 Heat Transfer and Fluid Mechanics Institute, Stanford University Press, June 1964.

13. Handbook of Chemistry and Physics, 38th Ed., Cleveland, Ohio, Chemical Rubber Publishing Co., 1956, p 2708.

14. Mayo, R. F. and Davis, Jr., D. D., "Magnetically Diffused Radial Electric Arc-Air Heater Employing Water Cooled Copper Electrodes" Electric Propulsion Development (Progress in Astronautics and Aeronautics Vol. 9), Academic Press, N. Y., 1963.

15. Weber, H. E., "Growth of an Arc Column in Flow and Pressure Fields", AGARD o graph 84, (Proceedings of NATO AGARD Specialists Meeting on Arc Heaters and MHD Accelerators for Aerodynamic Purposes), Rhode-Saint Genèse, Belgium, Sept. 1964.

16. Peng, T. and Pindroh, A. L., "An Improved Calculation of Gas Properties at High Temperatures - Air" Magnetohydrodynamics - Proceedings 4th Biennial Gas Dynamics Symposium, Northwestern University Press, Evanston, Ill, 1962.

17. Raezer, S. D., Bunt, E. A. and Olsen, H. L., "Development of Hypersonic Propulsion Tunnels Using D. C. Plasma Arc Heating" AIAA-ASME Hypersonic Ramjet Conference, NOL, White Oak, Md., April 1963.

18. Pivovonsky, M. and Nagel, M. R., Tables of Black Body Radiation Functions, New York, The MacMillan Co., 1961, p xiv.

19. Greaves, W. R., "Polynomial Curve Fitting, No Constraints", August 22, 1962, IBM, New Orleans, La.

20. Pearce, W. J., "Calculations of True Radial Distribution of Intensities in Symmetric Sources", General Electric Company, Philadelphia, Pennsylvania, MSD TIS 57SD761, 1957.

21. Sadjian, H., "Calculation of the Intensity Temperature Profile of A Spectral Line", General Electric Company, Philadelphia, Pennsylvania, Aerodynamics Technical Memorandum #1, 1958.

APPENDIX A

CALCULATION OF ENERGY FRACTION

For a given wavenumber interval, $\Delta n = n_2 - n_1$, let η be the fraction of the total energy flux radiated by a black body at a given temperature which falls within this interval

$$\eta = D_1 - D_2 \tag{A.1}$$

where

$$D = \frac{\int_n^\infty W_{B,n}\, dn}{\int_0^\infty W_{B,n}\, dn} \tag{A.2}$$

The function D is available in tabular form, (Ref. 18) but, for computer application, direct generation of η by series expansion was desired. Two series were used.

1. Pivovonsky and Nagel (Ref. 18) gives a series expansion for D as

$$D = 1 - \frac{15}{\pi^4} v^3 \left(\frac{1}{3} - \frac{v}{8} + \frac{v^2}{60} - \frac{v^4}{5040} + \frac{v^6}{272160} - \cdots \right) \tag{A.3}$$

where

$$v = \frac{c_2 n}{T} = \frac{1.4380n}{T} \tag{A.4}$$

This series converges for $v < 2\pi$ but convergence is slow when $v > 1$. Defining

$$\bar{v} \equiv \frac{v_2 + v_1}{2} \quad ; \quad \Delta v \equiv \frac{v_2 - v_1}{2} \tag{A.5}$$

Equation A.3 was transformed to

$$\eta = \frac{15}{\pi^4} \left\{ \Delta v \left(\bar{v}^2 - \frac{\bar{v}^3}{2} + \frac{\bar{v}^4}{12} - \frac{\bar{v}^6}{720} + \ldots . \right. \right.$$

$$+ (\Delta v)^3 \left(\frac{1}{12} - \frac{\bar{v}}{8} + \frac{\bar{v}^2}{24} - \frac{\bar{v}^4}{576} + \ldots . \right.$$

$$\left. \left. + (\Delta v)^5 \left(\frac{1}{960} - \frac{v^2}{3840} + \ldots . \right) + 0 \left[(\Delta v)^7 \right] + \ldots . \right\} \tag{A.6}$$

and used to calculate η when $\bar{v} \leq 1$. Inclusion of the terms shown through order $(\Delta v)^3$ results in a value of η accurate to $\pm 0.1\%$.

2. While D itself cannot be expressed in closed form, its derivatives can be. Since η is the difference between two values of D, the zero order term of a Taylor expansion of η vanishes. Expansion about $\bar{v}$ eliminates all even order derivatives, thus

$$\eta = \left[(v_1 - \bar{v}) - (v_2 - \bar{v}) \right] \left[\frac{\partial D}{\partial v} \right]_{v = \bar{v}}$$

$$+ \frac{1}{3!} \left[(v_1 - \bar{v})^3 - (v_2 - \bar{v})^3 \right] \left[\frac{\partial^3 D}{\partial v^3} \right]_{v=\bar{v}} + \ldots . \tag{A.7}$$

Since

$$\frac{\partial D}{\partial v} = - \frac{15}{\pi^4} \frac{v^3}{(e^v - 1)} \tag{A.8}$$

the energy fraction becomes

$$\eta = \frac{15}{\pi^4} \left\{ (\Delta v) \left[\frac{\bar{v}^3}{e^{\bar{v}} - 1} \right] + (\Delta v)^3 \left[\frac{\bar{v}}{3!(e^{v} - 1)^3} \right] \left[(6 + \bar{v}^2 + 6\bar{v} - 12)\, e^{v} + (\bar{v}^2 - 6\bar{v} + 6)\, e^{2v} \right] + \ldots \right\} \quad \text{(A. 9)}$$

Retaining only the term of order Δv, Eq. (A.9) was used to calculate η to $\pm$ 0.6% when $v > 1$. The curve $v = 1$ on Fig. 3.1 separates the region of application of the two methods.

APPENDIX B

PROGRAM ARCRAD

B.1 PURPOSE

The purpose of this program is the calculation of radiation heat flux from a cylindrical air arc based on spectral emission-absorption characteristics of air and a measured or assumed temperature profile.

B.2 GLOSSARY OF TERMS

Fortran Name	Formula Name	Description
ABEMIS(22)		Intermediate array used in calculation of EOUT.
AINC		Decrease in wave number.
ALPHA(10)	x	Angles used for absorption lengths for calculation EXTRMN and EXTRMX and EIN.
AMAX		Running sum of maximum radiation heat flux from all annuli of cylinder (excluding core) - final sum corresponds to only one wave number WN(I).
AMIN		Running sum of minimum radiation heat flux.
AKDR(45)		Components of linear absorption path.
ANGADD	x/2	Angle difference in radians of elements of ANGLE array.
ANGLE(20)		Angles used for absorption lengths and transmissivity for interior radiation.
B		Intermediate value in calculation of RI array.
BCDREC(14)		Storage locations for reading BCD input.
BUFF2(525)		Buffer for labeled and blocked tape on A6.
BUFFT(86)		I-O buffer storage total.
C		Intermediate value in calculation RI array RI(NQ, 1).

Fortran Name	Formula Name	Description
ENTRMN	$\tau_{i,\,LL}$	Minimum transmissivity for interior radiation.
ENTRMX	$\tau_{i,\,UL}$	Maximum transmissivity for interior radiation.
EOUT	ϵ_e	Emissivity exterior.
EPSMN		Minimum interior emissivity.
EPSMX		Maximum interior emissivity.
ETA(23, 121)	η	Fraction of total energy radiated by black body at annulus temperature and wave number.
ETASM(23)		ETA of each temperature summed over all wave numbers.
EXRQSN(22, 10)		Intermediate array used in calculation of R array.
EXSNRQ(22, 10)		Intermediate array used in calculation of R array.
EXTRMN	$\tau_{e,\,LL}$	Minimum transmissivity of exterior radiation.
EXTRMX	$\tau_{e,\,UL}$	Maximum transmissivity of exterior radiation.
FKR(20)		Empirical approximation of one of the integrals used in calculation of transmissivity and interior emissivity.
FMT(12)		Storage for input Hollerith identification.
I		Index for reading in data on tape A2, for printing output on tapes A3 and A6, and indexing wave numbers.

Fortran Name	Formula Name	Description
I1		Index used in reordering the part of TRYKDR array - associated with 2 consecutive ALPHA - in ascending order.
I2		Index used in reordering part of TRYKDR array in ascending order.
IAL		Subscript used in ordering linear absorption path for interior radiation.
IOPT 1		Option for printing on A6 - save tape used in printer.
IP 1		Lower limit of I2 index.
IPST		Adjustment value used in selecting linear absorption coefficients from proper input records.
J		Subscript used to find annulus position - used in determining AKDR array for interior radiation.
JAL		Upper limit for I1 limit.
K		Index used for reading record of files of input tape.
LAL		Index for reordering entire TRYKDR array.
MAL		Lower limit of I1 index.
N		Index for annuli.
NA		Index for ALPHA array.
NAH		Subscript used in calculating EXTRMN.

Fortran Name	Formula Name	Description
NAL		Upper limit of I2 index.
NALPHA		Number of members in ALPHA array.
NANGLE		Number of members in ANGLE array.
NAVE		Index for ANGLE array.
NCASE		Number of cases of data to be used for a computer run.
NDIV		Number of sectors of half cylinder.
NFAC		NTOUCH+1 - the first annulus counting from core outward that the linear absorption path of interior radiation intersects.
NFILE		Counter for file number used during read in process.
NH		Value used as part of subscript in calculation of EXTRMN.
NJ		Subscript used in ordering and summing the components of linear absorption path of interior radiation.
NPP		Upper limit of K index.
NQ		Index used in calculation of R along linear absorption path of both interior and exterior radiation - also used in interior radiation.
NRAVE	s	Number of divisions of the sectors of half cylinder.

Fortran Name	Formula Name	Description
C2T(23)	σ / T	Intermediate array used in calculation of V.
CORMN(121)		Minimum radiation heat flux of core - corresponds to one wave number.
CORMX (121)		Maximum radiation heat flux of core.
D		Intermediate value used in calculation of RI array-RI(NQ, 2)
DALPHA	$\pi/2s$	Angle difference in degrees of the elements of ALPHA array.
DELTA	δ	Radius of arc column.
DK		Absorption length along diameter of arc column.
DR(23)		Annulus thickness - outermost inward.
DRK		Absorption length at 0^{o} used in exterior radiation.
DSINA(20)		Sine of angles of ALPHA array.
DV(23)		Intermediate value in calculation of ETA array.
EIN	ϵ_i	Emissivity inward.
EKDR(10)		Absorption length used in calculation of EIN.
ENSNA(20)		Sine of angles of ANGLE array.
ENSNRQ(23, 20)		Intermediate array used in calculation of RI array.
ENRQSN(23, 20)		Intermediate array used in calculation of RI array.

Fortran Name	Formula Name	Description
NR		NT+1 number of annuli plus one.
NTEST		Number of annuli (depending on position of radiating annulus) including core and going outward which may be intersected in two positions - used in calculation of RI for interior linear absorption path.
NTOUCH		Last annulus (considering core as annuli one) not intersected by interior linear absorption path.
NT	m	Number of annuli of constant temperature of the cylinder.
NTR		NT-1 number of annuli minus one.
NUMDR		Number of components of interior linear absorption path.
NWBIN		Control parameter = 0 to read in entire binary word.
NWBCD		Control parameter = 0 to read in entire BCD record.
NW		Number of wave numbers.
OPT		Running sum of radiation heat flux from all annuli (not including core) - assuming gas non-self absorbing.
OPTCOR(121)		Radiation from core assuming gas non-self absorbing.
QMAX(121)	W_{UL}	Radiation heat flux per wave number at boundary of cylinder considering maximum transmissivity.

Fortran Name	Formula Name	Description
QMIN(121)	W_{LL}	Radiation heat flux per wave number at boundary of cylinder - considering minimum transmissivity.
QOPT(121)	W_{OP}	Radiation heat flux per wave number at boundary of cylinder - assuming gas non-self absorbing.
QOPTSM		Radiant heat flux QOPT(I) summed over all wave numbers.
QSUMMN		Minimum radiant heat flux QMIN(I) summed over all wave numbers.
QSUMMX		Maximum radiant heat flux QMAX(I) summed over all wave numbers.
RAD(23)	r	Array of radii ordered from outermost annulus in to core.
RADQ(23)		Array of radii order from core to outermost annulus.
RAVE	s	Floating NRAVE.
RADLPH		Increment in radians of elements of ALPHA array.
RDELTA(23)		Array of radii of annuli over radius of cylinder - from outermost annulus in to core.
REC(700)		Storage for reading in binary words.
RHO (23)	log P/Po	Log of density of annuli from outermost annuli in to core.
RI(23, 2)	R^+ R^-	Sector radii array along path of interior radiation.

Fortran Name	Formula Name	Description
R(22)	R	Sector radii along path of exterior radiation.
SIGMA		Intermediate value in calculation of RI array.
SINA		Sine of ALPHA array.
SKDR	$\overline{KR}$	Dimensionals absorption length used in calculation of transmissivity.
SMCRMN		Sum over all wave numbers of minimum radiant heat flux core (CORMN(I)).
SMCRMX		Sum over all wave numbers of maximum radiant heat flux from core (CORMX(I)).
SMOPTC		Sum over all wave numbers of radiant heat flux from core (OPTCOR(I)) - assuming gas is non self-absorbing.
SUM		Intermediate value used in summing.
TEMP(23)	T	Temperature array - corresponding to outermost annulus in to core.
TEMPL		Temporary storage used in reordering of TRYKDR array.
TEMPRW(23)		Intermediate array used in calculation - σT^4.
TEMPS		Temporary storage used in reordering TRYKDR array.
V	v	Parameter using Plank radiation function for the calculation of ETA array.

Fortran Name	Formula Name	Description
V2		Second power of V.
V3		Third power of V.
V4		Fourth power of V.
V6		Sixth power of V.
WBB		Intermediate value in calculation of WIN and WOUT.
WIN		Radiation inward - gas non self-absorbing.
WINMN		Radiation inward - considering minimum transmissivity.
WINMX		Radiation inward - considering maximum transmissivity.
WNA		Highest wave number plus AINC.
WN(121)	λ	Wave number array.
WOUT		Radiation outward - gas non self-absorbing.
WOUTMN		Radiation outward considering minimum transmissivity.
WOUTMX		Radiation outward considering maximum transmissivity.
X		Intermediate value in calculation of ETA.
Y(4)		Array used in printing on save tape A6.
Z		Intermediate value in calculation of ETA.

B.3 INITIALIZATION AND INPUT, PROGRAM NOTES

B.3.1 Initialization

1. General Initialization

   The Initial sequence sets aside 86 locations in the BUFFT array for the I-O buffer. Input requires 39 locations-output 47 locations.

2. Input Initialization

   Call ABUF1 sets up input buffer on A5. To read BCD, decimal tape number is 645. To read BIN, decimal tape number is 661. Logical tape number is 15.

3. Output Initialization

   BUFFS sets up output buffer on A6 to write labeled and blocked tape. To read BIN, decimal tape number is 662. Logical tape number is 16.

4. Header for File of LBT on A6

   Call LBID, specifies a BCD file name for label of a labeled and blocker tape to be written on A6. Call LBID for each file.

5. Identification of Case

   Call SPGHDR (FMT): page header is written with 12 BCD words of array FMT. Call SPGHDR for every case.

6. Error Initialization

   ERTRP allows printout and transfer to next case

B.3.2 Input

1. Tape

   Binary tape data is input for temperature 3000°K-25000°K. This is a tape with 23 files, one file per temperature. A description of tape will be given in B.3.3.

2. Cards

   a. number of cases (fixed point)

   b. Cards per case

      1) identification card

      2) Radius of cylinder, decrease in wave number, highest wave number - AINC, angle difference in degrees of array ALPHA, divisions of original sectors (ALPHA array) of half cylinder (floating point)

      3) number of wave numbers, number of annuli or temperatures, option for writing output tape, NT-1, NT+1, number of angles in ALPHA array, divisions of original sectors of half cylinder (fixed point)

      4) temperature array: temperatures of annuli from outermost temperatures must be multiples of thousands in ascending order into core (floating point).

      5) radius array: radii of annuli from outermost into core+1 (floating point)

      6) radius array: radii of annuli from core to outermost (floating point)

      7) log of density ratio array - log of density ratio of annuli from outermost into core (floating point)

B.3.3 Read in Process

Read in linear absorption coefficients for each case, interpolating as necessary.

1. General

   A table of absorption coefficient data is interpolated with density selected from input tape and set up as a function of temperature and wave number, f (TEMP, WN)

2. Format

Data is stored in files. Each file corresponds to a temperature. File temperatures range from 3000°K to 25000°K in 1000°K increments.
The first file (3000°K) is made up of 5 records. Record 1 is a BCD label. Record 2 is main table heading. The main table headings are: NT, TEMP(1), TEMP(2)... TEMP(23). Record 3 contains the number of words in the data subtable, plus heading: NW, ND, FMIC(1) FMIC(2)...FMIC(NW) DENS(1), DENS(2)...DENS(ND).

Note: NT is number of files

NW is number of wave numbers (21)

ND is the number of densities (5)

FMIC(1) is micron value of WN(1) = 10/WN(1)

FMIC(NW) is micron value of WN(NW)=10/WN(NW)

DENS(1) = -3 (RHO/RHOO)

DENS(ND) = 1 (RHO/RHOO)

Record 4 consists of one word, the temperature of the file. The last record, record 5, is the data subtable and contains linear absorption coefficients for the temperature of the file for all wave numbers for each of the 5 log density ratios. The remaining 22 files are composed of 3 records, corresponding to the format of the last 3 records of file 1: a subtable record, a temperature record, and a data record.

Temperatures (multiples of 1000°K) in array TEMP are stored in ascending order as are the file temperatures. Reading of files is controlled by DO N=1, NT (number of temperatures). Records of files are read up to and including temperature record. If the first and only word of the temperature record is not equal to the indexed TEMP(N), the file is closed and the next file is then read

in a similar manner. If TEMP(N) and the one word of the temperature record are equal, the following record is read and processed for all wave numbers (61500-1500) to obtain the absorption coefficients. PROP(N, 1) through PROP(N, 121) for TEMP(N) with its associated log of density ratio (RHO(N). The file is closed, the index for TEMP(N) is increased by 1 and the reading process continued to obrain linear absorption coefficients for all the indexed temperatures. The first file is read as a special case. The BCD record is read by a special instruction and then the 3 following records must be read to include the temperature record. The remaining 22 files are similar in read instructions; 2 records are read, the second being temperature record.

Records are all read in REC(700) which is large enough to include the largest record (the last) of the files.

The data for TEMP(N) is stored as a function of density and wavenumber in the following order: $f(d_1, NW_1)$ $f(d_2, NW_1), \ldots f(d_5, NW_1)$, $f(d_1, NW_2)$, $f(d_2, NW_2), \ldots$ $f(d_5, NW_2), \ldots f(d_5, NW_{121})$. Where d is density and NW is wave number. Thus the data record (last record of each file) can be treated as 121 groups of 5. Each group corresponding to one wave number. The 5 linear absorption coefficients in each group are arranged in ascending order of log density ratio -3, -2, -1, 0, 1.

If the RHO(N) corresponding to TEMP(N) is an integer value between -3 and 1, the value IPST, which is the subscript of array REC is assigned as follows:

IPST = 1 if RHO(N) = -3

IPST = 2 if RHO(N) = -2

IPST = 3 if RHO(N) = -1

IPST = 4 if RHO(N) = 0

IPST = 5 if RHO(N) = -1

Control is then transferred to DO loop - DO I = 1, NW(121). The value REC(IPST) is read directly for linear absorption coefficient for first wave number. IPST is increased by 5 in last step of DO loop. When the DO is satisfied the linear absorption coefficients PROP(N, 1) through PROP(N, 121) are obtained for TEMP(N) with its corresponding RHO(N).

If RHO(N) is not an integer value but within the integer range, the linear absorption coefficient is obtained by logarithmic interpolation between tabulated values. IPST is set corresponding to the next lower RHO(N), e.g. RHO(N) = -2.5, IPST=1, PCNT is the fractional difference between tabulated values, REC(IPST) and REC(IPST+1). PCNT is equal to RHO(N) minus integer values less than RHO(N). Control is then transferred to a DO loop - DO I = 1, NW(121). Linear absorption coefficient for first wave numbers equals antilog of PCNT {log [REC (IPST + 1)] - log [REC (IPST)] } + log [REC (IPST)]. IPST is increased by 5 in last step of DO loop. When the DO is satisfied the linear absorption coefficients to PROP(N, 1) through PROP(N, 121) are obtained for TEMP (N) with its corresponding RHO(N).

If RHO(N) is greater than 1, PCNT is calculated as previously stated, and IPST is set equal to 5. Absorption coefficient is logarithmically extrapolated based on values of REC (IPST) and REC (IPST - 1).

The log difference of REC(IPST) and REC(IPST-1) is added to REC(IPST) and an antilog is taken to obtain in DO loop similiar to the one previously described PROP (N, 1) through PROP(N, 121) for TEMP(N) with its corresponding RHO(N).

This concludes the read in part of the program. Notes related to the remainder of the program are incorporated in the block diagram, section B. 4.

B.4 BLOCK DIAGRAM AND PROGRAM NOTES

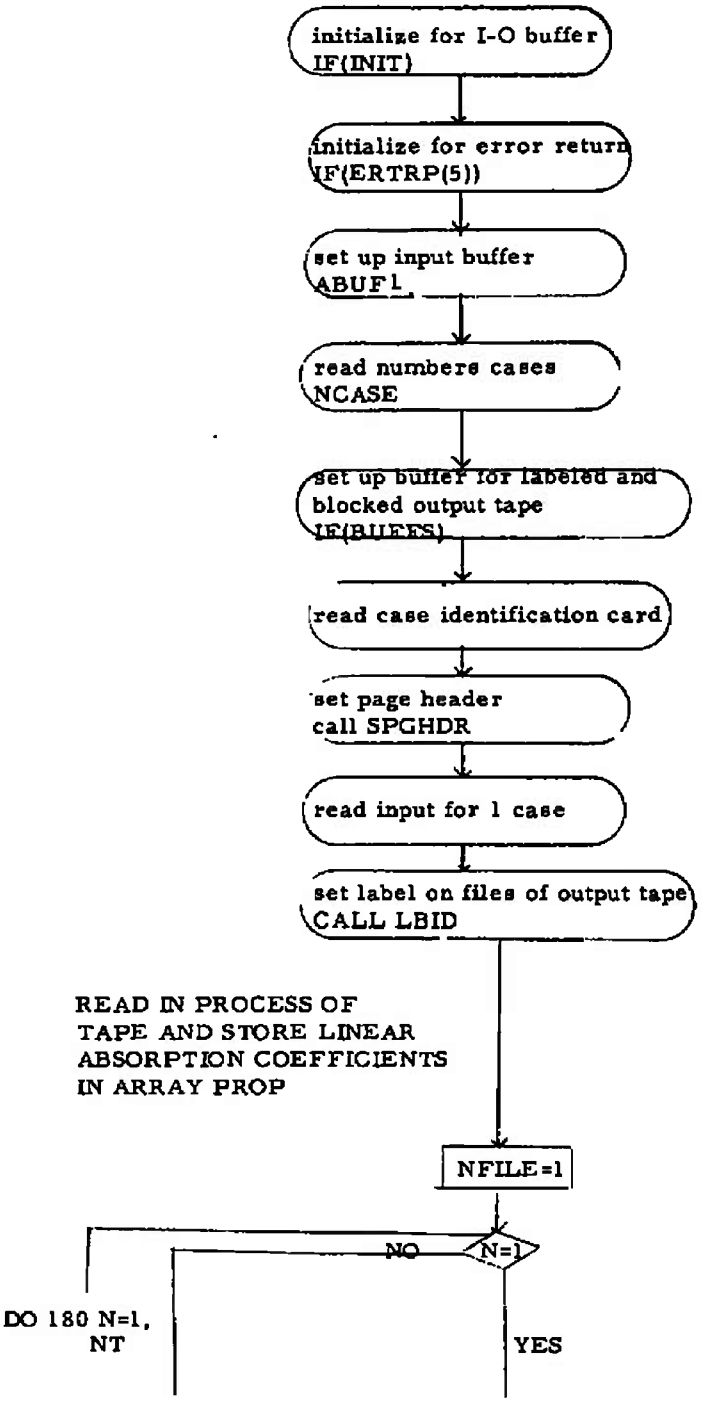

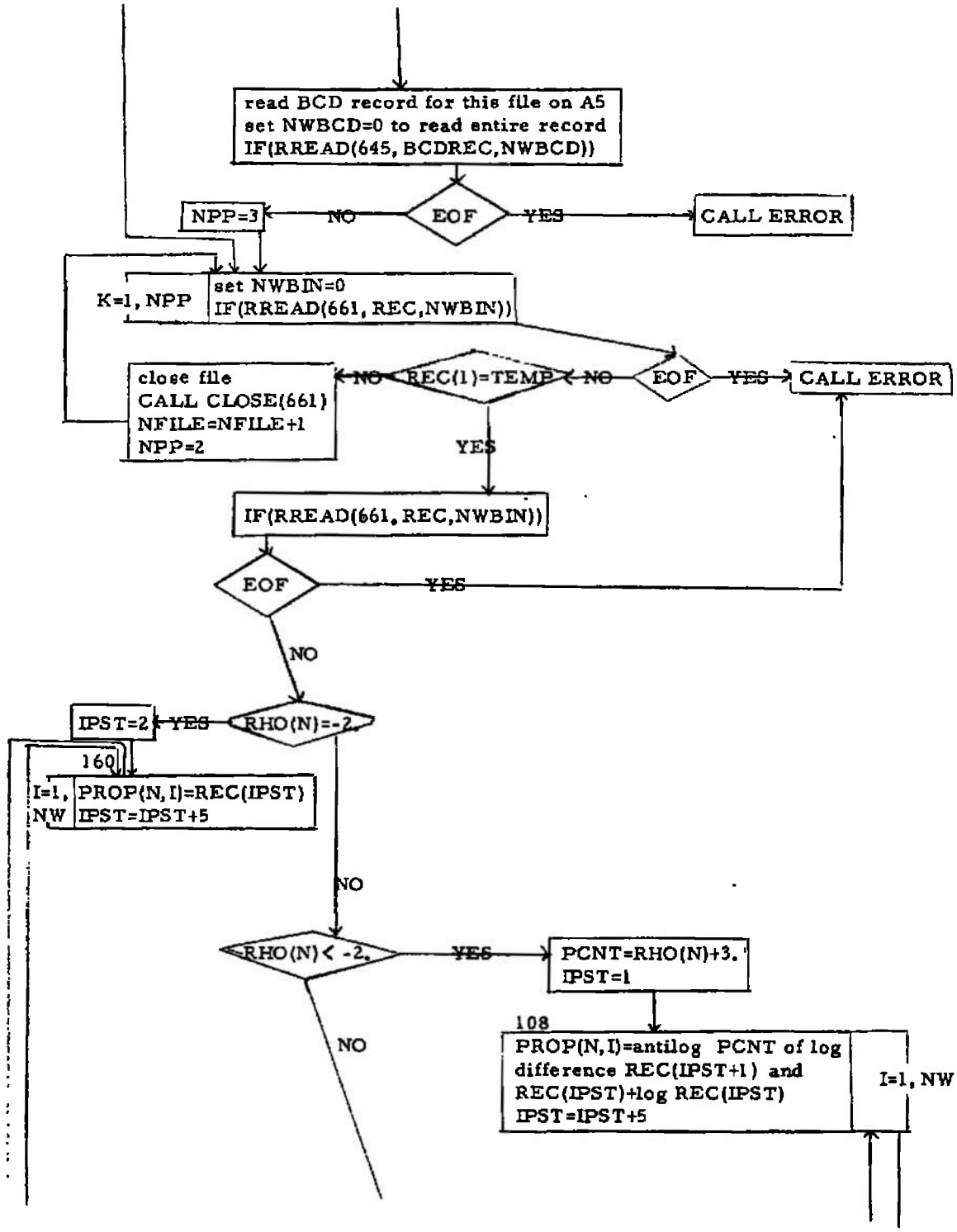
read BCD record for this file on A5
set NWBCD=0 to read entire record
IF(RREAD(645, BCDREC,NWBCD))
EOF
YES
CALL ERROR
NO
NPP=3
K=1, NPP
set NWBIN=0
IF(RREAD(661, REC,NWBIN))
EOF
YES
CALL ERROR
NO
REC(1)=TEMP
NO
close file
CALL CLOSE(661)
NFILE=NFILE+1
NPP=2
YES
IF(RREAD(661, REC,NWBIN))
EOF
YES
NO
RHO(N)=-2.
YES
IPST=2
160
I=1, NW
PROP(N, I)=REC(IPST)
IPST=IPST+5
NO
RHO(N)< -2.
YES
PCNT=RHO(N)+3.
IPST=1
NO
108
PROP(N,I)=antilog PCNT of log difference REC(IPST+1) and REC(IPST)+log REC(IPST)
IPST=IPST+5
I=1, NW

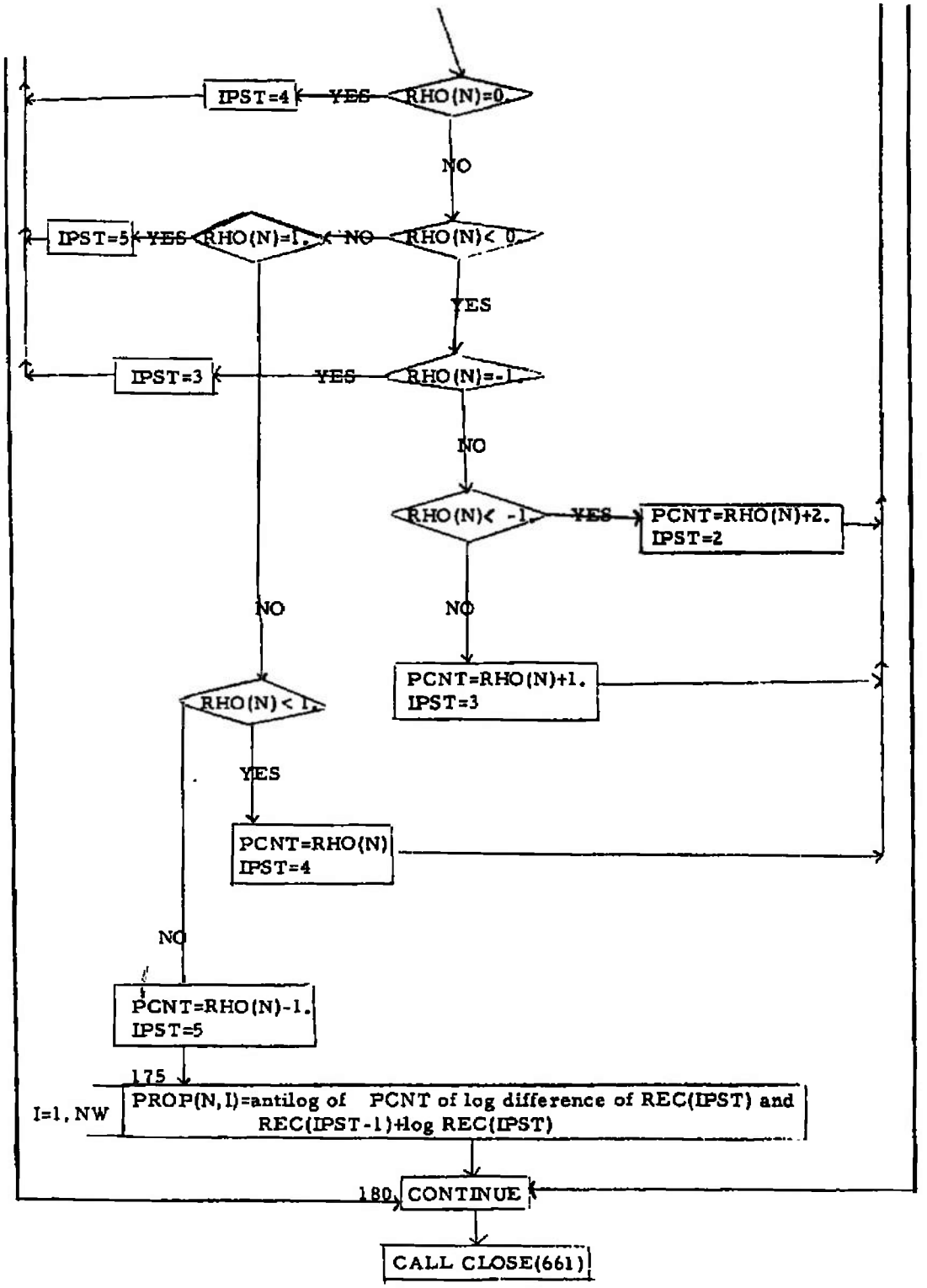
RHO(N)=0.
YES
IPST=4
NO
RHO(N)< 0.
NO
RHO(N)=1.
YES
IPST=5
YES
NO
RHO(N)=-1.
YES
IPST=3
NO
RHO(N)< -1.
YES
PCNT=RHO(N)+2.
IPST=2
NO
NO
PCNT=RHO(N)+1.
IPST=3
RHO(N) < 1.
YES
PCNT=RHO(N)
IPST=4
NO
PCNT=RHO(N)-1.
IPST=5
175
I=1, NW
PROP(N, I)=antilog of PCNT of log difference of REC(IPST) and REC(IPST-1)+log REC(IPST)
180
CONTINUE
CALL CLOSE(661)

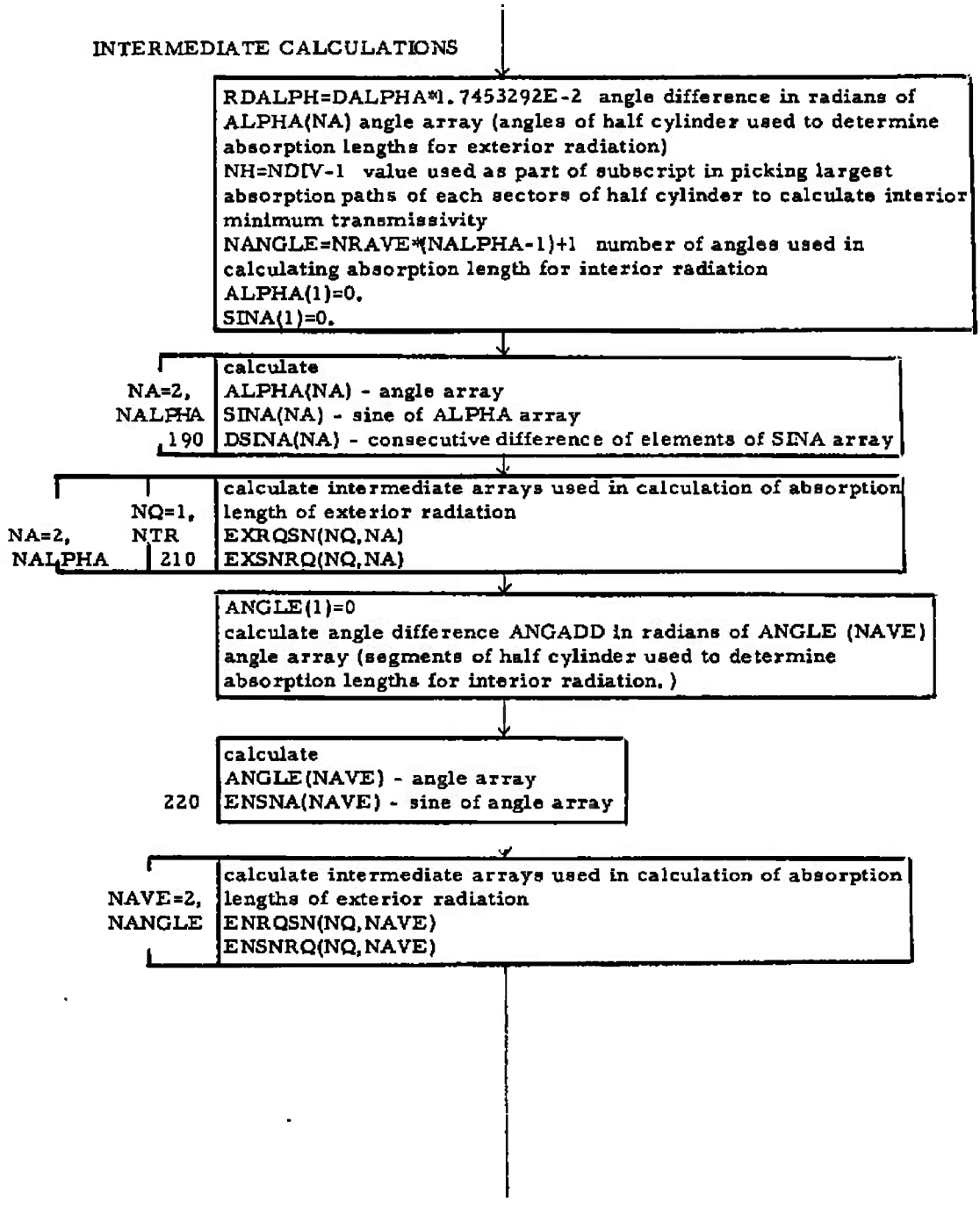
INTERMEDIATE CALCULATIONS
RDALPH=DALPHA*1.7453292E-2 angle difference in radians of ALPHA(NA) angle array (angles of half cylinder used to determine absorption lengths for exterior radiation)
NH=NDIV-1 value used as part of subscript in picking largest absorption paths of each sectors of half cylinder to calculate interior minimum transmissivity
NANGLE=NRAVE*(NALPHA-1)+1 number of angles used in calculating absorption length for interior radiation
ALPHA(1)=0.
SINA(1)=0.
NA=2, NALPHA
190
calculate
ALPHA(NA) - angle array
SINA(NA) - sine of ALPHA array
DSINA(NA) - consecutive difference of elements of SINA array
NA=2, NALPHA
NQ=1, NTR
210
calculate intermediate arrays used in calculation of absorption length of exterior radiation
EXRQSN(NQ,NA)
EXSNRQ(NQ,NA)
ANGLE(1)=0
calculate angle difference ANGADD in radians of ANGLE (NAVE) angle array (segments of half cylinder used to determine absorption lengths for interior radiation.)
220
calculate
ANGLE(NAVE) - angle array
ENSNA(NAVE) - sine of angle array
NAVE=2, NANGLE
calculate intermediate arrays used in calculation of absorption lengths of exterior radiation
ENRQSN(NQ,NAVE)
ENSNRQ(NQ,NAVE)

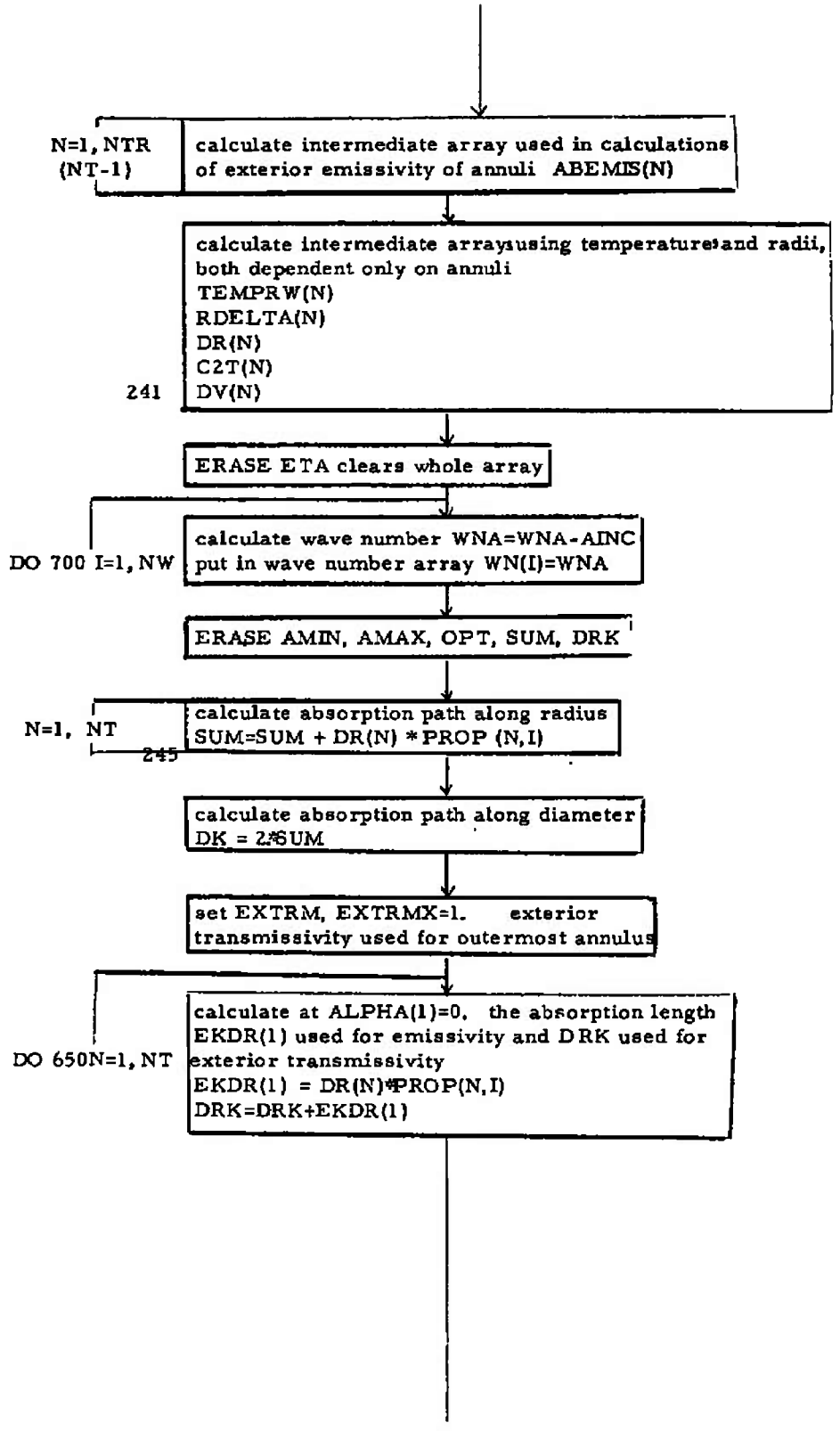
N=1, NTR
(NT-1)
calculate intermediate array used in calculations of exterior emissivity of annuli ABEMIS(N)
calculate intermediate arrays using temperatures and radii, both dependent only on annuli
TEMPRW(N)
RDELTA(N)
DR(N)
C2T(N)
241
DV(N)
ERASE ETA clears whole array
DO 700 I=1, NW
calculate wave number WNA=WNA-AINC
put in wave number array WN(I)=WNA
ERASE AMIN, AMAX, OPT, SUM, DRK
N=1, NT
245
calculate absorption path along radius
SUM=SUM + DR(N) * PROP (N,I)
calculate absorption path along diameter
DK = 2*SUM
set EXTRM, EXTRMX=1. exterior transmissivity used for outermost annulus
DO 650N=1, NT
calculate at ALPHA(1)=0. the absorption length EKDR(1) used for emissivity and DRK used for exterior transmissivity
EKDR(1) = DR(N)*PROP(N,I)
DRK=DRK+EKDR(1)

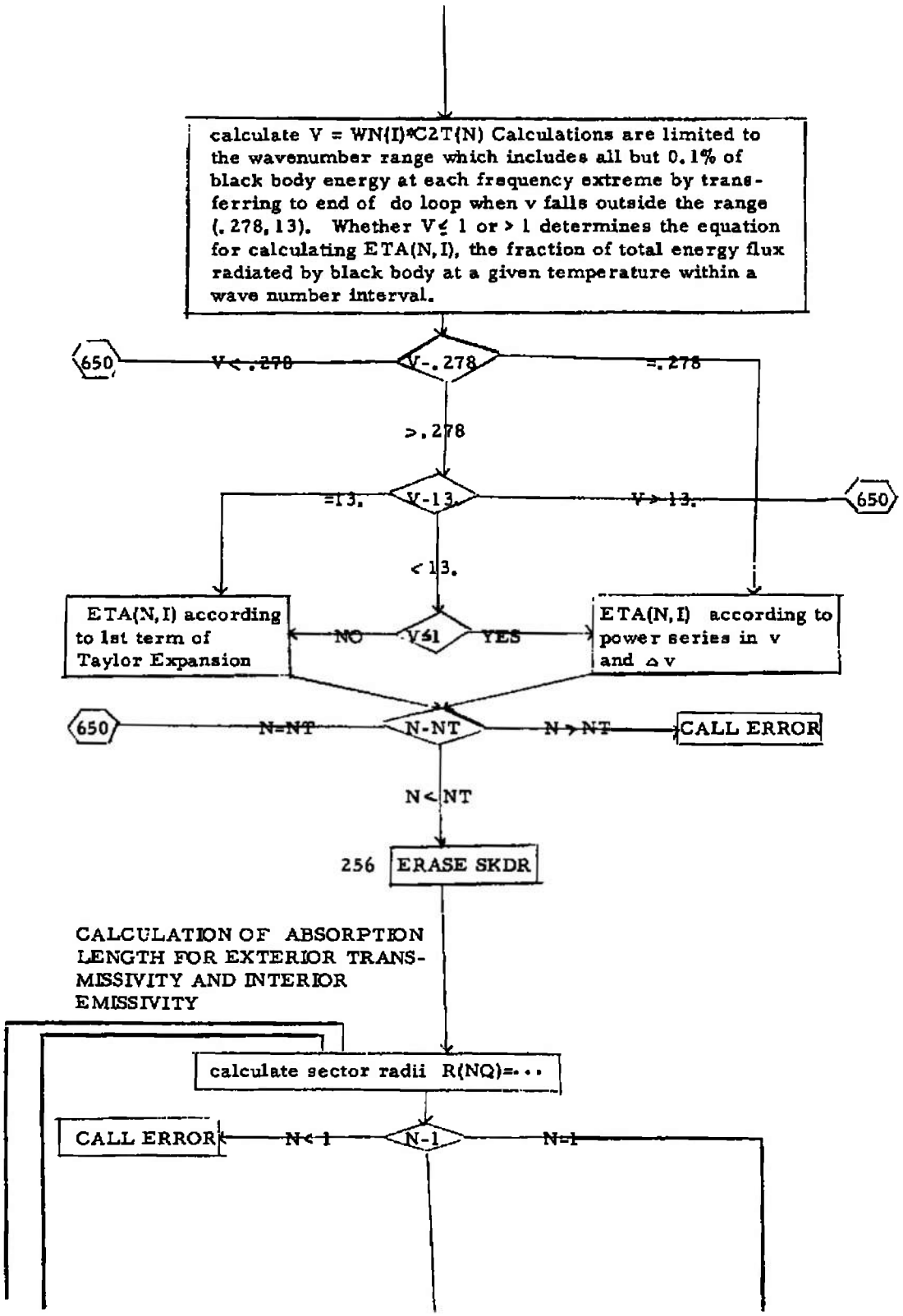
calculate V = WN(I)*C2T(N) Calculations are limited to the wavenumber range which includes all but 0.1% of black body energy at each frequency extreme by transferring to end of do loop when v falls outside the range (.278, 13). Whether V ≤ 1 or > 1 determines the equation for calculating ETA(N,I), the fraction of total energy flux radiated by black body at a given temperature within a wave number interval.
650
V<.278
V-.278
=.278
>.278
=13.
V-13.
V>13.
650
<13.
ETA(N,I) according to 1st term of Taylor Expansion
NO
V≤1
YES
ETA(N,I) according to power series in v and Δv
650
N=NT
N-NT
N>NT
CALL ERROR
N<NT
256
ERASE SKDR
CALCULATION OF ABSORPTION LENGTH FOR EXTERIOR TRANSMISSIVITY AND INTERIOR EMISSIVITY
calculate sector radii R(NQ)=...
CALL ERROR
N<1
N-1
N=1

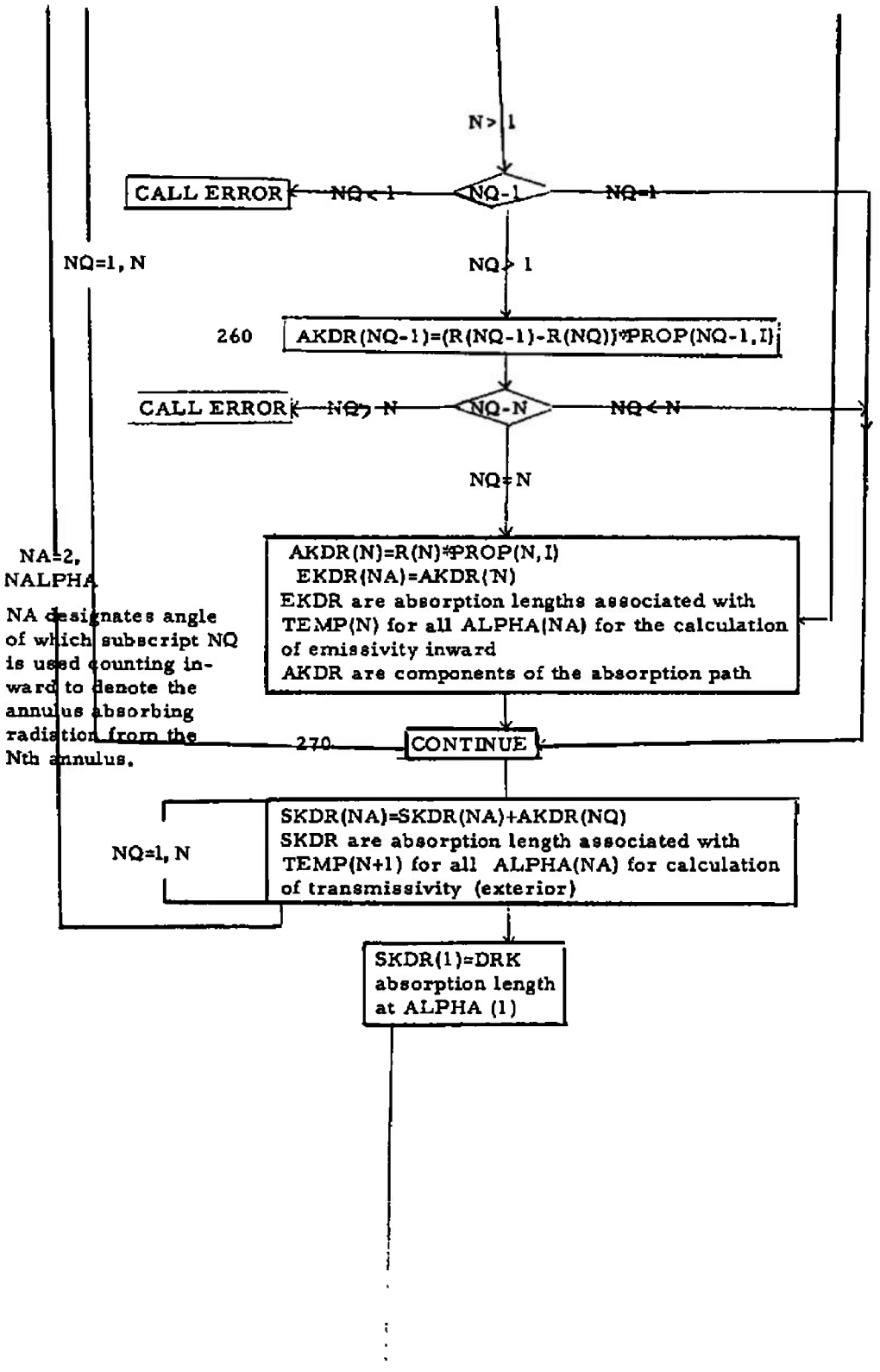
N> 1
CALL ERROR
NQ< 1
NQ-1
NQ=1
NQ=1, N
NQ> 1
260
AKDR(NQ-1)=(R(NQ-1)-R(NQ))*PROP(NQ-1,I)
CALL ERROR
NQ> N
NQ-N
NQ< N
NQ=N
AKDR(N)=R(N)*PROP(N,I)
EKDR(NA)=AKDR(N)
EKDR are absorption lengths associated with TEMP(N) for all ALPHA(NA) for the calculation of emissivity inward
AKDR are components of the absorption path
NA=2, NALPHA
NA designates angle of which subscript NQ is used counting inward to denote the annulus absorbing radiation from the Nth annulus.
270
CONTINUE
NQ=1, N
SKDR(NA)=SKDR(NA)+AKDR(NQ)
SKDR are absorption length associated with TEMP(N+1) for all ALPHA(NA) for calculation of transmissivity (exterior)
SKDR(1)=DRK
absorption length
at ALPHA (1)

CALCULATION OF INTERIOR EMISSIVITY

FKR(NA) is an empirical approximation to the transmissivity integral; the solution of FKR(NA) varies if EKDR(NA) ≤ 1. or ≥ 16.

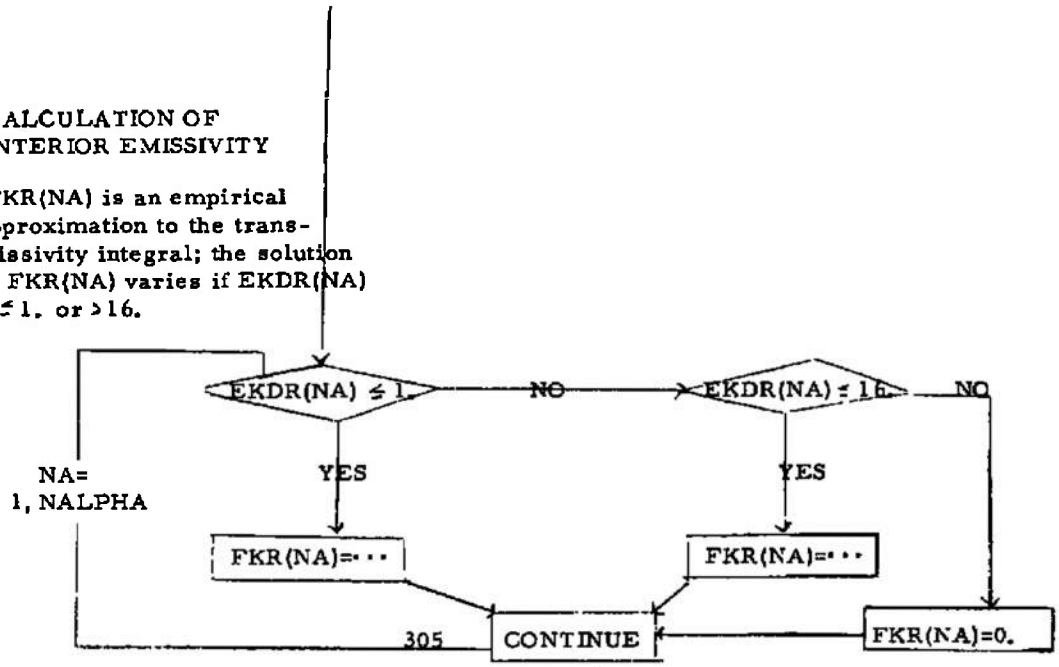

Interior emissivity of a single annulus is identical to transmissivity of that annulus alone relative to the next interior annulus.

Transmissivity is sum of products of 2 integrals, one being DSINA(NA) the other approximated by FKR(NA)

The lower limit of transmissivity corresponds to sector-segment coincidence at NA=2, ··· NALPHA - upper limit at NA=1, ··· NALPHA-1

Prior to the Do statement EXTRMN and EXTRMX are set equal to 1. and this is the value used when the Do loop index has its initial value (N=1). Later in the loop EXTRMN and EXTRMX are calculated for use when the index is increased by one.

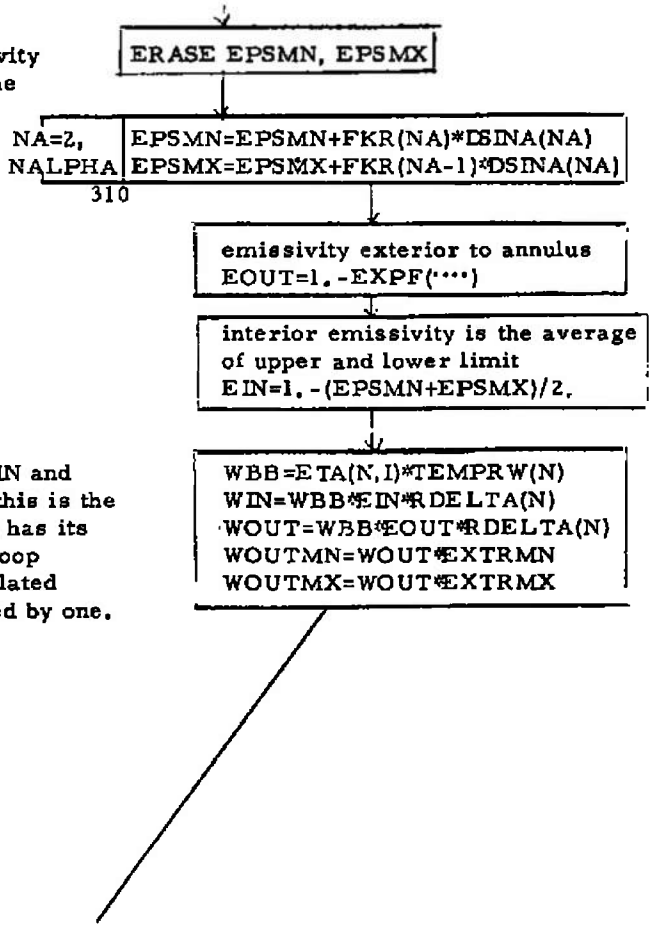

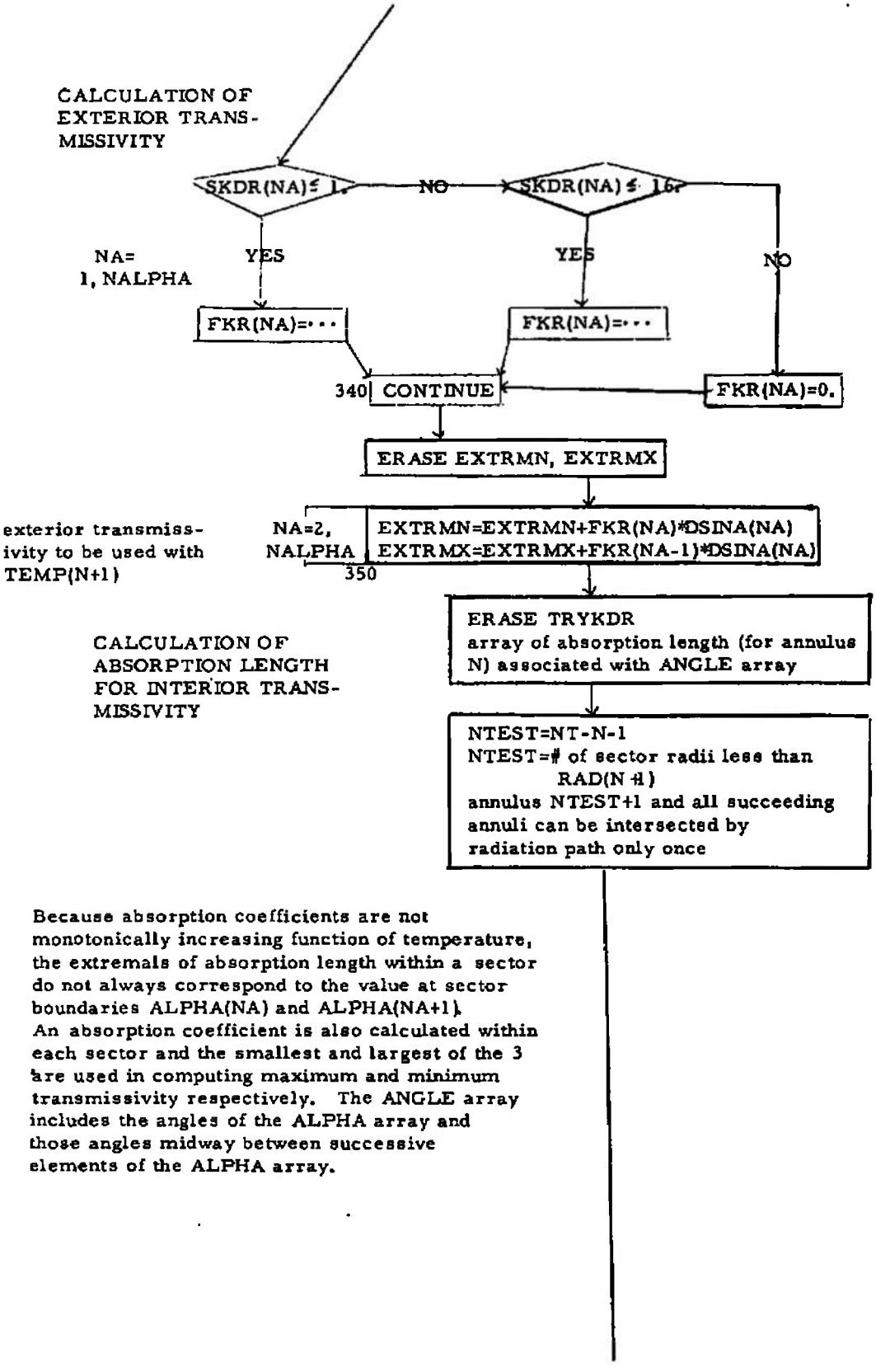
CALCULATION OF EXTERIOR TRANS-MISSIVITY
SKDR(NA)≤ 1.
NO
SKDR(NA) ≤ 16.
NA= 1, NALPHA
YES
YES
NO
FKR(NA)=...
FKR(NA)=...
340 CONTINUE
FKR(NA)=0.
ERASE EXTRMN, EXTRMX
exterior transmissivity to be used with TEMP(N+1)
NA=2, NALPHA
EXTRMN=EXTRMN+FKR(NA)*DSINA(NA)
EXTRMX=EXTRMX+FKR(NA-1)*DSINA(NA)
350
CALCULATION OF ABSORPTION LENGTH FOR INTERIOR TRANS-MISSIVITY
ERASE TRYKDR
array of absorption length (for annulus N) associated with ANGLE array
NTEST=NT-N-1
NTEST=# of sector radii less than RAD(N+1)
annulus NTEST+1 and all succeeding annuli can be intersected by radiation path only once
Because absorption coefficients are not monotonically increasing function of temperature, the extremals of absorption length within a sector do not always correspond to the value at sector boundaries ALPHA(NA) and ALPHA(NA+1). An absorption coefficient is also calculated within each sector and the smallest and largest of the 3 are used in computing maximum and minimum transmissivity respectively. The ANGLE array includes the angles of the ALPHA array and those angles midway between successive elements of the ALPHA array.

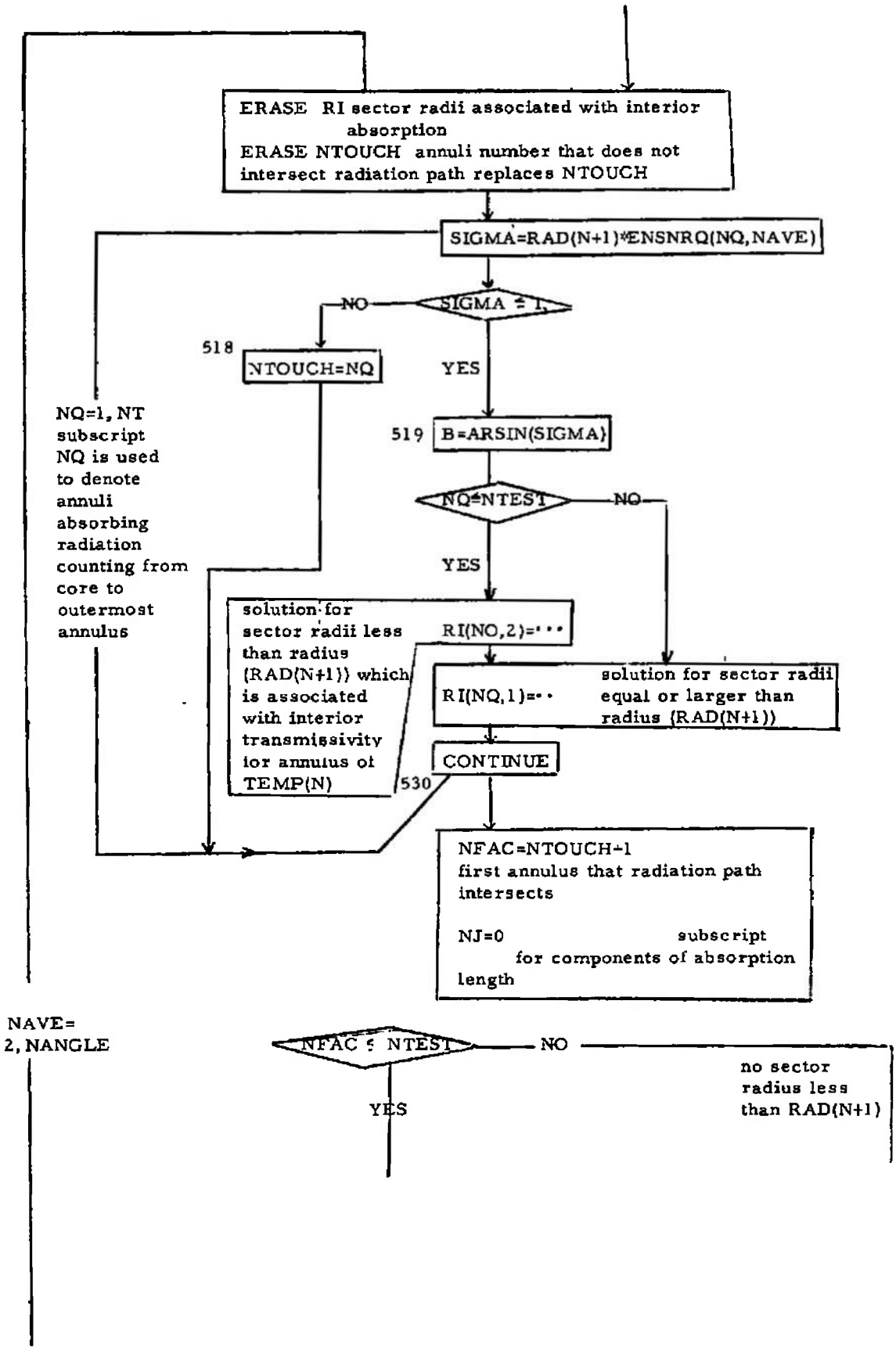
ERASE RI sector radii associated with interior absorption
ERASE NTOUCH annuli number that does not intersect radiation path replaces NTOUCH
SIGMA=RAD(N+1)*ENSNRQ(NQ,NAVE)
SIGMA ≥ 1.
NO
YES
518
NTOUCH=NQ
519
B=ARSIN(SIGMA)
NQ=NTEST
NO
YES
NQ=1, NT subscript NQ is used to denote annuli absorbing radiation counting from core to outermost annulus
solution for sector radii less than radius (RAD(N+1)) which is associated with interior transmissivity ior annulus of TEMP(N)
RI(NO,2)=···
RI(NQ,1)=··
solution for sector radii equal or larger than radius (RAD(N+1))
CONTINUE
530
NFAC=NTOUCH+1
first annulus that radiation path intersects
NJ=0
subscript
for components of absorption length
NAVE=
2, NANGLE
NFAC ≤ NTEST
NO
YES
no sector radius less than RAD(N+1)

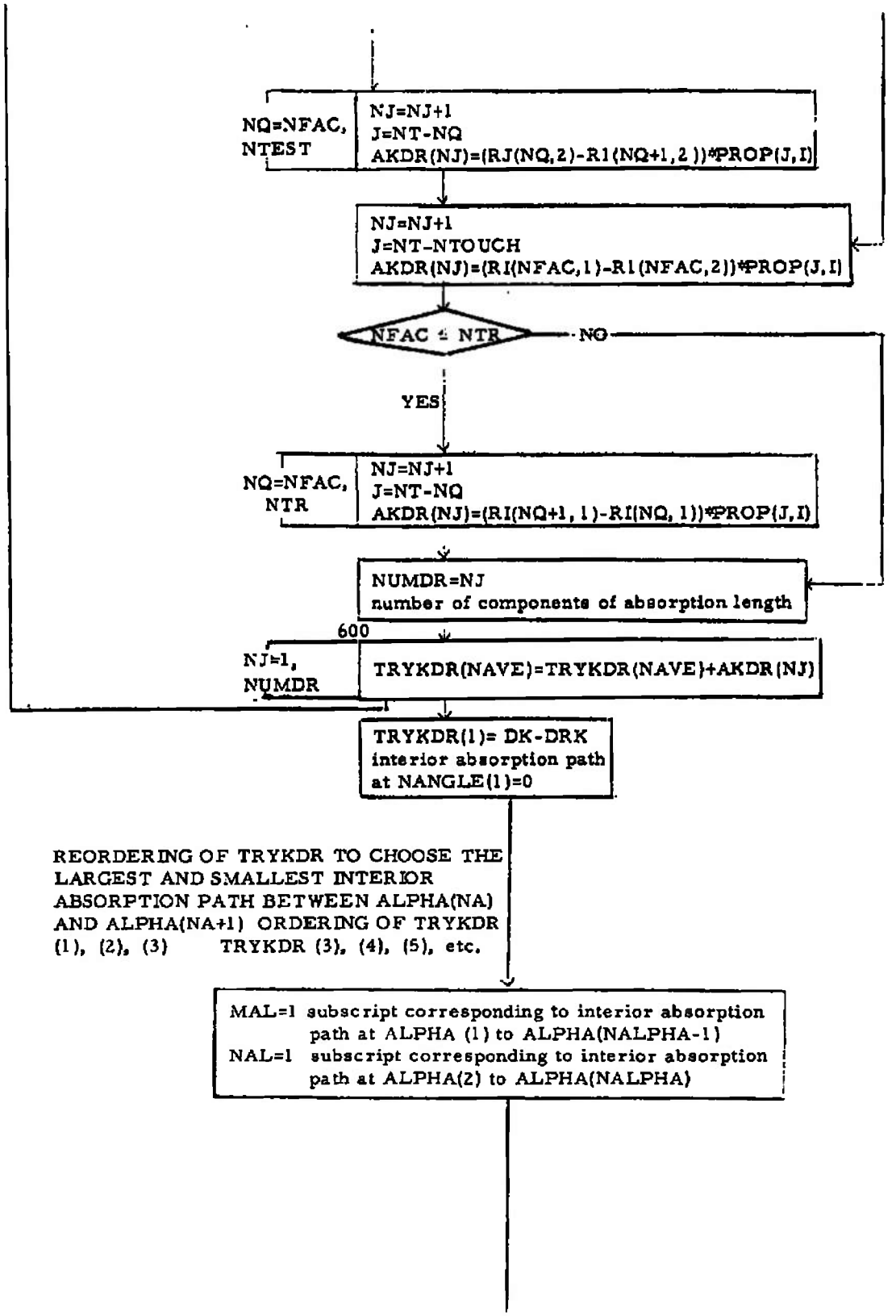
NQ=NFAC, NTEST
NJ=NJ+1
J=NT-NQ
AKDR(NJ)=(RJ(NQ,2)-RI(NQ+1,2))*PROP(J,I)
NJ=NJ+1
J=NT-NTOUCH
AKDR(NJ)=(RI(NFAC,1)-RI(NFAC,2))*PROP(J,I)
NFAC = NTR
NO
YES
NQ=NFAC, NTR
NJ=NJ+1
J=NT-NQ
AKDR(NJ)=(RI(NQ+1,1)-RI(NQ,1))*PROP(J,I)
NUMDR=NJ
number of components of absorption length
600
NJ=1, NUMDR
TRYKDR(NAVE)=TRYKDR(NAVE)+AKDR(NJ)
TRYKDR(1)= DK-DRK
interior absorption path
at NANGLE(1)=0
REORDERING OF TRYKDR TO CHOOSE THE LARGEST AND SMALLEST INTERIOR ABSORPTION PATH BETWEEN ALPHA(NA) AND ALPHA(NA+1) ORDERING OF TRYKDR (1), (2), (3) TRYKDR (3), (4), (5), etc.
MAL=1 subscript corresponding to interior absorption path at ALPHA (1) to ALPHA(NALPHA-1)
NAL=1 subscript corresponding to interior absorption path at ALPHA(2) to ALPHA(NALPHA)

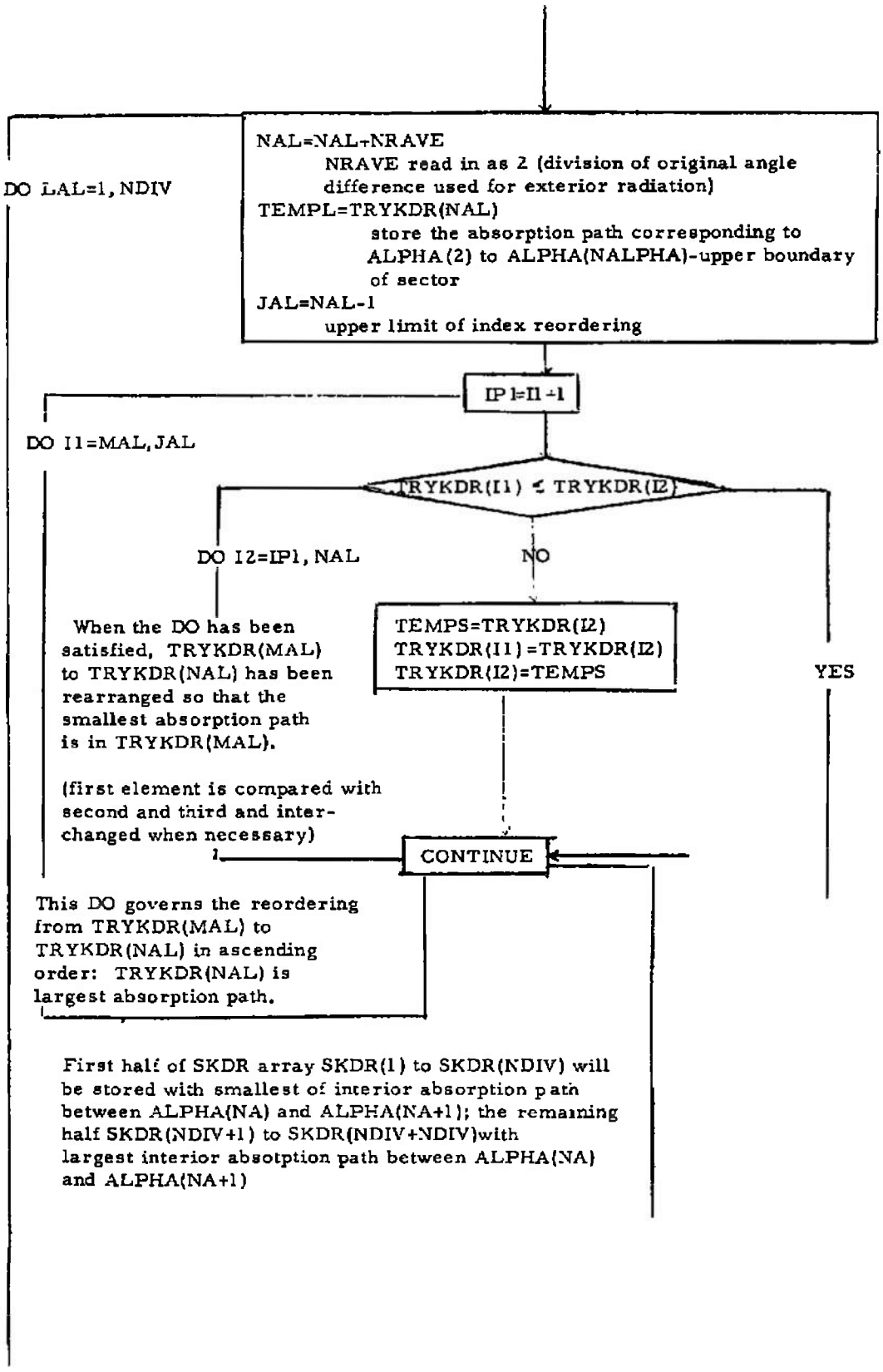
NAL=NAL+NRAVE
NRAVE read in as 2 (division of original angle difference used for exterior radiation)
TEMPL=TRYKDR(NAL)
store the absorption path corresponding to ALPHA(2) to ALPHA(NALPHA)-upper boundary of sector
JAL=NAL-1
upper limit of index reordering
DO LAL=1, NDIV
IP1=I1+1
DO I1=MAL, JAL
TRYKDR(I1) ≤ TRYKDR(I2)
YES
NO
DO I2=IP1, NAL
When the DO has been satisfied, TRYKDR(MAL) to TRYKDR(NAL) has been rearranged so that the smallest absorption path is in TRYKDR(MAL).
(first element is compared with second and third and interchanged when necessary)
TEMPS=TRYKDR(I2)
TRYKDR(I1)=TRYKDR(I2)
TRYKDR(I2)=TEMPS
CONTINUE
This DO governs the reordering from TRYKDR(MAL) to TRYKDR(NAL) in ascending order: TRYKDR(NAL) is largest absorption path.
First half of SKDR array SKDR(1) to SKDR(NDIV) will be stored with smallest of interior absorption path between ALPHA(NA) and ALPHA(NA+1); the remaining half SKDR(NDIV+1) to SKDR(NDIV+NDIV)with largest interior absotption path between ALPHA(NA) and ALPHA(NA+1)

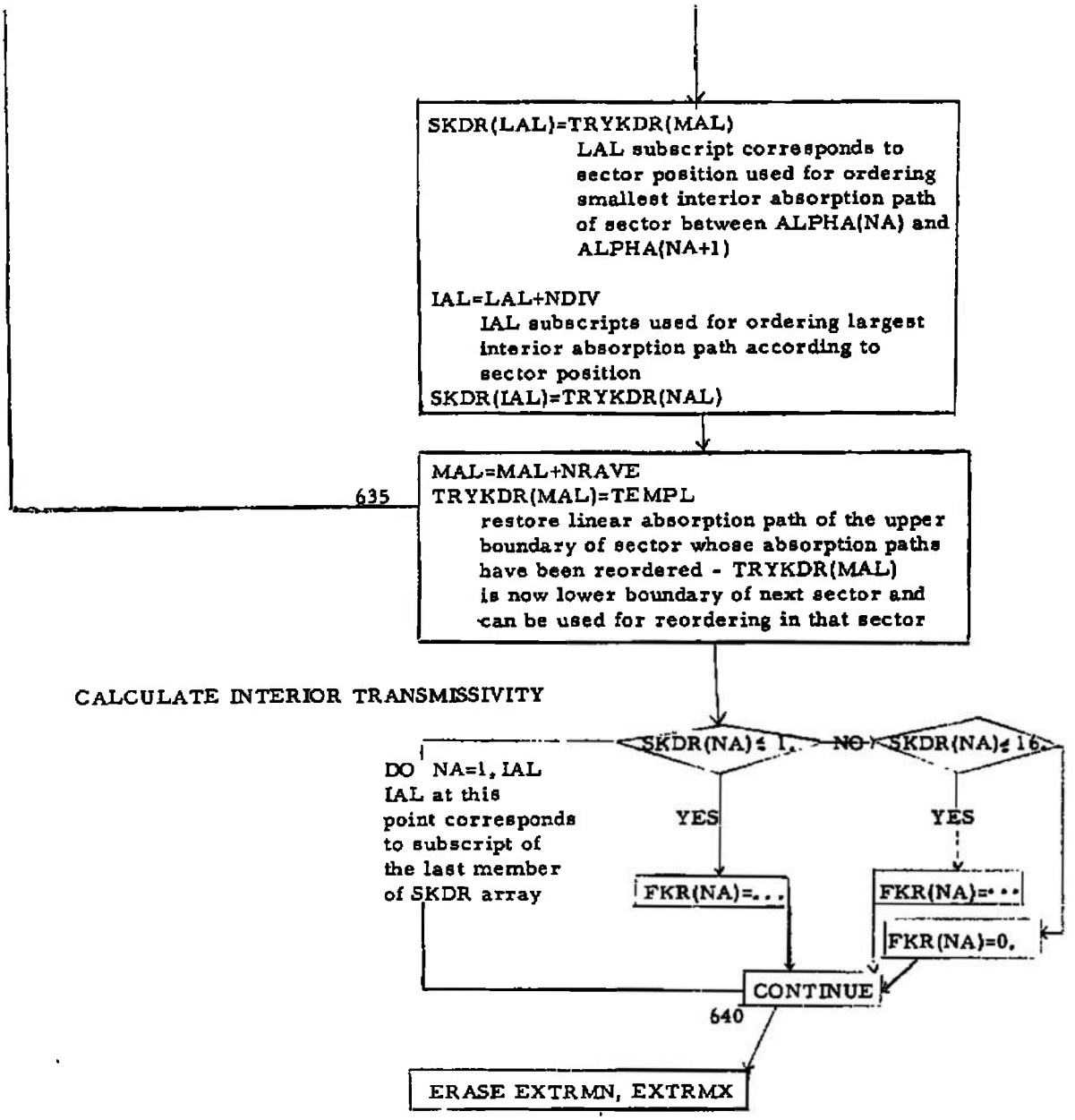
SKDR(LAL)=TRYKDR(MAL)
LAL subscript corresponds to sector position used for ordering smallest interior absorption path of sector between ALPHA(NA) and ALPHA(NA+1)
IAL=LAL+NDIV
IAL subscripts used for ordering largest interior absorption path according to sector position
SKDR(IAL)=TRYKDR(NAL)
MAL=MAL+NRAVE
TRYKDR(MAL)=TEMPL
restore linear absorption path of the upper boundary of sector whose absorption paths have been reordered - TRYKDR(MAL) is now lower boundary of next sector and can be used for reordering in that sector
635
CALCULATE INTERIOR TRANSMISSIVITY
DO NA=1, IAL
IAL at this point corresponds to subscript of the last member of SKDR array
SKDR(NA)≤ 1.
NO
SKDR(NA)≤ 16.
YES
YES
FKR(NA)=...
FKR(NA)=...
FKR(NA)=0.
CONTINUE
640
ERASE EXTRMN, EXTRMX

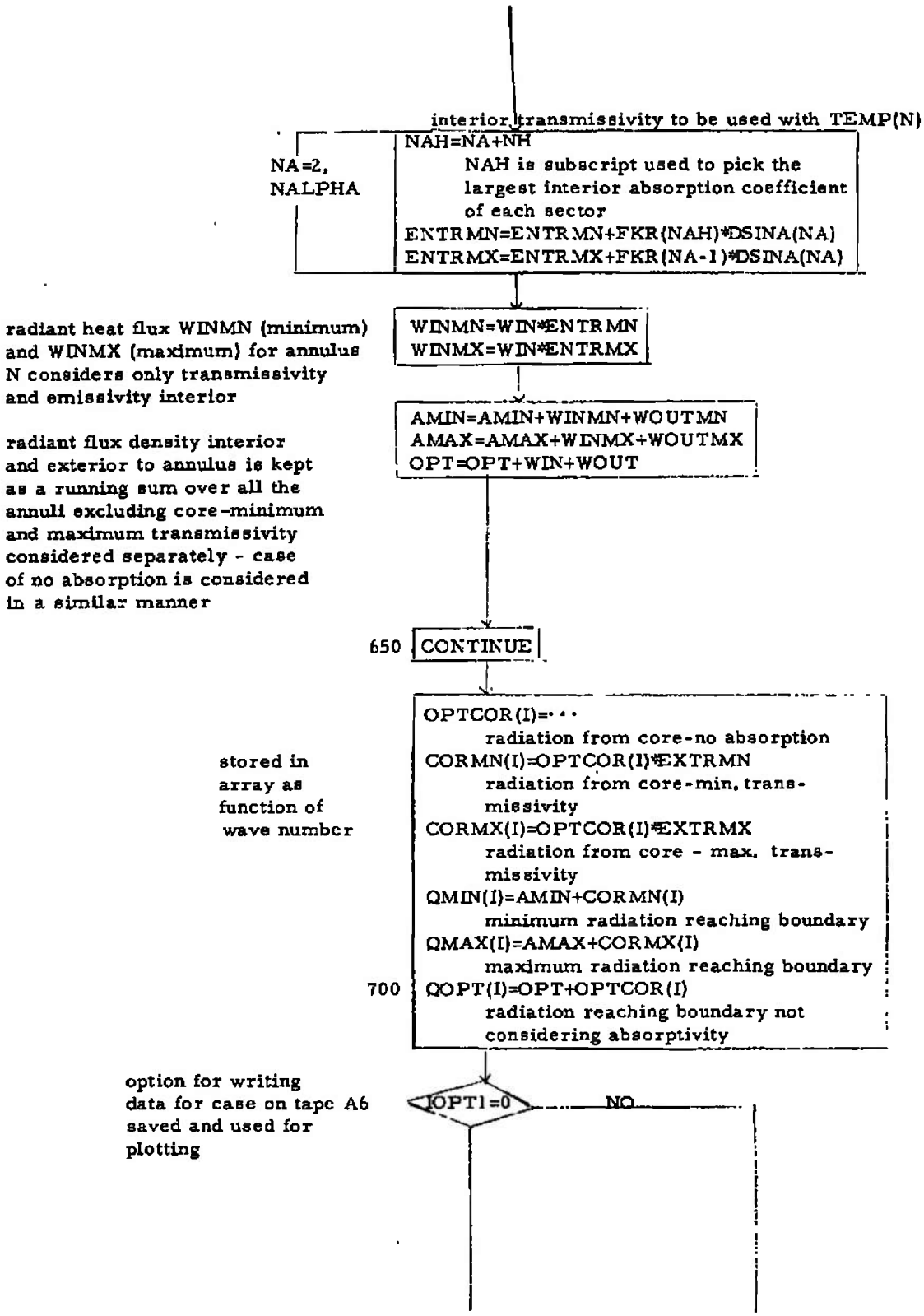
interior transmissivity to be used with TEMP(N)
NAH=NA+NH
NAH is subscript used to pick the largest interior absorption coefficient of each sector
ENTRMN=ENTRMN+FKR(NAH)*DSINA(NA)
ENTRMX=ENTRMX+FKR(NA-1)*DSINA(NA)
NA=2, NALPHA
radiant heat flux WINMN (minimum) and WINMX (maximum) for annulus N considers only transmissivity and emissivity interior
WINMN=WIN*ENTRMN
WINMX=WIN*ENTRMX
radiant flux density interior and exterior to annulus is kept as a running sum over all the annuli excluding core-minimum and maximum transmissivity considered separately - case of no absorption is considered in a similar manner
AMIN=AMIN+WINMN+WOUTMN
AMAX=AMAX+WINMX+WOUTMX
OPT=OPT+WIN+WOUT
650 CONTINUE
stored in array as function of wave number
OPTCOR(I)=...
radiation from core-no absorption
CORMN(I)=OPTCOR(I)*EXTRMN
radiation from core-min, trans-missivity
CORMX(I)=OPTCOR(I)*EXTRMX
radiation from core - max. trans-missivity
QMIN(I)=AMIN+CORMN(I)
minimum radiation reaching boundary
QMAX(I)=AMAX+CORMX(I)
maximum radiation reaching boundary
700 QOPT(I)=OPT+OPTCOR(I)
radiation reaching boundary not considering absorptivity
option for writing data for case on tape A6 saved and used for plotting
IOPT1=0
NO

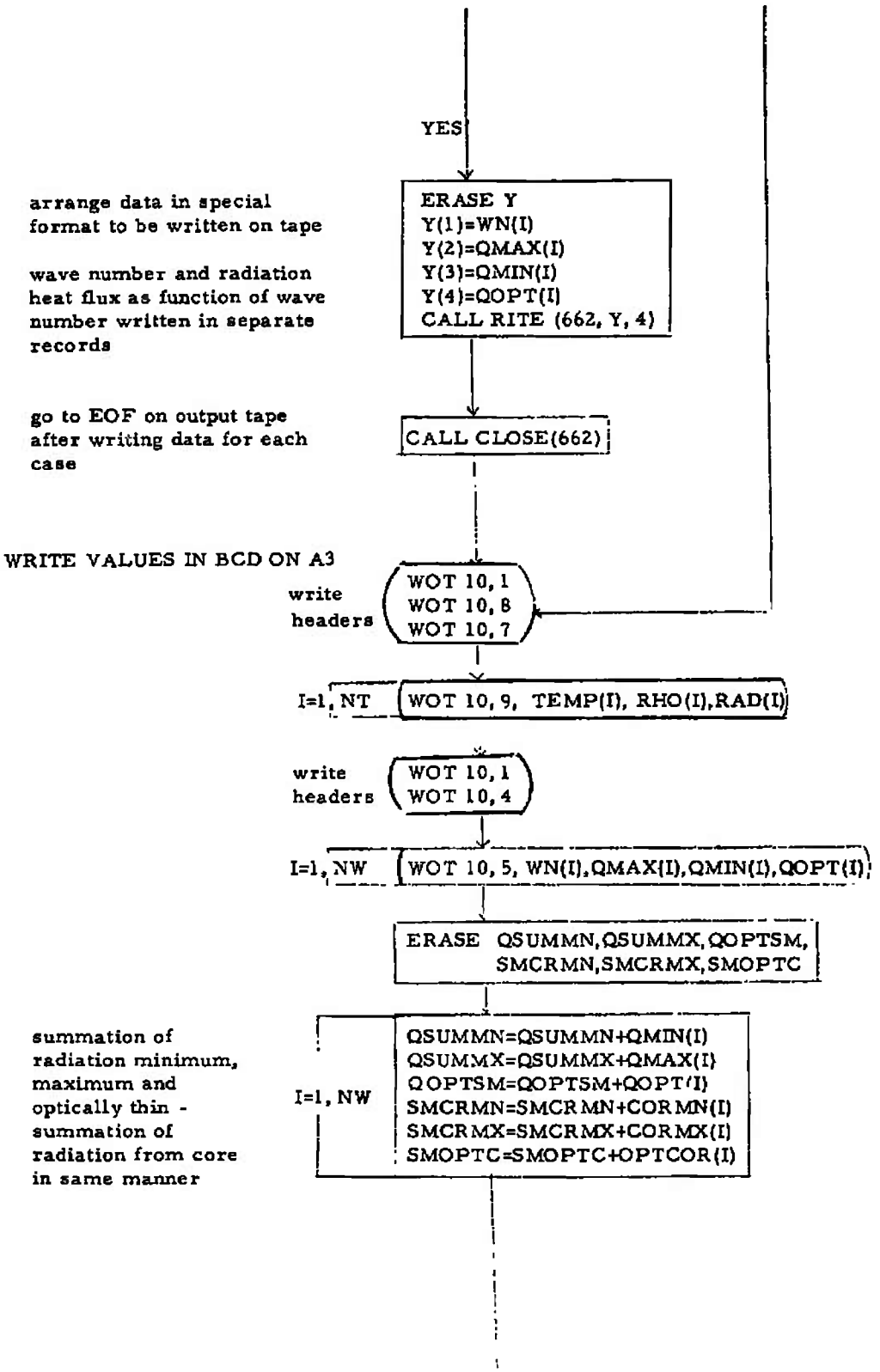
YES
arrange data in special format to be written on tape
wave number and radiation heat flux as function of wave number written in separate records
ERASE Y
Y(1)=WN(I)
Y(2)=QMAX(I)
Y(3)=QMIN(I)
Y(4)=QOPT(I)
CALL RITE (662, Y, 4)
go to EOF on output tape after writing data for each case
CALL CLOSE(662)
WRITE VALUES IN BCD ON A3
write headers
WOT 10, 1
WOT 10, 8
WOT 10, 7
I=1, NT
WOT 10, 9, TEMP(I), RHO(I), RAD(I)
write headers
WOT 10, 1
WOT 10, 4
I=1, NW
WOT 10, 5, WN(I), QMAX(I), QMIN(I), QOPT(I)
ERASE QSUMMN, QSUMMX, QOPTSM, SMCRMN, SMCRMX, SMOPTC
summation of radiation minimum, maximum and optically thin - summation of radiation from core in same manner
I=1, NW
QSUMMN=QSUMMN+QMIN(I)
QSUMMX=QSUMMX+QMAX(I)
QOPTSM=QOPTSM+QOPT(I)
SMCRMN=SMCRMN+CORMN(I)
SMCRMX=SMCRMX+CORMX(I)
SMOPTC=SMOPTC+OPTCOR(I)

fraction of total energy flux radiation by black body within wave number interval WN(I) to WN(NW)

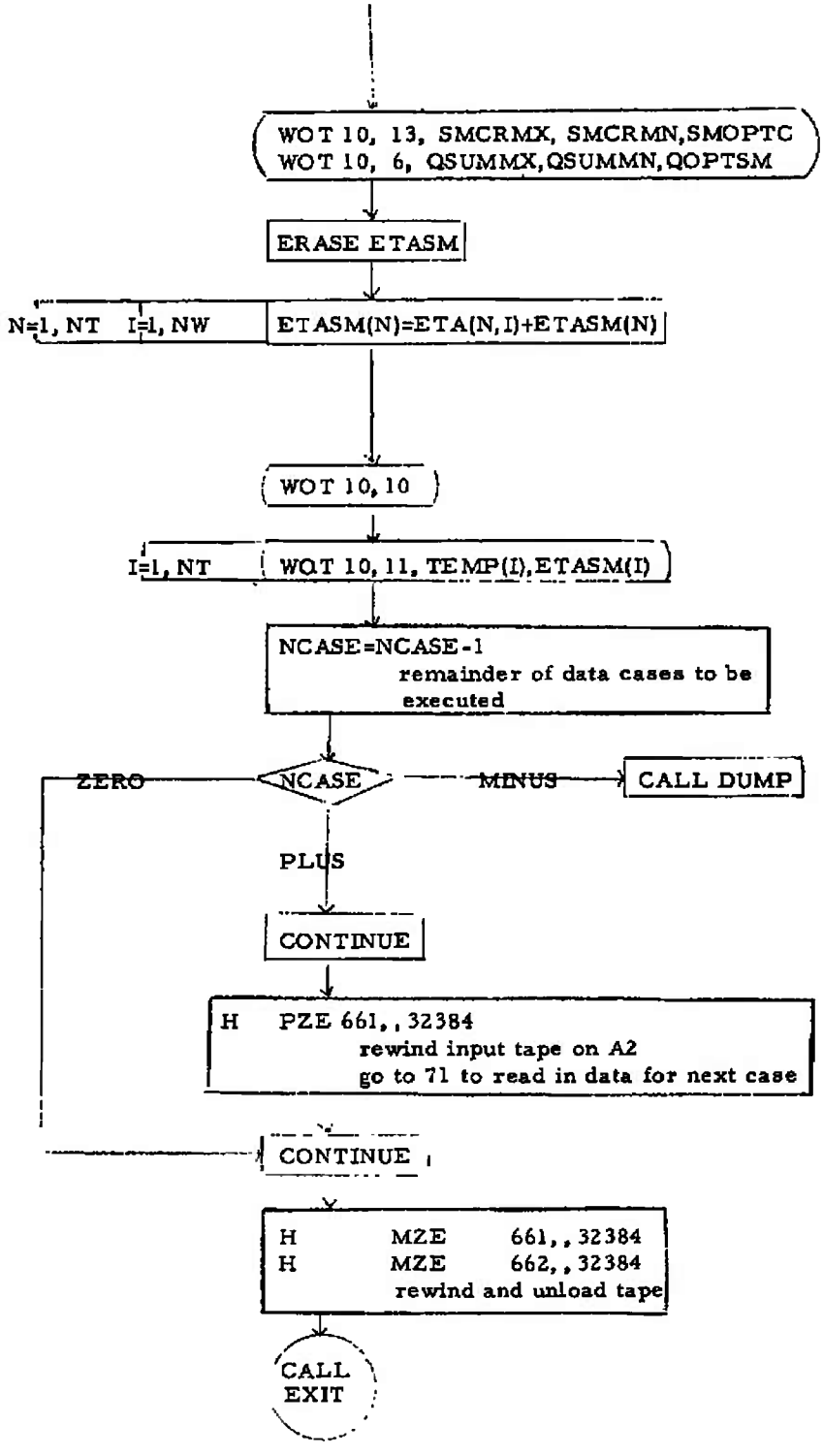

B.5 PROGRAM LISTING

STUDY OF RADIATION HEAT FLUX FROM HIGH PRESSURE AIR ARCS AT LOW F09/11/64

```
C
C
      COMMON ABEMIS(22),AINC,AKDR(45),ALPHA(10),ANGLE(20)
      COMMON BCONEC(25)
      COMMON BUFF2(525),BUFFT(86),CORMN(121),CORMX(121),C2T(23)
      COMMON DALPHA,DELTA,DPHI
      COMMON DR(23),DSINA(10),DV(23),EKDR(10),ENSNA(20)
      COMMON ENSNRQ(23,20),ENRQSN(23,20),ETA(23,121)
      COMMON ETASM(23)
      COMMON EXSNRQ(22,20),EXRQSN(22,20),FKR(20),FMT(12),IT(23)
      COMMON ICPT1,   NALPHA,NDIV
      COMMON NRAVE,NTR,NT,NW,OPTCOR(121)
      COMMON PRCP(23,121),QMAX(121),QMIN(121)
      COMMON QOPT(121),RADQ(23),RAD(23),RAVE,RDALPH,RDELTA(23),REC(700)
      COMMON RHO(23)
      COMMON      RI(23,2),R(22),SINA(20),SKDR(20),TEMP(23),TEMPRW(23)
      COMMON TRYKDR(20),WNA,WN(121),Y(4)
    1 FORMAT(1H1)
    2 FORMAT(12A6)
    4 FORMAT (1HC3X8HWAVE NO.,11X4HQMAX,13X4HQMIN,13X4HQOPT)
    5 FORMAT(1H 4(1PE14.7,3X))
    6 FORMAT(1HO3X8HSQMAX = 1PE14.7,3X8HSQMIN = 1PE14.7,3X8HSQOPT = 1PE1
     14.7)
    7 FORMAT (1HC2X11HTEMPETATURE,5X12HLOG RHO/RHCO,8X6HRADIUS)
    8 FORMAT(1HO30X19HTEMPERATURE PROFILE)
    9 FORMAT(1H 3(1PE14.7,3X))
   10 FORMAT (1HO2X11HTEMPERATURE,8X6HETASLM)
   11 FORMAT (1H 2(1PE14.7,3X))
   13 FORMAT (1HC1X10HSQCORMX = 1PE14.7,1X10HSQCORMN = 1PE14.7,
     11X11HSQCORCPT = 1PE14.7)
C      INITIALIZE FOR INPUT OUTPUT
   50 IF(INIT(642,643,BUFFT(86),39,47))60,55,60
   55 CALL DUMP
C     INITIALIZE FOR ERROR ROUTINE
   60 IF (ERTRP(5))70,726,726
C     INITIALIZE FOR BUFFERS
C     ABUFI IS FOR INPUT ON A5
   70 CALL ABUF1
      RIT 2,2, NCASE
      IF (BUFFS(662,BUFF2(525),525,0,1,1,1))71,55,71
C       READ IDENTIFICATION CARD
C       READ IN CARDS ON A2
   71 RIP12,2,(FMT(I),I=1,12)
      CALL SPGHDR (FMT)
C     INPUT
      RIT 2,2,DELTA,AINC,WNA,DALPHA,RAVE
      RIT 2,2, NW,NT,ICPT1,NTR,NR,NALPHA,NRAVE,NDIV
      RIT 2,2, (TEMP(I),I=1,NT)
      RIT 2,2, (RAD(I),I=1,NR )
      RIT 2,2, (RADQ(I), I=1,NT)
      RIT 2,2, (RHO(I),I=1,NT)
      CALL LBID (662,  ARC ,  RAD )
C     READ IN AND STORE DATA ONE FILE PER TEMPERATURE
   72 NFILE=1
      DO 180 N=1,NT
```

```
      STUDY OF RADIATION HEAT FLUX FROM HIGH PRESSURE AIR ARCS AT LCW F09/11/64

      IF (N-1)73C,73,83
C     READ BCDREC FOR FIRST FILE ON AS
C     NWBCD IS SET TO ZERO TO READ ENTIRE RECORD
   73 ERASE NWBCD
      IF  (RREAD(645,BCDREC,NWBCD))75,74,75
   74 CALL ERROR (29HOBCDREC SHOULD START NEW FILE)
   75 NPP=3
   76 CO 77 K=1,NPP
      ERASE NWBIN
      IF (RREAD(661,REC,NWBIN))77,78,77
   77 CONTINUE
      GO TO 85
   78 WOT 10,79, NFILE,K
   79 FORMAT(13HOFILE NO. IS I2,2X11HREC NC. IS I2)
      CALL ERROR (18HEOF WHILE READ REC)
   83 CALL CLOSE (661)
      NFILE = NFILE +1
      NPP=2
      GO TC 76
   85 IF(ABSF(TEMP(N)-REC(1))-1.E-6)90,9C,83
   9C K=NPP+1
      ERASE NWBIN
      IF (RREAD(661,REC,NWBIN))94,78,94
   94 IF (ABSF(RHO(N)+2.)-1.E-6) 110,110,95
   95 IF (RHO(N)+2.)96,110,97
   96 PCNT =RHO(N)+3.
      IPST = 1
      GO TC 108
   97 IF(ABSF(RHC(N))-1.E-6)14C,14C,98
   98 IF (RHO(N))100,140,105
  10C IF(ABSF(RHC(N)+1.)-1.E-6)125,125,101
  101 IF(RHC(N)+1.)102,125,103
  102 PCNT = RHO(N) +2.
      IPST = 2
      GO TO 108
  103 PCNT = RHO(N) + 1.
      IPST = 3
      GO TC 108
  105 IF (ABSF(RHO(N)-1.)-1.E-6)155,155,106
  106 IF (RHC(N)-1.)107,155,17C
  107 PCNT = RHO(N)
      IPST = 4
  108 CO 109 I =1,NW
      PROP(N,I)    = EXPF((LOGF(REC(IPST+1)/REC(IPST)))*PCNT+LOGF(REC(IPS
     1T)))
  109 IPST = IPST+5
      GO TC 180
  11C IPST = 2
      GO TC 160
  125 IPST = 3
      GO TC 160
  14C IPST = 4
      GO TC 16C
  155 IPST = 5
  160 CO 165 I=1,NW
      PROP(N,I)    =REC(IPST)
```

```
      STUDY OF RADIATION HEAT FLUX FROM HIGH PRESSURE AIR ARCS AT LCW F09/11/64

165 IPST = IPST +5
    GO TC 180
170 PCNT =RHO(N)-1.
    IPST =5
    CO 175 I=1,NW
    PROP(N,I)    = EXPF((LOGF(REC(IPST)/REC(IPST-1)))*PCNT+
   1LOGF(REC(IPST)))
175 IPST = IPST +5
180 CONTINUE
    CALL CLOSE (661)
    RDALPH=DALPHA*1.7453292E-2
    NH=NCIV-1
    NANGLE =NRAVE*(NALPHA-1)+1
    ALPHA(1)=0.
    SINA(1)=0.
    CO 190 NA=2,NALPHA
    ALPHA(NA)=ALPHA(NA-1)+RDALPH
    SINA(NA)=SINF(ALPHA(NA))
190 CSINA(NA)=SINA(NA)-SINA(NA-1)
    CO 210 NQ=1,NTR
    CO 210 NA=2,NALPHA
    EXRQSN(NQ,NA)=RAD(NQ)/SINA(NA)
210 EXSNRQ(NQ,NA)=1./EXRQSN(NQ,NA)
    ANGLE(1)=0.
    ANGADD=RDALPH/RAVE
    CO 220 NAVE=2,NANGLE
    ANGLE (NAVE)=ANGLE(NAVE-1)+ANGADD
220 ENSNA(NAVE)=SINF(ANGLE(NAVE))
    CO 230 NQ=1,NT
    CO 230 NAVE=2,NANGLE
    ENRQSN(NQ,NAVE)=RADQ(NQ)/ENSNA(NAVE)
230 ENSNRQ(NQ,NAVE)=1./ENRQSN(NQ,NAVE)
    CO 240 N=1,NTR
240 ABEM(SIN)=-1.9((1.-(RAC(N+1)/RAD(N))**2/2.)-(ARSIN(RAD(N+1)/RAC(N
   1))+SINF(2.*ARSIN(RAD(N+1)/RAD(N)))/2.)/3.1415926)
    CO 241 N=1,NT
    TEMPRW(N)=(TEMP(N)**4)*5.6686E-12
    RDELTA(N)=RAD(N)/DELTA
    DR(N)=RAD(N)-RAD(N+1)
    C2T(N)=1.438/TEMP(N)
241 CV(N)=AINC*C2T(N)
    ERASE ETA
    CC 7CO I=1,NW
    WNA=WNA-AINC
    WN(I)=WNA
    ERASE AMIN,AMAX,OPT,SUM,CRK
    CO 245 N=1,NT
245 SUM=SUM+DR(N)*PROP(N,I)
    CK=2.*SUM
    EXTRMN=1.
    EXTRMX=1.
    CO 650 N=1,NT
    EKDR(1)=DR(N)*PROP(N,1)
    CRK=DRK+EKCR(1)
    V=WN(I)*C2T(N)
    IF (V-.278)650,253,250
```

```
      STUDY OF RADIATION HEAT FLUX FROM HIGH PRESSURE AIR ARCS AT LOW F09/11/64

250   IF (V-13.)251,252,650
251   IF (V-1.)253,253,252
252   ETA(N,I)=.15399*DV(N)*(V**3)/(EXPF(V)-1.)
      GO TO 255
253   V2=V*V
      V3=V2*V
      V4=V3*V
      V6=V4*V2
      X=V2-V3/2.+V4/12.-V6/720.
      Z=(DV(N)**2)*(1./12.-V /8.+V3/24.-V4/576.)
      ETA(N,I)=.15399*DV(N)*(X+Z)
255   IF (N-NT) 256,650,730
256   ERASE SKDR
      DO 275 NA=2,NALPHA
      DO 270 NQ=1,N
      R(NQ)=EXRQSN(NQ,NA)*(SINF(ALPHA(NA)-ARSIN(RAD(N+1)*
     1EXSNRQ(NQ,NA))))
      IF( N -1) 730,265,257
257   IF (NQ-1) 730,270,260
260   AKDR(NQ-1)=(R(NQ-1)-R(NQ))*PROP(NQ-1,I)
      IF (NQ- N )270,265,730
265   AKDR( N )=R( N )*PROP( N ,I)
      EKDR(NA)=AKDR( N )
270   CONTINUE
      DO 275 NQ=1,N
275   SKDR(NA)=SKDR(NA)+AKDR(NQ)
      SKDR(1)=DRK
      DO 305 NA =1,NALPHA
      IF(EKDR(NA)-1.)295,295,300
295   FKR(NA)=EXPF(-1.206*EKDR(NA))
      GO TO 305
300   IF (EKDR(NA)-16.)301,301,302
301   FKR(NA)=(EXPF(-1.206*EKDR(NA)))*(1.0774-.09539*EKDR(NA)+
     1.055577*(EKDR(NA))**2-4.29143E-3*(EKDR(NA))**3+2.082602E-4*
     2(EKDR(NA))**4)
      GO TO 305
302   FKR(NA)=0.
305   CONTINUE
      ERASE EPSMN,EPSMX
      DO 310 NA=2,NALPHA
      EPSMN=EPSMN+FKR(NA)*CSINA(NA)
310   EPSMX=EPSMX+FKR(NA-1)*CSINA(NA)
      EOUT=1.-EXPF(ABEMIS(N)*PROP(N,I)*RAD(N) )
      EIN=1.-(EPSMN+EPSMX)/2.
      WBB=ETA(N,I)*TEMPRW(N)
      WIN=WBB*EIN*RDELTA(N+1)
      WOUT=WBB*EOUT*RDELTA(N)
      WOUTMN=WOUT*EXTRMN
      WOUTMX=WOUT*EXTRMX
      DO 340 NA=1,NALPHA
      IF (SKDR(NA)-1.)320,320,325
320   FKR(NA)=EXPF(-1.206*SKDR(NA))
      GO TO 340
325   IF (SKDR(NA)-16.) 330,330,335
330   FKR(NA)=(EXPF(-1.206*SKDR(NA)))*(1.0774-.09539*SKDR(NA)+
     1.055577*(SKDR(NA))**2-4.29143E-3*(SKDR(NA))**3+2.082602E-4*
```

```
      STUDY OF RADIATION HEAT FLUX FROM HIGH PRESSURE AIR ARCS AT LOW F09/11/64

     2(SKDR(NA))**4)
      GO TO 340
  335 FKR(NA)=0.
  340 CONTINUE
      ERASE EXTRMN,EXTRMX
      DO 350 NA=2,NALPHA
      EXTRMN=EXTRMN+FKR(NA)*DSINA(NA)
  350 EXTRMX=EXTRMX+FKR(NA-1)*DSINA(NA)
      ERASE TRYKDR
      NTEST=NT-N-1
      DO 600 NAVE=2,NANGLE
      ERASE RI
      ERASE NTOUCH
      DO 530 NQ=1,NT
      SIGMA=RAD(N+1)*ENSNRQ(NQ,NAVE)
      IF (SIGMA-1.)519,519,518
  518 NTOUCH =NQ
      GO TO 530
  519 B=ARSIN(SIGMA)
      IF (NQ-NTEST)520,520,523
  520 D=ANGLE(NAVE)-B+3.1415926
      IF(D-1.5707963) 522,522,521
  521 D=3.1415926-D
  522 RI(NQ,2)=ENRQSN(NQ,NAVE)*SINF(D)
  523 C=ANGLE(NAVE)+B
      IF(C-1.5707963) 525,525,524
  524 C=3.1415926-C
  525 RI(NQ,1)=ENRQSN(NQ,NAVE)*SINF(C)
  530 CONTINUE
      NFAC=NTOUCH+1
      NJ=0
      IF(NFAC-NTEST)545,545,565
  545 DO 560 NQ=NFAC,NTEST
      NJ=NJ+1
      J=NT-NQ
  560 AKDR(NJ)=(RI(NQ,2)-RI(NQ+1,2))*PROP(J,I)
  565 NJ=NJ+1
      J=NT-NTOUCH
      AKDR(NJ)=(RI(NFAC,1)-RI(NFAC,2))*PROP(J,I)
      IF (NFAC-NTR) 580,580,595
  580 DO 590 NQ=NFAC,NTR
      NJ=NJ+1
      J=NT-NQ
  590 AKDR(NJ)=(RI(NQ+1,1)-RI(NQ,1))*PROP(J,I)
  595 NUMDR=NJ
      DO 600 NJ=1,NUMDR
  600 TRYKDR(NAVE)=TRYKDR(NAVE)+AKDR(NJ)
  606 TRYKDR(1)=DK-DRK
      MAL=1
      NAL=1
      DO 635 LAL=1,NDIV
      NAL=NAL+NRAVE
      TEMPL=TRYKDR(NAL)
      JAL=NAL-1
      DO 630 II=MAL,JAL
      IP1=II+1
```

```
      STUDY OF RADIATION HEAT FLUX FROM HIGH PRESSURE AIR ARCS AT LCW F09/11/64

     DO 630 I2=IP1,NAL
     IF(TRYKDR(I1)-TRYKDR(I2))630,630,627
627  TEMPS=TRYKDR(I1)
     TRYKDR(I1)=TRYKDR(I2)
     TRYKDR(I2)=TEMPS
630  CONTINUE
     SKDR(LAL)=TRYKDR(MAL)
     IAL =LAL+NDIV
     SKDR(IAL)=TRYKDR(NAL)
     MAL=MAL+NRAVE
635  TRYKDR(MAL)=TEMPL
     DO 640     NA=1,IAL
     IF (SKDR(NA)-1.)636,636,637
636  FKR(NA)=EXPF(-1.206*SKDR(NA))
     GO TO 640
637  IF (SKDR(NA)-16.) 638,638,639
638  FKR(NA)=(EXPF(-1.206*SKDR(NA)))*(1.0774-.09539*SKDR(NA)+
    1.055577*(SKDR(NA))**2-4.29143E-3*(SKDR(NA))**3+2.082602E-4*
    2(SKDR(NA))**4)
     GO TO 640
639  FKR(NA)=0.
640  CONTINUE
     ERASE ENTRMN,ENTRMX
     DO 645 NA=2,NALPHA
     NAH=NA+NH
     ENTRMN=ENTRMN+FKR( NAH )*DSINA(NA)
645  ENTRMX=ENTRMX+FKR(NA-1)*DSINA(NA)
     WINMN=WIN*ENTRMN
     WINMX=WIN*ENTRMX
     AMIN=AMIN+WINMN+WOUTMN
     AMAX=AMAX+WINMX+WOUTMX
     OPT=OPT+WIN+WOUT
650  CONTINUE
     OPTCOR(I)=TEMPRW(NT)*RDELTA(NT)*ETA(NT,I)*(1.-EXPF(-1.9*EKDR(I)))
     CORMN(I)=OPTCOR(I)*EXTRMN
     CORMX(I)=OPTCOR(I)*EXTRMX
     QMIN(I)=AMIN+CORMN(I)
     QMAX(I)=AMAX+CORMX(I)
700  QOPT(I)=OPT+OPTCOR(I)
     IF (1QPT1)705,703,705
703  DO 704 I=1,NW
     ERASE Y
     Y(1)=WN(I)
     Y(2)=QMAX(I)
     Y(3)=QMIN(I)
     Y(4)=QOPT(I)
704  CALL RITE (662,Y,4)
     CALL CLOSE (662)
705  WOT 10,1
     WOT 10,8
     WOT10,7
     DO 707  I=1, NT
707  WOT 10, 9, TEMP(I), RHO(I), RAD(I)
     WOT 10,1
     WOT 10,4
     DO 710 I=1,NW
```

```
      STUDY OF RADIATION HEAT FLUX FROM HIGH PRESSURE AIR ARCS AT LGH F09/11/6'

  71C WOT 10,5, WN(I), QMAX(I), QMIN(I), QOPT(I)
      ERASE QSUMMN,QSUMMX,QOPTSM,SMCRMN,SMCRMX,SMOPTC
      DO 711 I=1,NW
      QSUMMN=QSUMMN+QMIN(I)
      QSUMMX=QSUMMX+QMAX(I)
      QOPTSM=QOPTSM+QOPT(I)
      SMCRMN=SMCRMN+CORMN(I)
      SMCRMX=SMCRMX+CORMX(I)
  711 SMOPTC=SMOPTC+OPTCOR(I)
      WOT 10,13,SMCRMX,SMCRMN,SMOPTC
      WOT 10,6, QSUMMX,QSUMMN,QOPTSM
      ERASE ETASM
       DO 722 N=1,NT
      DO 722 I=1,NW
  722 ETASM(N)=ETA(N,I)+ETASM(N)
      WOT 10,10
      DO 725 I=1,NT
  725 WOT 10,11, TEMP(I),ETASM(I)
  726 NCASE=NCASE-1
      IF (NCASE)'55,740,727
  727 CONTINUE
H      PZE     661,,32384
      GO TO 71
  730 CALL ERROR (18HINDEX OUT OF LIMIT)
  74C CONTINUE
H      MZE     661,,32384
H      MZE     662,,32384
      CALL EXIT
      END(1,1,0,0,0,1,1,1,C,1,C,0,C,C,C)
```

STUDY OF RADIATION HEAT FLUX FROM HIGH PRESSURE AIR ARCS AT HIGH FRE09/11/64

```
C
      COMMON ABEMIS(22),AINC,AKDR(45),ALPHA(10),ANGLE(20)
      COMMON BCDREC(25)
      COMMON BUFF2(525),BUFFT(86),CORMN(121),CORMX(121),C2T(23)
      COMMON DALPHA,DELTA,DPHI
      COMMON DR(23),DSINA(10),EKDR(10),ENSNA(20)
      COMMON ENSNRQ(23,20),ENRQSN(23,20),ETA(23,121)
      COMMON ETASM(23)
      COMMON EXSNRQ(22,20),EXRQSN(22,20),FKR(20),FMT(12),IT(23)
      COMMON IOPT1,   NALPHA,NDIV
      COMMON NRAVE,NTR,NT,NW,OPTCOR(121)
      COMMON PRCP(23,121),QMAX(121),QMIN(121)
      COMMON QOPT(121),RADQ(23),RAD(23),RAVE,RDALPH,RDELTA(23),REC(700)
      COMMON RHO(23)
      COMMON      RI(23,2),R(22),SINA(20),SKDR(20),TEMP(23),TEMPRW(23)
      COMMON TRYKDR(20),WNA,WN(121),Y(4)
    1 FORMAT(1H1)
    2 FORMAT(12A6)
    4 FORMAT (1HO3X8HWAVE NO.,11X4HQMAX,13X4HQMIN,13X4HQOPT)
    5 FORMAT(1H 4(1PE14.7,3X))
    6 FORMAT(1HO3X8HSQMAX = 1PE14.7,3X8HSQMIN = 1PE14.7,3X8HSQOPT = 1PE1
     14.7)
    7 FORMAT (1HC2X11HTEMPETATURE,5X12HLOG RHO/RHOO,8X6HRADIUS)
    8 FORMAT(1HO30X19HTEMPERATURE PROFILE)
    9 FORMAT(1H 3(1PE14.7,3X))
   10 FORMAT (1HC2X11HTEMPERATURE,8X6HETASUM)
   11 FORMAT (1H 2(1PE14.7,3X))
   13 FORMAT (1HO1X10HSQCORMX = 1PE14.7,1X10HSQCORMN = 1PE14.7,
     11X11HSQCORCPT = 1PE14.7)
C      INITIALIZE FOR INPUT OUTPUT
   50 IF(INIT(642,643,BUFFT(86),39,47))60,55,60
   55 CALL DUMP
C     INITIALIZE FOR ERROR ROUTINE
   60 IF (ERTRP(5))70,726,726
C     INITIALIZE FOR BUFFERS
C     ABUF1 IS FOR INPUT ON A5
   70 CALL ABUF1
      RIT 2,2, NCASE
      IF (BUFFS(662,BUFF2(525),525,0,1,1,1))71,55,71
C       READ IDENTIFICATION CARD
C       READ IN CARDS ON A2
   71 RIPT2,2,(FMT(I),I=1,12)
      CALL SPGHOR (FMT)
C     INPUT
      RIT 2,2,DELTA,WNA,WNL,CALPHA,RAVE
      RIT 2,2, NT,IOPT1,IOPT2,NTR,NR,NALPHA,NRAVE,NDIV
      RIT 2,2,(TEMP(I),I=1,NTR)
      RIT 2,2, (RAO(I),I=1,NR)
      RIT 2,2, (RADQ(I),I=1,NT)
      RIT 2,2, (RHO(I),I=1,NTR)
      ERASE PROP
      NFILE =0
      ERASE NWBCD
      IF (RREAD(645,BCDREC,NWBCD))75,74,75
   74 CALL ERROR (25H BCDREC SHOULD START TAPE)
```

```
 STUDY OF RADIATION HEAT FLUX FROM HIGH PRESSURE AIR ARCS AT HIGH FRE09/11/64

  75 ERASE NWBIN
     IF(RREAD(661,REC,NWBIN))76,74,76
  76 DO 180 N=1,NTR
  77 NFILE =NFILE+1
     K=1
     ERASE NWBIN
     IF(RREAD(661,REC,NWBIN))83,78,83
  78 WOT 10,79,NFILE,K
  79 FORMAT(13HOFILE NO. IS I2,2X11HREC NO. IS I2)
     CALL ERROR (18HEOF WHILE READ REC)
  83 IF(ABSF(TEMP(N)-REC(1))-1.E-6)90,90,85
  85 CALL CLOSE (661)
     GO TO 77
  90 K=K+1
     ERASE NWBIN
     IF (RREAD(661,REC,NWBIN))94,78,94
  94 NW=REC(1)
     IF(N-NTR)192,1190,192
1190 DO 191 I=1,NW
 191 WN(I)=REC(I+2)
     WN(NW+1)=WNL
 192 K=K+1
     ERASE NWBIN
     IF (RREAD(661,REC,NWBIN))194,78,194
 194 IF (ABSF(RHO(N)+2.)-1.E-6)110,110,95
  95 IF (RHO(N)+2.)96,110,97
  96 PCNT =RHO(N)+3.
     IPST = 1
     GO TO 108
  97 IF(ABSF(RHO(N))-1.E-6)140,140,98
  98 IF (RHO(N))100,140,105
 100 IF(ABSF(RHO(N)+1.)-1.E-6)125,125,101
 101 IF(RHO(N)+1.)102,125,103
 102 PCNT = RHO(N) +2.
     IPST = 2
     GO TO 108
 103 PCNT = RHO(N) + 1.
     IPST = 3
     GO TO 108
 105 IF (ABSF(RHO(N)-1.)-1.E-6)155,155,106
 106 IF (RHO(N)-1.)107,155,170
 107 PCNT = RHO(N)
     IPST = 4
 108 DO 109 I =1,NW
     PROP(N,I)    = EXPF((LOGF(REC(IPST+1)/REC(IPST)))*PCNT+LOGF(REC(IPS
    1T)))
 109 IPST = IPST+5
     GO TO 180
 110 IPST = 2
     GO TO 160
 125 IPST = 3
     GO TO 160
 140 IPST = 4
     GO TO 160
 155 IPST = 5
 160 DO 165 I=1,NW
```

```
  STUDY OF RADIATION HEAT FLUX FROM HIGH PRESSURE AIR ARCS AT HIGH FRE09/11/64

     PROP(N,I)    =REC(IPST)
165  IPST = IPST +5
     GO TO 180
170  PCNT =RHO(N)-1.
     IPST =5
     DO 175 I=1,NW
     PROP(N,I)    = EXPF((LOGF(REC(IPST)/REC(IPST-1)))*PCNT+
    1LOGF(REC(IPST)))
175  IPST = IPST +5
180  CALL CLOSE (661)
     IF (IOPT2)184,183,184
183  NTA=NTR+1
     NTB=NTR
     GO TO 185
184  NTA=NTR
     NTB=NTR-1
185  NTP=NT-1
     RDALPH=DALPHA*1.7453292E-2
     NH=NDIV-1
     NANGLE =NRAVE*(NALPHA-1)+1
     ALPHA(1)=0.
     SINA(1)=0.
     DO 190 NA=2,NALPHA
     ALPHA(NA)=ALPHA(NA-1)+RDALPH
     SINA(NA)=SINF(ALPHA(NA))
190  DSINA(NA)=SINA(NA)-SINA(NA-1)
     DO 210 NQ=1,NTB
     DO 210 NA=2,NALPHA
     EXRQSN(NQ,NA)=RAD(NQ)/SINA(NA)
210  EXSNRQ(NQ,NA)=1./EXRQSN(NQ,NA)
     ANGLE(1)=0.
     ANGADD=RDALPH/RAVE
     DO 220 NAVE=2,NANGLE
     ANGLE (NAVE)=ANGLE(NAVE-1)+ANGADD
220  ENSNA(NAVE)=SINF(ANGLE(NAVE))
     DO 230 NQ=1,NT
     DO 230 NAVE=2,NANGLE
     ENRQSN(NQ,NAVE)=RADQ(NQ)/ENSNA(NAVE)
230  ENSNRQ(NQ,NAVE)=1./ENRQSN(NQ,NAVE)
     DO 241 N=1,NTR
     ABEMIS(N)=-1.9*((1.-(RAD(N+1)/RAD(N))**2/2.)-(ARSIN(RADIN+1)/RADIN
    1))+SINF(2.*ARSIN(RAD(N+1)/RAD(N)))/2.)/3.1415926)
     TEMPRN(N)=(TEMP(N)**4)*5.6686E-12
     RDELTA(N)=RAD(N)/DELTA
     DR(N)=RAD(N)-RAD(N+1)
241  C2T(N)=1.438/(TEMP(N)*4.)
     ERASE ETA
     DO 700 I=1,NW
     ERASE AMIN,AMAX,OPT,SUM,DRK
     DO 245 N=1,NTR
245  SUM=SUM+DR(N)*PROP(N,I)
     DK=2.*SUM
     EXTRMN=1.
     EXTRMX=1.
     DO 650 N=1,NTA
     DV=(WN(I+1)-WNA)*2.*C2T(N)
```

```
  STUDY OF RADIATION HEAT FLUX FROM HIGH PRESSURE AIR ARCS AT HIGH FREQ09/11/64

     EKDR(1)=DR(N)*PROP(N,I)
     DRK=DRK+EKDR(1)
     V=C2T(N)*(2.*WN(I)+WNA+WN(I+1))
     IF (V-13.)252,252,650
252  ETA(N,I)=.15399*DV    *(V**3)/(EXPF(V)-1.)
255  IF (N-NTA)256,650,730
256  ERASE SKDR
     DO 275 NA=2,NALPHA
     DO 270 NQ=1,N
     R(NQ)=EXRQSN(NQ,NA)*(SINF(ALPHA(NA)-ARSIN(RAD(N+1)*
    1EXSNRQ(NQ,NA)))
     IF( N -1) 730,265,257
257  IF (NQ-1) 730,270,260
260  AKDR(NQ-1)=(R(NQ-1)-R(NQ))*PROP(NQ-1,I)
     IF (NQ- N )270,265,730
265  AKDR( N )=R( N )*PROP( N ,I)
     EKDR(NA)=AKDR( N )
270  CONTINUE
     DO 275 NQ=1,N
275  SKDR(NA)=SKDR(NA)+AKDR(NQ)
280  SKDR(1)=DRK
     DO 305 NA =1,NALPHA
     IF(EKDR(NA)-1.)295,295,300
295  FKR(NA)=EXPF(-1.206*EKDR(NA))
     GO TO 305
300  IF (EKDR(NA)-16.)301,301,302
301  FKR(NA)=(EXPF(-1.206*EKDR(NA)))*(1.0774-.09539*EKDR(NA)+
    1.055577*(EKDR(NA))**2-4.29143E-3*(EKDR(NA))**3+2.082602E-4*
    2(EKDR(NA))**4)
     GO TO 305
302  FKR(NA)=0.
305  CONTINUE
     ERASE EPSMN,EPSMX
     DO 310 NA=2,NALPHA
     EPSMN=EPSMN+FKR(NA)*DSINA(NA )
310  EPSMX=EPSMX+FKR(NA-1)*DSINA(NA)
     EOUT=1.-EXPF(ABEMIS(N)*PROP(N,I)*RAD(N) )
     EIN=1.-(EPSMN+EPSMX)/2.
     WBB=ETA(N,I)*TEMPRW(N)
     WIN=WBB*EIN*RDELTA(N+1)
     WOUT=WBB*EOUT*RDELTA(N)
     WOUTMN=WOUT*EXTRMN
     WOUTMX=WOUT*EXTRMX
     DO 340 NA=1,NALPHA
     IF (SKDR(NA)-1.)320,320,325
320  FKR(NA)=EXPF(-1.206*SKDR(NA))
     GO TO 340
325  IF (SKDR(NA)-16.) 330,330,335
330  FKR(NA)=(EXPF(-1.206*SKDR(NA)))*(1.0774-.09539*SKDR(NA)+
    1.055577*(SKDR(NA))**2-4.29143E-3*(SKDR(NA))**3+2.082602E-4*
    2(SKDR(NA))**4)
     GO TO 340
335  FKR(NA)=0.
340  CONTINUE
     ERASE EXTRMN,EXTRMX
     DO 350 NA=2,NALPHA
```

```
STUDY OF RADIATION HEAT FLUX FROM HIGH PRESSURE AIR ARCS AT HIGH FREQ09/11/64

      EXTRMN=EXTRMN+FKR(NA)*DSINA(NA)
  350 EXTRMX=EXTRMX+FKR(NA-1)*DSINA(NA)
      ERASE TRYKDR
      NTEST=NT-N-1.
      DO 600 NAVE=2,NANGLE
      ERASE RI
      ERASE NTOUCH
      DO 530 NQ=1,NT
      SIGMA=RAD(N+1)*ENSNRQ(NQ,NAVE)
      IF (SIGMA-1.)519,519,518
  518 NTOUCH =NQ
      GO TO 530
  519 B=ARSIN(SIGMA)
      IF (NQ-NTEST)520,520,523
  520 D=ANGLE(NAVE)-B+3.1415926
      IF(D-1.5707963) 522,522,521
  521 D=3.1415926-D
  522 RI(NQ,2)=ENRQSN(NQ,NAVE)*SINF(D)
  523 C=ANGLE(NAVE)+B
      IF(C-1.5707963) 525,525,524
  524 C=3.1415926-C
  525 RI(NQ,1)=ENRQSN(NQ,NAVE)*SINF(C)
  530 CONTINUE
      NFAC=NTOUCH+1
      NJ=0
      IF(NFAC-NTEST)545,545,565
  545 DO 560 NQ=NFAC,NTEST
      NJ=NJ+1
      J=NT-NQ
  560 AKDR(NJ)=(RI(NQ,2)-RI(NQ+1,2))*PROP(J,I)
  565 NJ=NJ+1
      J=NT-NTOUCH
      AKDR(NJ)=(RI(NFAC,1)-RI(NFAC,2))*PROP(J,I)
      IF (NFAC-NTP)580,580,595
  580 DO 590 NQ=NFAC,NTP
      NJ=NJ+1
      J=NT-NQ
  590 AKDR(NJ)=(RI(NQ+1,1)-RI(NQ,1))*PROP(J,1)
  595 NUMDR=NJ
      DO 600 NJ=1,NUMDR
  600 TRYKDR(NAVE)=TRYKDR(NAVE)+AKDR(NJ)
  606 TRYKDR(1)=DK-DRK
      MAL=1
      NAL=1
      DO 635 LAL=1,NDIV
      NAL=NAL+NRAVE
      TEMPL=TRYKDR(NAL)
      JAL=NAL-1
      DO 630 I1=MAL,JAL
      IP1=I1+1
      DO 630 I2=IP1,NAL
      IF(TRYKDR(I1)-TRYKDR(I2))630,630,627
  627 TEMPS=TRYKDR(I1)
      TRYKDR(I1)=TRYKDR(I2)
      TRYKDR(I2)=TEMPS
  630 CONTINUE
```

```
  STUDY OF RADIATION HEAT FLUX FROM HIGH PRESSURE AIR ARCS AT HIGH FREQ09/11/64

     SKOR(LAL)=TRYKOR(NAL)
     IAL =LAL+NDIV
     SKOR(IAL)=TRYKOR(NAL)
     MAL=MAL+NRAVE
635  TRYKOR(MAL)=TEMPL
     CO 640     NA=1,IAL
     IF (SKOR(NA)-1.)636,636,637
636  FKR(NA)=EXPF(-1.206*SKOR(NA))
     GO TC 640
637  IF (SKOR(NA)-16.) 638,638,639
638  FKR(NA)=(EXPF(-1.206*SKOR(NA)))*(1.0774-.09539*SKOR(NA)+
    1.055577*(SKOR(NA))**2-4.29143E-3*(SKOR(NA))**3+2.082602E-4*
    2(SKOR(NA))**4)
     GO TC 640
635  FKR(NA)=0.
640  CONTINUE
     ERASE ENTRMN,ENTRMX
     CO 645 NA=2,NALPHA
     NAH=NA+NH
     ENTRMN=ENTRMN+FKR( NAH )*DSINA(NA)
645  ENTRMX=ENTRMX+FKR(NA-1)*DSINA(NA)
     WINMN=WIN*ENTRMN
     WINMX=WIN*ENTRMX
     AMIN=AMIN+WINMN+WOUTMN
     AMAX=AMAX+WINMX+WOUTMX
     OPT=OPT+WIN+WOUT
650  CONTINUE
     WNA=WN(I)
     IF (IOPT2)670,680,670
670  OPTCOR(I)=TEMPRW(NTR)*RDELTA(NTR)*ETA(NTR,I)
    1*(1.-EXPF(-1.9*EKOR(I)))
     CORMN(I)=OPTCOR(I)*EXTRMN
     CORMX(I)=OPTCOR(I)*EXTRMX
680  QMIN(I)=AMIN+CORMN(I)
     QMAX(I)=AMAX+CORMX(I)
700  QOPT(I)=OPT+OPTCOR(I)
     IF (IOPT)705,703,705
703  CO 704 I=1,NW
     ERASE Y
     Y(1)=WN(I)
     Y(2)=QMAX(I)
     Y(3)=QMIN(I)
     Y(4)=QOPT(I)
704  CALL RITE (662,Y,4)
     CALL CLOSE (662)
705  WOT 10,1
     WOT 10,8
     WOT10,7
     CO 707 I=1,NTR
707  WOT 10, 9, TEMP(I), RHO(I), RAD(I)
     WOT 10,1
     WOT 10,4
     CO 710 I=1,NW
710  WOT 10,5, WN(I), QMAX(I), QMIN(I), QOPT(I)
     ERASE QSUMMN,QSUMMX,QOPTSM,SMCRMN,SMCRMX,SMOPTC
     IF (IOPT2)1710,712,1710
```

```
      STUDY OF RADIATION HEAT FLUX FROM HIGH PRESSURE AIR ARCS AT HIGH FRE09/11/64
  171C CO 711 I=1,NW
       SMCRMN=SMCRMN+CORMN(I)
       SMCRMX=SMCRMX+CORMX(I)
   711 SMOPTC=SMOPTC+OPTCOR(I)
   712 CO 715 I=1,NW
       QSUMMN=QSUMMN+QMIN(I)
       QSUMMX=QSUMMX+QMAX(I)
   715 COPTSM=QOPTSM+QOPT(I)
       WOT 10,13,SMCRMX,SMCRMN,SMOPTC
       WOT 10,6, QSUMMX,QSUMMN,QOPTSM
       ERASE ETASM
       CO 722 N=1,NTR
       CO 722 I=1,NW
   722 ETASM(N)=ETA(N,I)+ETASM(N)
       WOT 10,10
       CO 725 I=1,NTR
   725 WOT 10,11, TEMP(I),ETASM(I)
   726 NCASE=NCASE-1
       IF (NCASE) 55,740,727
   727 CONTINUE
H       PZE     661,,32384
       GO TC 71
   73C CALL ERROR (18HINDEX OUT OF LIMIT)
   74C CONTINUE
H       MZE     661,,32384
H       MZE     662,,32384
       CALL EXIT
       END(1,1,0,0,0,1,1,1,C,1,C,0,C,0,0)
```

APPENDIX C

CALCULATION OF ANNULUS RADII

C.1 ANALYSIS

If one assumes that an individual annulus is optically thin, then there exists a mean value J of total spectral radiance (watts/cm^3 - steradian) such that

$$4\pi\bar{J}\left[\pi(r_j^2 - r_{j+1}^2)\right] = \int_{r_{j+1}}^{r_j} 2\pi r(4\pi J)\,dr \qquad (C-1)$$

where Eq. (C-1) is written for a unit length of arc column. Further assuming that J is proportional to T^4 and knowing T as a function of r, Eq. (C-1) can be rewritten

$$T_j = \left\{ \frac{2}{r_j^2 - r_{j+1}^2} \int_{r_{j+1}}^{r_j} \left[T(r)\right]^4 r\,dr \right\}^{1/4} \qquad (C-2)$$

For measured profiles, the function T(r) was approximated as a polynomial using a standard "least squares" curve fit computer program (Appendix D). Starting at the outer boundary of the arc column, successive values of r_{j+1} were determined such that T_j was a temperature at which absorption data were tabulated (multiples of 1000°K).

Since r_{j+1} appears both explicitly and as an integration limit, the following computerized iteration scheme was used. The outside and inside radii of the j^{th} annulus are r_j and r_{j+1} respectively and the radius at which $T = T_j$ is $r(T_j)$ (see sketch). The radii $r(T_j)$ and $r(T_{j+1})$ were chosen as trial values of r_{j+1} and the weighted average temperature computed from Eq. (C-2). Additional successive trial values of r_{j+1} were obtained by linear interpolation from the two preceding trials. Typically four trials were needed to match the weighted average temperature to the tabulated T_j within one degree Kelvin.

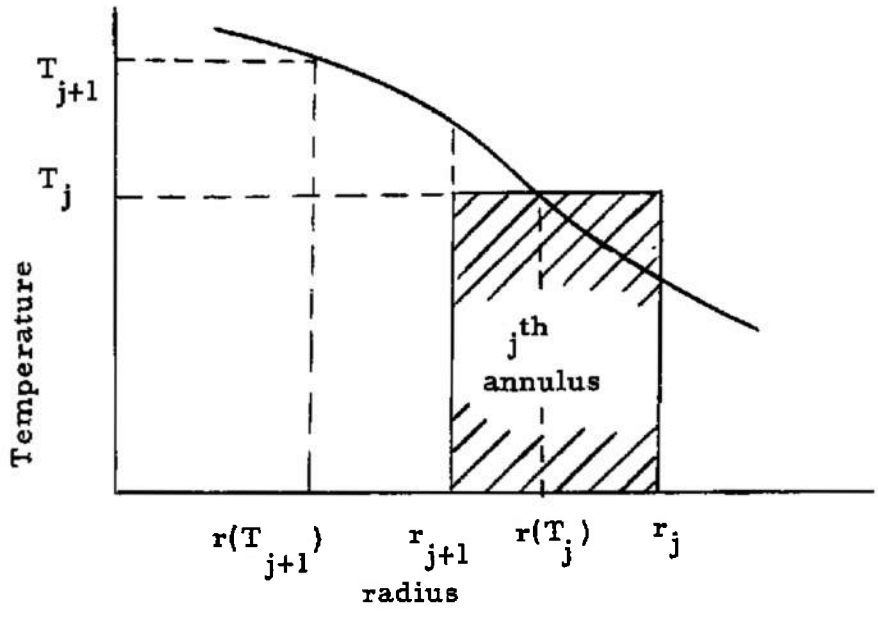

C.2 DESCRIPTION OF ANALYTIC TEMPERATURE PROFILE COMPUTER PROGRAM

A FORTRAN program called ANALYTIC TEMPERATURE PROFILE was written for the IBM 1620 Digital Computer and used to calculate the successive values of r_{j+1} satisfying Eq. (C.2). It requires as input data the constants of the polynomial describing the profile (see Appendix D) and a list of the T_j*.

Profiles derived from experimental data generally were incomplete. That is, the data extended neither to the centerline nor to the outer boundary. This program therefore automatically completed the profiles with parabolas which joined the curve fit polynomial smoothly and also satisfied the conditions of zero tem-

*From 10,000°K up, increments of 1000°K in T_j were used to make maximum use of available data. Below 10,000°K increments were usually 2000°K because in this temperature range the temperature gradient was generally very steep and the 1000°K increment would result in annuli unnecessarily thin compared to the higher temperature ones.

perature gradient at the centerline and a given outer boundary temperature. Next, a calculation of the values of $r(T_j)$ was necessary. Since the curve fit polynomial was usually at least 3rd order the Newton-Raphson iteration method was used.

Arbitrary profiles of the form of Eq. 3.3 were complete without end parabolas and could be solved exactly for the $r(T_j)$. A simplified version of the Analytic Temperature Profile program was used with these profiles. The statements in the program listing, Section C.5, which are bracketed were deleted and four statements were added to compute the $r(T_j)$.

C.3 DEFINITION OF SYMBOLS FOR COMPUTER PROGRAM

A(N)	Constants associated with curve fit polynomial
B, B2	Constants associated with inner parabola
C, C1	Constants associated with interpolation of RLLIM
COEF	Coefficient used in calculation of R(N) by Newton-Raphson Method
DELT	Number of intervals for numerical integration
DRAD	Radius increment
E, E1, E2	Constants associated with outer parabola
F(I)	Function of radius $F(I) = [T(R)]^4 \times R$
FINTG	$\int F dR$
FPOW	After some calculation steps FPOW = T(R)
I	Index for integration
UMAX	Maximum value of I
K	Index
L	Index for computing R(N) and for computing [RLLIM(L), TAVG(L)]
N	Index for temperature
NCST	Number of constants in curve fit polynomial
NORD	Order of curve fit polynomial
NT	Number of temperatures
PRNUM	Profile number
R(N)	Radius associated with N^{th} temperature
RAD	Radius

RB	Intermediate variable in computing R(N)
RD, RE	Radii at which inner and outer parabolas, respectively, join the curve fit polynomial
RDIF	Error in Newton-Raphson calculation of R(N)
RJ(N)	Inside radius of annulus having a weighted average temperature T(N)
RPOW	Intermediate variable in computing R(N)
RLLIM(L)	Lower limit radius for TAVG(L) integration
RTOL	Tolerance on Newton Raphson calculation of R(N)
RULIM	Upper limit radius for TAVG(L) integration
SUM1, SUM2, SUM3	Intermediate variables in TAVG integration
T(N)	N^{th} temperature
TAVG(L)	Weighted average temperature
TD	Temperature at R = RD
TDIF	Difference between TAVG(3) and T(N)
TDIFA	Absolute value of TDIF
TDP	Slope of temperature profile at R = RD
TE	Slope of temperature at R = RE
TEP	Slope of temperature profile at R = RE
TNR	Temperature as used in Newton-Raphson calculation
TPNR	Slope of temperature profile as used in Newton-Raphson calculation of R(N)
TTOL	Tolerance on TDIF

C.4 BLOCK DIAGRAM

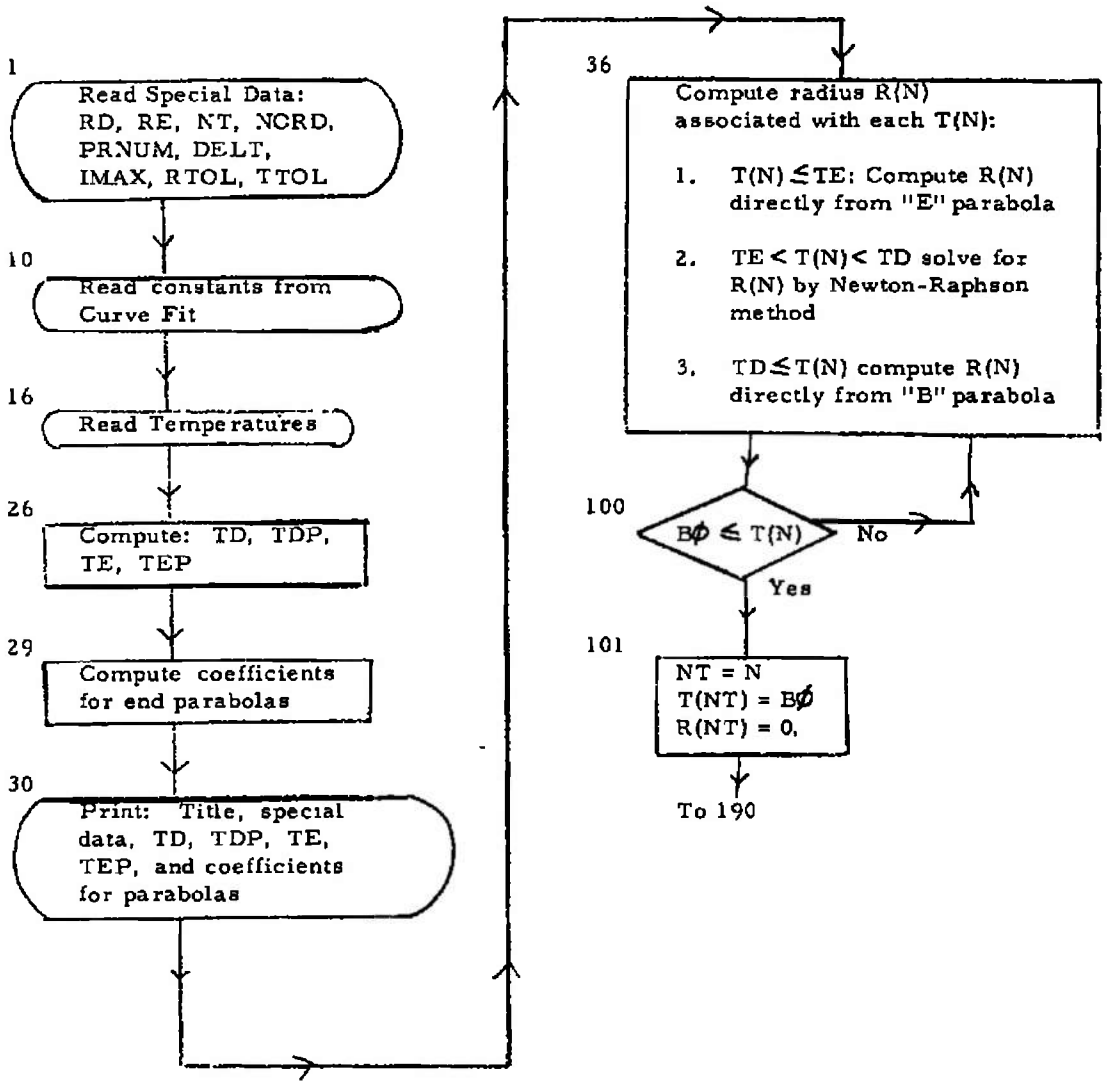

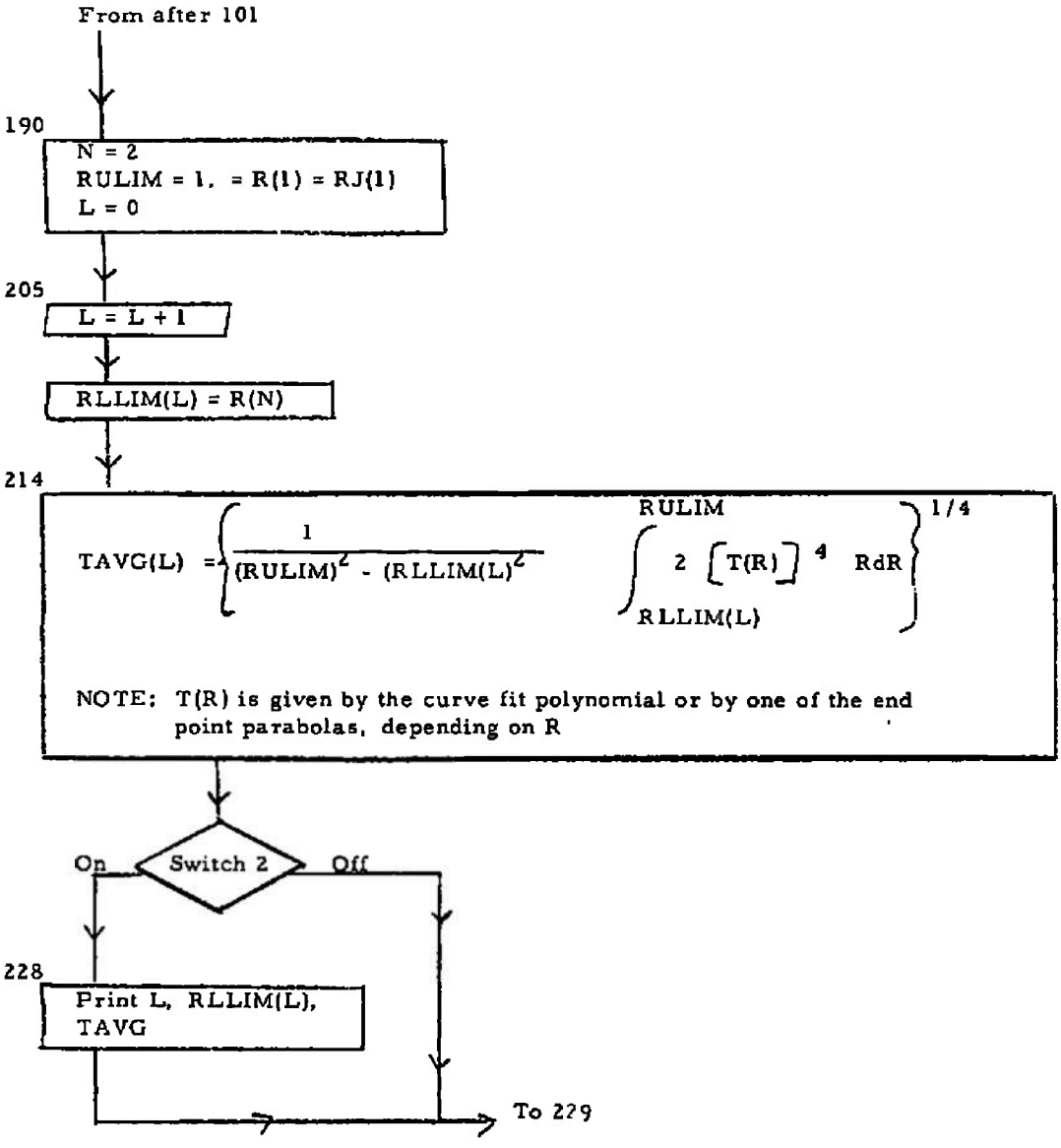
From after 101
190
N = 2
RULIM = 1. = R(1) = RJ(1)
L = 0
205
L = L + 1
RLLIM(L) = R(N)
214
TAVG(L) = { 1 / (RULIM)^2 - (RLLIM(L))^2 ∫ 2 [T(R)]^4 RdR }^1/4
RULIM
RLLIM(L)
NOTE: T(R) is given by the curve fit polynomial or by one of the end point parabolas, depending on R
On
Switch 2
Off
228
Print L, RLLIM(L), TAVG
To 229

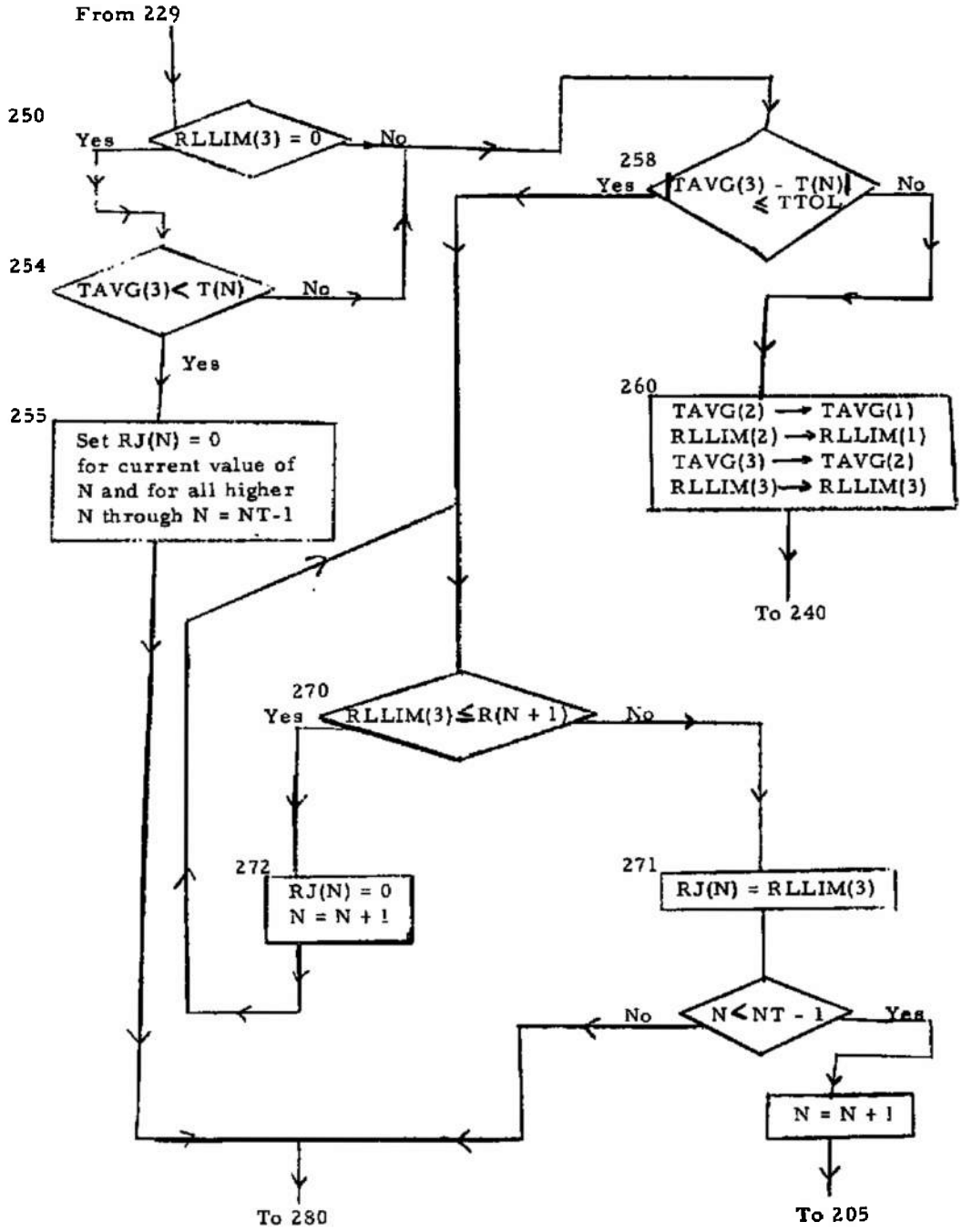
From 229
250
Yes
RLLIM(3) = 0
No
254
TAVG(3) < T(N)
No
Yes
255
Set RJ(N) = 0
for current value of
N and for all higher
N through N = NT-1
258
Yes
TAVG(3) - T(N) ≤ TTOL
No
260
TAVG(2) → TAVG(1)
RLLIM(2) → RLLIM(1)
TAVG(3) → TAVG(2)
RLLIM(3) → RLLIM(3)
To 240
270
Yes
RLLIM(3) ≤ R(N + 1)
No
272
RJ(N) = 0
N = N + 1
271
RJ(N) = RLLIM(3)
No
N < NT - 1
Yes
N = N + 1
To 280
To 205

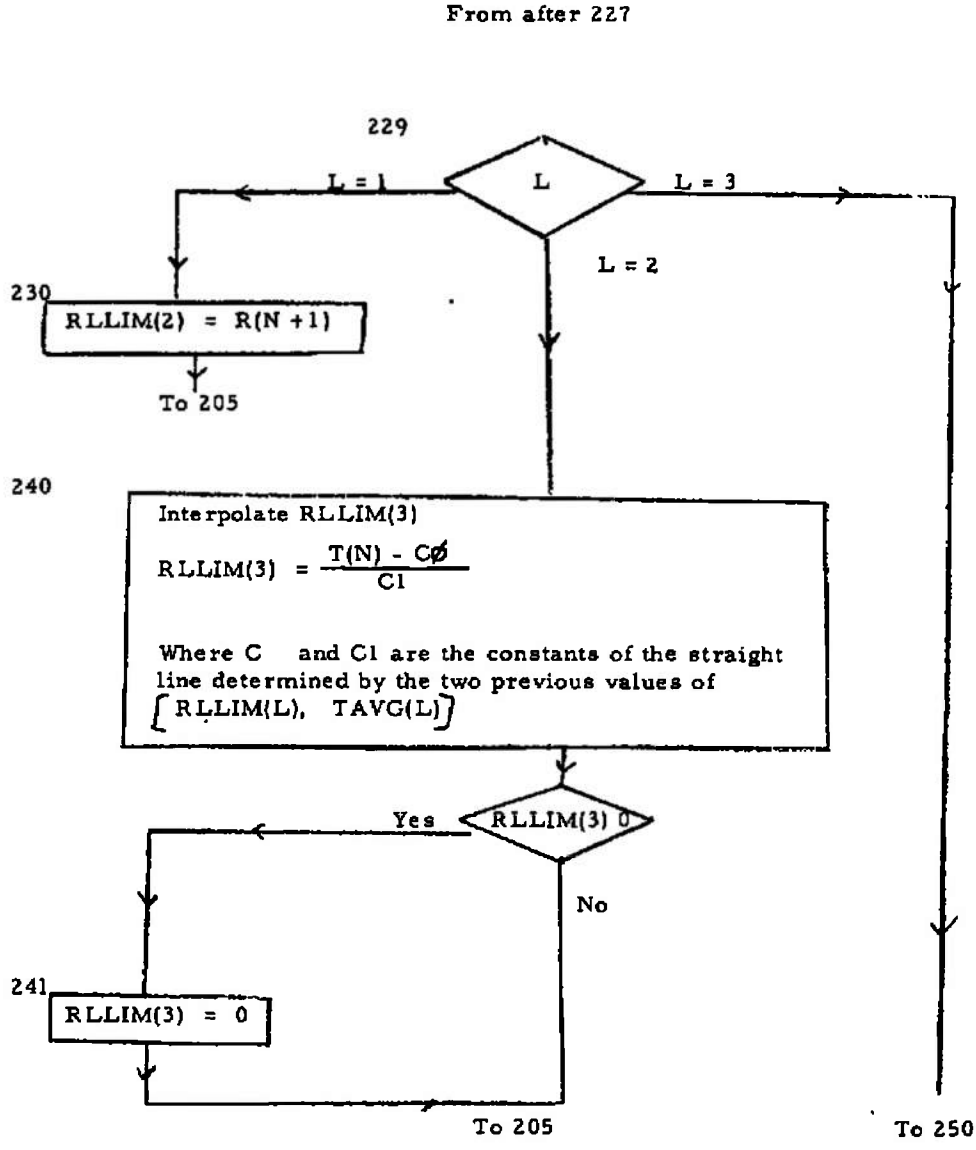
From after 227
229
L
L = 1
L = 2
L = 3
230
RLLIM(2) = R(N +1)
To 205
240
Interpolate RLLIM(3)
RLLIM(3) = T(N) - Cø / C1
Where C and C1 are the constants of the straight line determined by the two previous values of [RLLIM(L), TAVG(L)]
Yes
RLLIM(3) 0
No
241
RLLIM(3) = 0
To 205
To 250

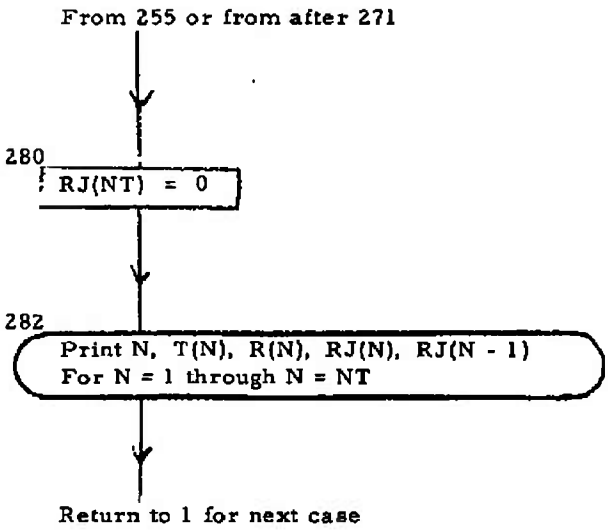
From 255 or from after 271
280
RJ(NT) = 0
282
Print N, T(N), R(N), RJ(N), RJ(N - 1)
For N = 1 through N = NT
Return to 1 for next case

C.5 PROGRAM LISTING

```
Ø8300 C     ANALYTIC TEMPERATURE PROFILE 22 MARCH 1964
Ø8300    20 FORMAT(2F10.5,2X13,2X12,2X14)
Ø8376       DIMENSION T(24), R(24), A(7), RJ(24), RLLIM(3), TAVG(3), F(17)
Ø8376    22 FORMAT(F5.1)
Ø8398    23 FORMAT(F5.Ø,15,2F1Ø.5)
Ø8436    24 FORMAT(E14.5)
Ø8458   151 FORMAT(8X22HARCRAD PROFILE NUMBER ,14)
Ø8554   152 FORMAT(8X5HNORD=,12,3X3HRD=,F6.3,3X3HRE=,F6.3)
Ø8678   153 FORMAT(8X5HRTOL=,F8.6,3X5HTTOL=,F8.6)
Ø8776   275 FORMAT(9X4ØHN      TEMP      RADIUS       RI          RO)
Ø8906   281 FORMAT(7X13,3XF6.2,4XF7.4,3XF8.5,3XF8.5)
Ø9024   300 FORMAT(5X12,3XF8.5,3XF9.5)
Ø9100   530 FORMAT(5X8HTMAX=BØ=,F11.5,3X3HB2=,F11.5)
Ø9194   531 FORMAT(5X3HEØ=,F11.5,3X3HE1=,F11.5,3X3HE2=,F11.5)
Ø9308   532 FORMAT(5X3HTD=,F9.5,3X4HTDP=,F10.5,3X3HTE=,F9.5,3X4HTEP=,F10.5)
Ø9458     1 READ 2Ø,RD,RE, NT, NORD, PRNUM
Ø9530       NCST=NORD+1
Ø9578       N=1
Ø9614    10 READ 24, A(N)
Ø9662       N=N+1
Ø9710       IF(NCST-N) 15, 10, 10
Ø9778    15 N=1
Ø9814    16 READ 22, T(N)
Ø9862       N=N+1
Ø9910       IF(NT-N) 25, 16, 16
Ø9978    25 READ 23, DELT, IMAX, RTOL, TTOL
T0038  5025 L=1
T0074       RB=RD
T0110    26 RPOW=1.
```

Note: Bracketed statements deleted for arbitrary profiles, Eq. 3.2.

```
T0146      TNR=A(1)
T0182      TPNR=0.
T0218      COEF=0.
T0254      DO 27 K=2, NCST
T0266      COEF =COEF+1.
T0314      TPNR=TPNR+A(K)*RPOW*COEF
T0410      RPOW=RPOW*RB
T0458   27 TNR=TNR+RPOW*A(K)
T0578      IF(L-1) 1000, 28, 29
T0646   28 TD=TNR
T0682      TDP=TPNR
T0718      RB=RE
T0754      L=2
T0790      GO TO 26
T0798   29 TE=TNR
T0834      TEP=TPNR
T0870      B0=TD-TDP*RD/2.
T0954      B2=TDP/2./RD
T1014      E2=((TEP*(RE-1.))-(TE-T(1)))/(RE-1.)**2
T1194      E1=TEP-2.*E2*RE
T1278      E0=T(1)-E2-E1
T1338   30 PRINT 151, PRNUM
T1362   31 PRINT 152, NORD, RD, RE
T1410   32 PRINT 153, RTOL, TTOL
T1446   33 IF(SENSE SWITCH 3) 36, 35
T1466   35 PRINT 530, B0, B2
T1502      PRINT 531, E0, E1, E2
T1550      PRINT 532, TD, TDP, TE, TEP
T1610   36 N=1
T1646      R(N)=1.
T1706   40 N=N+1
T1754   44 IF(TE-T(N)) 60, 45, 45
T1846   45 R(N)=-E1/2./E2+SQRTF((E1/2./E2)**2+(T(N)-E0)/E2)
```

```
T2098        GO TO 40
T2106    60  R(N)=RE
T2166    61  IF(TD-T(N)) 100, 81, 62
T2258    62  TNR=A(1)-T(N)
T2330        TPNR=0.
T2366        RPOW=1.
T2402        COEF=0.
T2438        DO 63 K=2, NCST
T2450        COEF=COEF+1.
T2498        TPNR=TPNR+A(K)*RPOW*COEF
T2594        RPOW=RPOW*R(N)
T2666    63  TNR=TNR+RPOW*A(K)
T2786        RDIF=TNR/TPNR
T2834        R(N)=R(N)-RDIF
T2930        RDIF=SQRTF(RDIF*RDIF)
T2990    70  IF(RDIF-RTOL) 90, 90, 62
T3058    81  R(N)=RD
T3118        N=N+1
T3166        GO TO 100
T3174    90  N=N+1
T3222        R(N)=R(N-1)
T3306        GO TO 61
T3314   100  IF(B0-T(N)) 101, 101, 110
T3406   101  NT=N
T3442        T(NT)=B0
T3502        R(N)=0.
T3562        GO TO 190
T3570   110  R(N)=SQRTF((B0-T(N))/B2)
T3690        N=N+1
T3738        GO TO 100
T3746   190  DO 200 I=1, 17
T3758   200  F(I)=0.
T3854        RJ(1)=R(1)
```

Statements added for arbitrary profiles, Eq. 3.2

```
        P = NORD
        Q = SQRTF(A(NCST)*A(NCST))
        DO 110, N=1, NT
100 R(N) = (1. - (T(N)-2.)/Q)**(1./P)
```

```
T3890        N=2
T3926   202  L=0
T3962        RULIM=RJ(N-1)
T4022        RLLIM(1)=R(N)
T4082   205  L=L+1
T4130        DRAD=(RULIM-RLLIM(L))/DELT
T4214        RAD=RLLIM(L)
T4274        DO 220 I=1, IMAX
T4286   214  IF(RAD-RD) 217, 217, 215
T4354   215  IF(RAD-RE) 216, 218, 218
T4422   216  FPOW=A(1)
T4458        RPOW=1.
T4494        DO 2161 K=2, NCST
T4506        RPOW=RPOW*RAD
T4554  2161  FPOW=FPOW+RPOW*A(K)
T4674        F(I)=FPOW**4*RAD
T4758        GO TO 220
T4766   217  F(I)=((B0+B2*RAD**2)**4)*RAD
T4886        GO TO 220
T4894   218  F(I)=((E0+E1*RAD+E2*RAD**2)**4)*RAD
T5062   220  RAD =RAD+DRAD
T5146        SUM1=F(1)+F(IMAX)
T5218        SUM2=F(2)+F(4)+F(6)+F(8)+F(10)+F(12)+F(14)+F(16)
T5338        SUM3=0.
T5374        I=3
T5410   226  SUM3=SUM3+F(I)
T5482        I=I+2
T5530        IF(I-IMAX) 226, 227, 227
T5598   227  FINTG=.66666667*DRAD*(SUM1+4.*SUM2+2.*SUM3)
T5754        TAVG(L)=(FINTG/(RULIM**2-RLLIM(L)**2))**0.25
T5934        IF(SENSE SWITCH 2) 228, 229
T5954   228  PRINT 300,L, RLLIM(L), TAVG(L)
T6050   229  IF(L-2) 230, 240, 250
```

```
T6118   230 RLLIM(2)=R(N+1)
T6178       GO TO 205
T6186   240 C1=(TAVG(L-1)-TAVG(L))/(RLLIM(L-1)-RLLIM(L))
T6378       CØ=TAVG(L-1)-C1*RLLIM(L-1)
T6498       RLLIM(3)=(T(N)-CØ)/C1
T6582       IF(RLLIM(3)) 241, 205, 205
T6638   241 RLLIM(3)=Ø.
T6674       GO TO 205
T6682   250 TDIF=TAVG(L)-T(N)
T6778   253 IF(RLLIM(3)) 1000, 254, 258
T6834   254 IF(TDIF) 255, 258, 258
T6890   255 RJ(N)=Ø.
T6950       IF(NT-N-1) 280, 280, 256
T7030   256 N=N+1
T7078       GO TO 255
T7086   258 TDIFA=SQRTF(TDIF*TDIF)
T7146       IF(TDIFA-TTOL) 270, 270, 260
T7214   260 DO265 K=1,2
T7226       TAVG(K)=TAVG(K+1)
T7310   265 RLLIM(K)=RLLIM(K+1)
T7430       L=L-1
T7478       GO TO 240
T7486   270 IF(RLLIM(3)-R(N+1)) 272, 271, 271
T7578   271 RJ(N)=RLLIM(3)
T7638       IF(NT-N-1) 280, 280, 273
T7718   272 RJ(N)= Ø.
T7778       N=N+1
T7826       GO TO 270
T7834   273 N=N+1
T7882       GO TO 202
T7890   280 RJ(NT)=Ø.
T7950       PRINT 275
T7974       N=1
```

```
T8010        PRINT 281, N, T(N), R(N)
T8106        N=2
T8142   282  PRINT 281, N, T(N), R(N), RJ(N), RJ(N-1)
T8310        N=N+1
T8358        IF(NT-N) 1, 282, 282
T8426  1000  STOP
T8474        END

PROG SW 1 ONFOR SYMBOL TABLE, PUSH START
SW 1 OFF TO IGNORE SUBROUTINES, PUSH START

PROCESSING COMPLETE
```

APPENDIX D

CURVE FIT FOR TEMPERATURE PROFILE DATA

D.1 ARCRAD CURVE FIT PROGRAM DESCRIPTION

Reduction of temperature profile data to analytic form was accomplished by making use of a modification of a standard computer program by W. R. Greaves (Ref. 19) entitled POLYNOMIAL CURVE FITTING, NO CONSTRAINTS.

The following changes were made in Greaves' program.

1. Format statements were added to change from "No Format" FORTRAN to FORTRAN I.

2. The maximum order polynomial was reduced from 50 to 7.

3. Provision for weighting data was eliminated.

4. Control statements were rewritten to the form shown in the accompanying block diagram.

The ARCRAD CURVE FIT program fits a straight line and successively higher order curves to the input data on a "least squares" basis. For each order curve the polynomial constants and the standard error are printed. As the order of the fitted curve increases the standard error at first decreases, then levels off and either increases or oscillates. A curve which is the best compromise between minimum order and minimum standard error is selected as most representative of the data. The program automatically causes a card to be punched for each constant in the polynomial for use as input to the ANALYTIC TEMPERATURE PROFILE program. Finally, for the order selected, the value of the polynomial at each input data point is printed, along with the input data value and the difference.

The number of data points must be at least 2 greater than the order of the maximum order polynomial. The program can handle up to 50 sets of data and computes polynomials up to seventh order but these limits can easily be changed by appropriate changes in the DIMENSION statement.

D.2 SENSE SWITCH SETTINGS

Flexibility in program utilization is made possible by the Sense Switches. Switch 1 OFF causes automatic selection of the 3rd order polynomial. Switch 1 ON causes the computer to pause after printing the constants and the standard error for the preselected maximum order. The desired order polynomial can then be selected and inserted in the machine by on-line typewriter (ACCEPT statement).

Switch 2 ON eliminates automatic card punching of the polynomial constants.

D.3 ARCRAD CURVE FIT DEFINITION SYMBOLS

AM (I, J)	Matrix of coefficients of normal equations
DIF	Difference between Y(I) and YFLEX(I)
LAST	Highest order polynomial to be fitted
NDATA	Number of data points
PRNUM	Serial number of temperature profile
SUMX(J)	$\sum_{i=1}^{N} (Xi)^{J-1}$
SUMY(J)	$\sum_{i=1}^{N} (Yi)(Xi)^{J-1}$
S1	Same as YFLEX(I)
S2	Standard error, $\sqrt{\frac{\sum_{i=1}^{N} (Yi - YFLEXi)^2}{NDATA-NORD-1}}$
S3	Same as DIF
X(I)	i^{th} value of independent variable (radius)
Y(I)	i^{th} value of dependent variable (temperature)
YFLEX(I)	Value of the polynomial at X(I)

D.4 BLOCK DIAGRAM

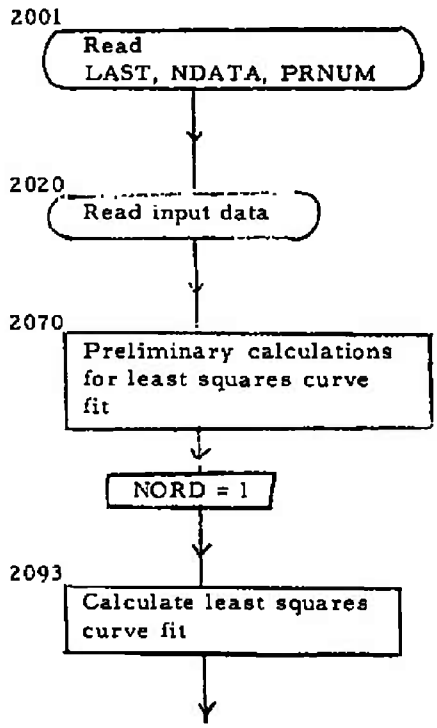

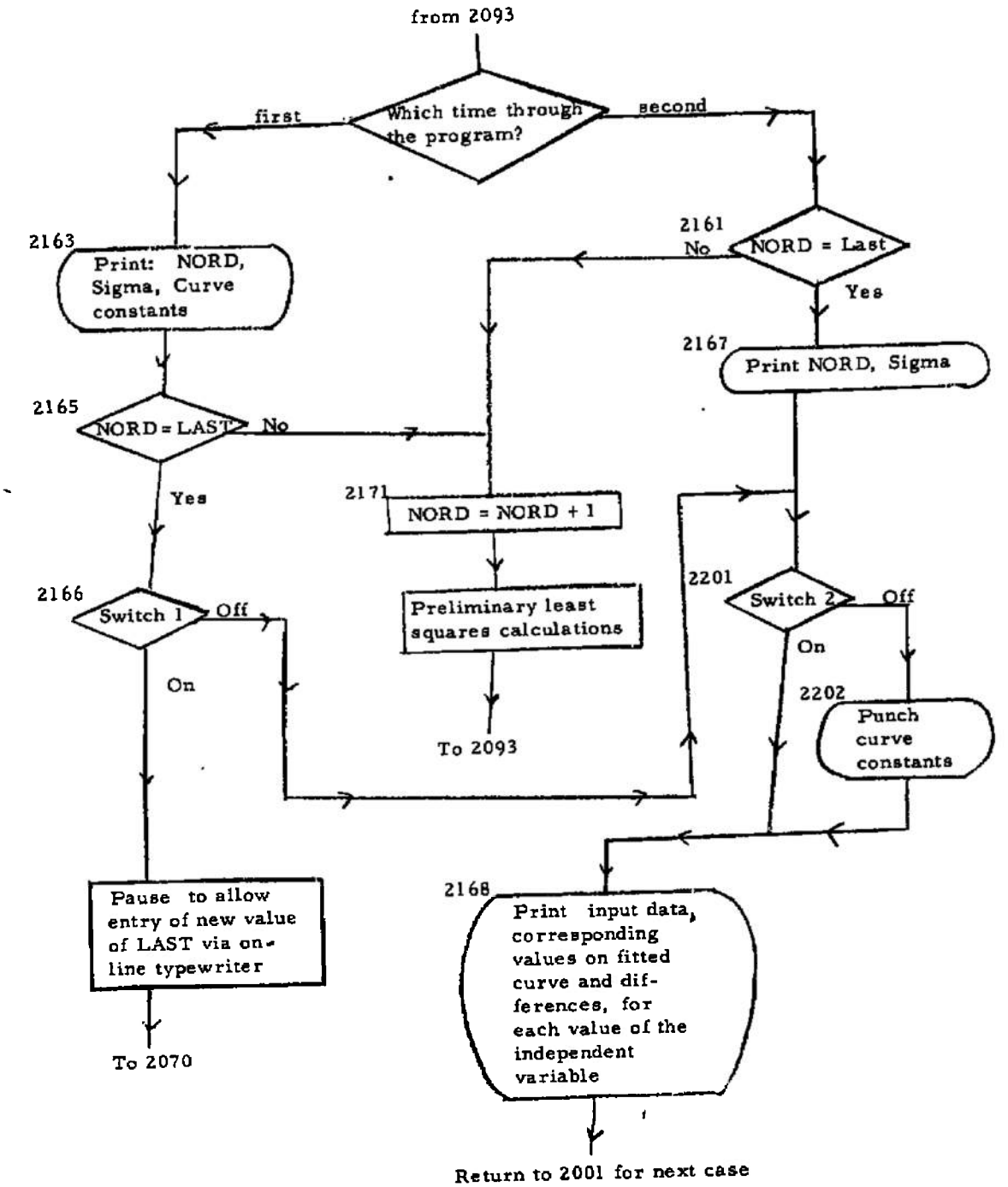
from 2093
Which time through the program?
first
second
2163
Print: NORD, Sigma, Curve constants
2161
No
NORD = Last
Yes
2167
Print NORD, Sigma
2165
NORD = LAST
No
Yes
2171
NORD = NORD + 1
Preliminary least squares calculations
To 2093
2166
Switch 1
Off
On
2201
Switch 2
Off
On
2202
Punch curve constants
Pause to allow entry of new value of LAST via on-line typewriter
To 2070
2168
Print input data, corresponding values on fitted curve and differences, for each value of the independent variable
Return to 2001 for next case

D.5 PROGRAM LISTING

```
08300 C      ARCRAD CURVE FIT 10 MARCH 1964
08300        DIMENSION X(52), Y(52), AM(9,9), SUMX(15), SUMY(17)
08300  2501 FORMAT(I2,2XI3,2XI4)
08354  2502 FORMAT(F6.2,2XE14.7)
08392  2503 FORMAT()
08410  2504 FORMAT(5X5HNORD=,I2,3X6HSIGMA=,F7.4)
08504  2505 FORMAT(5XI2,3XF11.5)
08562  2506 FORMAT(8X11HCASE NUMBER,I4,3X6HNDATA=,I3)
08674  2507 FORMAT(5XF7.4,3XF6.2,3XF8.4,3XF7.4)
08768  2508 FORMAT(5X47HSW1 OFF LAST=3, SW1 ON ACCEPT, LAST, PUSH START)
08904  2509 FORMAT(7X34HX(I)      Y(I)     YFLEX(I)       DIF)
09018  2510 FORMAT(E14.5)
09040  2001 READ 2501, LAST, NDATA, PRNUM
09088        PRINT 2506, PRNUM, NDATA
09124        NRPT=0
09148        I=0
09172  2020 I=I+1
09208        READ 2502, X(I), Y(I)
09292        IF(I-NDATA) 2020, 2070, 2070
09360  2070 SUMX(1)=0.
09384         SUMX(2)=0.
09408         SUMX(3)=0.
09432         SUMY(1)=0.
```

```
Ø9456          SUMY(2)=Ø.
Ø9480          DO 2Ø9Ø I=1, NDATA
Ø9492          SUMX(1)=SUMX(1)+1.
Ø9528          SUMX(2)=SUMX(2)+X(I)
Ø9588          SUMX(3)=SUMX(3)+X(I)*X(I)
Ø9684          SUMY(1)=SUMY(1)+Y(I)
Ø9744    2Ø9Ø  SUMY(2)=SUMY(2)+X(I)*Y(I)
Ø9876          NORD=1
Ø9ØØØ    2Ø93  L=NORD+1
Ø9936          KK=L+1
Ø9972          DO 21Ø1 I=1, L
Ø9984          DO 21ØØ J=1, L
Ø9996          IK=J-1+I
T ØØ44   21ØØ  AM(I,J)=SUMX(IK)
T Ø188   21Ø1  AM(I,KK)=SUMY(I)
T Ø332         DO 2140 I=1, L
T Ø3Ø4         AM(KK,I)=-1.
T Ø44Ø         KKK=I+1
T Ø476         DO 2110 J=KKK, KK
T Ø488   2110  AM(KK,J)=Ø.
T Ø6ØØ         C=1./AM(1,I)
T Ø692         DO 2120 II=2, KK
T Ø7Ø4         DO 2120 J=KKK,KK
T Ø716   2120  AM(II,J)=AM(II,J)-AM(1,J)*AM(II,I)*C
T 1Ø88         DO 2140 II=1, L
T 11ØØ         DO 2140 J=KKK,KK
T 1112   2140  AM(II,J)=AM(II+1,J)
T 1364         S2=Ø.
T 1388         DO 216Ø J=1, NDATA
T 14ØØ         S1=Ø.
T 1424         S1= S1+ AM(1, KK)
T 15Ø8         DO 2150 I=1, NORD
T 152Ø   2150  S1=S1+AM(I+1,KK)*X(J)**I
```

```
T1700  2160 S2=S2+(S1-Y(J))*(S1-Y(J))
T1880       B=NDATA-L
T1928        S2=(S2/B)**.5
T1976       IF(NRPT) 2163, 2163, 2161
T2032  2161 IF(NORD-LAST) 2171, 2167, 2167
T2100  2163 PRINT 2503
T2124       PRINT 2504, NORD, S2
T2160       I=0
T2184  2164 I=I+1
T2220       J=I-1
T2256       PRINT 2505, J, AM(I,KK)
T2352       IF(I-L) 2164, 2165, 2165
T2420  2165 IF (NORD-LAST) 2171, 2166, 2166
T2488  2166 IF(SENSE SWITCH 1) 2173, 2167
T2508  2167 PRINT 2504, NORD, S2
T2544       PRINT 2509
T2568       IF(SENSE SWITCH 2) 2203, 2201
T2588  2201 I=0
T2612  2202 I=I+1
T2648       PUNCH 2510, AM(I, KK)
T2732       IF(I-L) 2202, 2203, 2203
T2800  2203 I=0
T2824  2204 I=I+1
T2860        S1=0.
T2884       S1= AM(1,KK)
T2956       DO 2168 J=1, NORD
T2968  2168 S1=S1+AM(J+1,KK)*X(I)**J
T3148        S3=Y(I)-S1
T3208       PRINT 2507, X(I), Y(I), S1, S3
T3316       IF(I-NDATA) 2204, 2001, 2001
T3384  2171 NORD=NORD+1
T3420        J=2*NORD
T3456        SUMX(J)=0.
```

```
T3504          SUMX(J+1)=0.
T3552          SUMY(NORD+1)=0.
T3600         DO 2172 I=1, NDATA
T3612         SUMX(J)=SUMX(J)+X(I)**(J-1)
T3768         SUMX(J+1)=SUMX(J+1)+X(I)**J
T3888   2172 SUMY(NORD+1)=SUMY(NORD+1)+Y(I)*X(I)**NORD
T4080         GO TO 2093
T4088   2173 NRPT=NRPT+1
T4124         PRINT 2508
T4148         PAUSE
T4160         IF (SENSE SWITCH 1) 2175, 2176
T4180   2175 ACCEPT 2501, LAST
T4204         GO TO 2070
T4212   2176 LAST=3
T4236         GO TO 2070
T4244          END

PROG SW 1 ONFOR SYMBOL TABLE, PUSH START
SW 1 OFF TO IGNORE SUBROUTINES, PUSH START

PROCESSING COMPLETE
```

APPENDIX E

MEASUREMENT OF TEMPERATURE PROFILES

Conditions required for application of the intensity ratio technique are: (1) steady symmetric source, (2) Boltzmann distribution of the atomic energy levels (i.e., local thermal equilibrium of the plasma particles) and (3) optically thin plasma at the frequency of the emission line. The first condition was checked photographically with a Fastax camera operating at 3000 to 5000 frames per second. In this speed range, which was of the same order as the spectrograph exposures of 1/1000 sec, the source appeared steady and uniform. The existence of local thermal equilibrium is discussed in Section 2.1. Optical thinness is one of the factors governing the choice of suitable lines. At one atmosphere several lines can be used, but at 2 atmospheres only the oxygen pair 7774 Å - 7947 Å is suitable and it is near marginal. Relative intensity at a given wavelength is related to transition probability A, atom number density N and photon energy $h\nu$ by

$$\frac{I_{\lambda 1}}{I_{\lambda 2}} = \frac{A_1 N_1 (h\nu)_1}{A_2 N_2 (h\nu)_2} \tag{E-1}$$

For spectral lines of the same species, assuming a Boltzmann distribution of energy states

$$\frac{I_{\lambda 1}}{I_{\lambda 2}} = \frac{g_1 A_1 \lambda_1 e^{-\left(\frac{E_1 - E_2}{kT}\right)}}{g_2 A_2 \lambda_2} \tag{E-2}$$

where g is the statistical weight of an energy state and E is the excitation energy of the upper state energy level. Solving for T

$$T = \frac{(E_1 - E_2)(1/k)}{\ln(g_1 A_1 \nu_1 / g_2 A_2 \nu_2) - \ln(I_{\lambda 2}/I_{\lambda 1})} \tag{E-3}$$

The excitation energies and transition probabilities are known, so spectrographic measurement of the intensity ratios establishes an "average" temperature of the column. To determine the temperature distribution the true intensity distribution must be calculated from the "average" observed intensity using Abel's integral equation

$$I(x) = 2\int_{r=x}^{\delta} \frac{n(r)\ r\,dx}{\sqrt{r^2 - x^2}} \qquad \text{(E-4)}$$

where I(x) is observed intensity over radius x and n(r) is the number density of emitters in particular radial bands of radius r. This function has been tabulated by Pearce (Ref. 20).

Temperature level can be established because the spectral line intensity goes through a maximum at a unique temperature for a given pressure. This maximum, the so called peaking function, results from the counter-balancing effects of increased excitation of the upper states, which increases the number of emitters per unit volume, and increased ionization which reduces the number of emitters per unit volume. The technique has been described in detail by Sadjian (Ref. 21). For this study the oxygen atom pair, λ = 7947 Å and 7774 Å were used as well as the nitrogen atom/ion pair, λ = 4137 Å and 3995 Å.

UNCLASSIFIED
Security Classification

DOCUMENT CONTROL DATA - R&D

(Security classification of title, body of abstract and indexing annotation must be entered when the overall report is classified)

1 ORIGINATING ACTIVITY (Corporate author)
General Electric Company, Space Sciences Laboratory, Valley Forge Space Technology Center, King of Prussia, Pennsylvania

2a REPORT SECURITY CLASSIFICATION
UNCLASSIFIED

2b GROUP
N/A

3. REPORT TITLE
STUDY OF RADIATION HEAT FLUX FROM HIGH PRESSURE AIR ARCS

4. DESCRIPTIVE NOTES (Type of report and inclusive dates)
N/A

5 AUTHOR(S) (Last name, first name, initial)
Marston, C. H.

This document has been approved for public release its distribution is unlimited. Per AD TR-75-5 AFSC ltr 709 July 1975

6 REPORT DATE	7a. TOTAL NO. OF PAGES	7b. NO. OF REFS
January 1965	160	21

8a CONTRACT OR GRANT NO.
AF40(600)-1080

b. PROJECT NO. 8952

c. Program Element 62405334

d. Task 895202

9a. ORIGINATOR'S REPORT NUMBER(S)
AEDC-TR-65-11

9b. OTHER REPORT NO(S) (Any other numbers that may be assigned this report)
N/A

10. AVAILABILITY/LIMITATION NOTICES
N/A

11. SUPPLEMENTARY NOTES
N/A

12. SPONSORING MILITARY ACTIVITY
Arnold Engineering Development Center, Air Force Systems Command, Arnold AF Station, Tennessee

13 ABSTRACT

A computational model has been developed and applied for calculating radiant heat flux from an electric arc using real gas properties and taking into account both self absorption and space varying temperature. The model requires knowledge of the temperature profile as an input. Temperature profiles were measured spectrographically using an air arc at one and 2.4 atmospheres. These measured profiles plus some simple analytic ones which satisfied boundary conditions were used to calculate radiant heat flux at pressures from 1 to 300 atmospheres. The experimental program also included measurements of radiant flux density at 2.2 and 5.7 atmospheres for comparison with calculations based on the measured profiles. Estimates were made of radiation losses in the AEDC 20-megawatt arc air heater now under development.

DD FORM 1 JAN 64 1473

UNCLASSIFIED
Security Classification

14 KEY WORDS	LINK A		LINK B		LINK C	
	ROLE	WT	ROLE	WT	ROLE	WT
Heat Flux						
Radiant Heat Flux						
Air Arcs						

INSTRUCTIONS

1. ORIGINATING ACTIVITY: Enter the name and address of the contractor, subcontractor, grantee, Department of Defense activity or other organization *(corporate author)* issuing the report.

2a. REPORT SECURITY CLASSIFICATION: Enter the overall security classification of the report. Indicate whether "Restricted Data" is included. Marking is to be in accordance with appropriate security regulations.

2b. GROUP: Automatic downgrading is specified in DoD Directive 5200.10 and Armed Forces Industrial Manual. Enter the group number. Also, when applicable, show that optional markings have been used for Group 3 and Group 4 as authorized.

3. REPORT TITLE: Enter the complete report title in all capital letters. Titles in all cases should be unclassified. If a meaningful title cannot be selected without classification, show title classification in all capitals in parenthesis immediately following the title.

4. DESCRIPTIVE NOTES: If appropriate, enter the type of report, e.g., interim, progress, summary, annual, or final. Give the inclusive dates when a specific reporting period is covered.

5. AUTHOR(S): Enter the name(s) of author(s) as shown on or in the report. Enter last name, first name, middle initial. If military, show rank and branch of service. The name of the principal author is an absolute minimum requirement.

6. REPORT DATE: Enter the date of the report as day, month, year, or month, year. If more than one date appears on the report, use date of publication.

7a. TOTAL NUMBER OF PAGES: The total page count should follow normal pagination procedures, i.e., enter the number of pages containing information.

7b. NUMBER OF REFERENCES: Enter the total number of references cited in the report.

8a. CONTRACT OR GRANT NUMBER: If appropriate, enter the applicable number of the contract or grant under which the report was written.

8b, 8c, & 8d. PROJECT NUMBER: Enter the appropriate military department identification, such as project number, subproject number, system numbers, task number, etc.

9a. ORIGINATOR'S REPORT NUMBER(S): Enter the official report number by which the document will be identified and controlled by the originating activity. This number must be unique to this report.

9b. OTHER REPORT NUMBER(S): If the report has been assigned any other report numbers *(either by the originator or by the sponsor)*, also enter this number(s).

10. AVAILABILITY/LIMITATION NOTICES: Enter any limitations on further dissemination of the report, other than those imposed by security classification, using standard statements such as:

(1) "Qualified requesters may obtain copies of this report from DDC."

(2) "Foreign announcement and dissemination of this report by DDC is not authorized."

(3) "U. S. Government agencies may obtain copies of this report directly from DDC. Other qualified DDC users shall request through

_____."

(4) "U. S. military agencies may obtain copies of this report directly from DDC. Other qualified users shall request through

_____."

(5) "All distribution of this report is controlled. Qualified DDC users shall request through

_____."

If the report has been furnished to the Office of Technical Services, Department of Commerce, for sale to the public, indicate this fact and enter the price, if known.

11. SUPPLEMENTARY NOTES: Use for additional explanatory notes.

12. SPONSORING MILITARY ACTIVITY: Enter the name of the departmental project office or laboratory sponsoring *(paying for)* the research and development. Include address.

13. ABSTRACT: Enter an abstract giving a brief and factual summary of the document indicative of the report, even though it may also appear elsewhere in the body of the technical report. If additional space is required, a continuation sheet shall be attached.

It is highly desirable that the abstract of classified reports be unclassified. Each paragraph of the abstract shall end with an indication of the military security classification of the information in the paragraph, represented as *(TS), (S), (C), or (U)*

There is no limitation on the length of the abstract. However, the suggested length is from 150 to 225 words.

14. KEY WORDS: Key words are technically meaningful terms or short phrases that characterize a report and may be used as index entries for cataloging the report. Key words must be selected so that no security classification is required. Identifiers, such as equipment model designation, trade name, military project code name, geographic location, may be used as key words but will be followed by an indication of technical context. The assignment of links, rules, and weights is optional.